SHIPPING TO AMERICA

XIWEN BAI
Tsinghua University

JESÚS FERNÁNDEZ-VILLAVERDE
University of Pennsylvania

YILIANG LI
University of International Business and Economics

RICARDO MARTO
Federal Reserve Bank of St. Louis

FRANCESCO ZANETTI
University of Oxford

February 2026

Preliminary

We study the macroeconomic impact of route-specific shipping disruptions on the U.S. economy and their implications for trade policy. Using high-frequency satellite data covering *all* U.S.-bound container vessels between 2016 and 2025, we construct measures of disruptions from port congestion, canal bottlenecks, and rerouting associated with security threats in the Red Sea to document new facts on the U.S.-bound shipping supply. We then develop a multi-route general equilibrium model to quantify the impact of shipping disruptions. The welfare impact of the 2021 shipping disruptions from congestion at the ports of LA and Long Beach amounted to 1.3% of GDP. The rerouting of vessels via the Cape of Good Hope following the Houthi attacks in early 2024 had a welfare impact of 0.6%. The response of the Navy helped contain the effect of these attacks. Our estimate of the value of Navy protection in the Red Sea is equivalent to 0.2% of GDP. We also show that the shipping market can dampen the impact of tariffs depending on how congested routes are and how much market power firms have.

KEYWORDS: AIS, congestion, container ships, navy protection, Panama Canal, port fees, satellite data, shipping capacity, shipping disruptions, shipping routes, Suez Canal, tariffs.

JEL CLASSIFICATION: E23, L91, O18, O41, R40.

Xiwen Bai: xiwenbai@tsinghua.edu.cn
Jesús Fernández-Villaverde: jesusfv@sas.upenn.edu
Yiliang Li: yiliang_li@uibe.edu.cn
Ricardo Marto: ricardo.marto@stls.frb.org
Francesco Zanetti: francesco.zanetti@economics.ox.ac.uk

We thank Myrto Kalouptsidi, Theodore Papageorgiou, and Stephen Redding for their insightful comments and suggestions. We are also grateful to seminar participants at the Bank of Portugal Winter Research Conference, NBER Transportation Networks and the Spatial Distribution of Economic Activity, SED in Copenhagen, and St. Louis Fed. We thank Hoang Le and Shengyao Xu for excellent research assistance. The views expressed here are those of the authors and do not necessarily reflect the views of the Federal Reserve Bank of St. Louis or the Federal Reserve System.

1. Introduction

Over the past few years, a sequence of high-profile disruptions has exposed critical vulnerabilities within the global shipping sector. The COVID-19 pandemic, the blockage of the Suez Canal in 2021, the Red Sea crisis in 2023 and 2024, and renewed tensions in the Strait of Hormuz in 2025 have collectively triggered sharp delays, soaring freight costs, and profound ripple effects across global supply chains. Despite the central role of seaborne shipping in modern commerce, standard macroeconomic models typically treat the sector as a passive, frictionless intermediary.

This paper challenges that paradigm. We demonstrate that the shipping sector acts as a strategic intermediary whose endogenous responses to disruptions—through capacity reallocation, speed adjustments, and dynamic pricing—can substantially amplify or attenuate the macroeconomic consequences of supply chain shocks and trade policies.

We make four primary contributions. First, we construct a novel dataset covering the universe of container vessels arriving at U.S. ports from January 2016 through March 2025. This dataset combines real-time, high-frequency satellite data from the Automatic Identification System (AIS) with vessel-level characteristics from the Lloyd's List registry. Using these data, we develop granular, route-specific measures of *potential* and *effective* shipping supply. We decompose the gap between these two measures into four distinct wedges: disruptions from port congestion, canal bottlenecks, vessel rerouting, and slow steaming. Second, we develop a multi-region, multi-route general equilibrium model in which shipping firms actively allocate capacity across routes, choose sailing speeds and loading factors, and set prices within a monopolistically competitive market subject to route-specific congestion externalities. This framework generates novel theoretical predictions regarding how logistical disruptions and trade policies interact with market structure and congestion. Third, we map the model to the data to quantify the welfare costs of the two most significant recent disruption episodes: the 2021 West Coast port crisis and the 2024 Red Sea attacks. Fourth, we utilize this framework to analyze the macroeconomic implications of tariffs in an economy where maritime shipping markets are explicitly modeled.

Our empirical analysis uncovers several new stylized facts about U.S.-bound container shipping. First, the expansion of shipping supply during the 2021-2022 period was highly asymmetric. Total deadweight tonnage of U.S.-bound vessels surged more than 60% above pre-pandemic levels by early 2022, reaching 48 million metric tons, despite a much more modest increase in global capacity (Section 2). This expansion was disproportionately concentrated along the Asia-West Coast route, which offered the shortest transit times. As a result, regions such as Africa, Latin America, and the Caribbean bore the cost of this reallocation, losing over 12% of their direct liner connections during this period.

Second, disruptions absorbed a staggering share of potential supply (Section 3). At the peak of the supply chain crisis in late 2021, nearly one-third of deployed U.S.-bound potential supply was effectively removed from the market—absorbed by ships waiting at anchor, steaming at half-speed across the Pacific, or diverting around logistical bottlenecks. Similarly, the attacks in the Red Sea in early 2024 drove shipping firms to reroute via the Cape of Good Hope, adding between 800 and 1,200 nautical miles to journeys from Asia or the Middle East to the U.S. East Coast. At its peak, these security threats reduced potential supply by as much as 40 percentage points.

To interpret these empirical patterns and quantify their aggregate implications, we develop a general equilibrium model of the shipping sector (Section 4). Shipping firms operate under monopolistic competition and are endowed with a fleet of vessels that can be held idle or allocated across six major U.S.-bound routes. Along each route, firms optimize sailing speeds, loading intensities, and prices. A critical feature of our model is the presence of an endogenous congestion externality: greater capacity flowing into a route lowers the effective shipping productivity on that route, capturing port and canal congestion in reduced form. Retailers source goods from various origin regions, choosing both how much to import from each route (the intensive margin) and whether to specialize in a given route at all (the extensive margin). Consumers exhibit nested CES preferences over domestically produced goods and imports from four distinct global regions.

The model is calibrated to match the AIS data as of February 2016 and simulated to trace the full evolution of U.S.-bound shipping from March 2016 to March 2025. This simulation perfectly fits our targeted moments: shipping productivity ratios, potential supply by route, sailing speeds, and import shares (Section 5).

We leverage the calibrated model to quantify the welfare costs of two major disruption episodes (Section 6). For the 2021 West Coast port congestion, we construct a counterfactual in which shipping productivity along the Asia-West Coast route remains fixed at its February 2016 baseline. We find that, absent congestion, effective shipping supply would have been 58% higher at the end of 2021. Imports from Asia would have reached 11.6% of GDP (compared to the observed 9%), and the retail price of Asian goods would have fallen by more than 16% (driving a 1.7% decrease in the aggregate price index). Measured as an equivalent variation, the welfare cost of the 2021 disruptions amounted to 1.3% of GDP.

For the 2024 Houthi attacks, a similar counterfactual—holding shipping productivity on the Asia-Suez and Middle East routes at their pre-disruption levels—reveals that avoiding the Cape of Good Hope rerouting would have raised effective shipping supply by 18% in May 2024. This would have increased the import share by 0.5 percentage points and reduced retail prices by 0.6%. Between March 2024 and March 2025, the welfare cost of the Red Sea crisis amounted

to 0.6% of GDP. The disparity in aggregate impact between these two episodes reflects, in part, the mitigating role of the U.S. Navy. In response to the attacks, U.S. destroyers were deployed to intercept projectiles targeting commercial vessels. By constructing a counterfactual where shipping productivity continued to deteriorate at its March 2024 pace throughout 2025 (Section 6.4), we estimate the value of this military intervention at 0.2% of GDP.

The final set of results evaluates port infrastructure improvements and trade policy (Sections 7 and 8). We introduce port fees and tariffs into the model to study their interaction with shipping congestion and market power. Our primary finding is that tariffs are *not* universally welfare-reducing in this environment. When tariffs on Asian goods suppress import demand, shipping firms reallocate capacity away from Asian routes, thereby alleviating congestion. This "decongestion effect" acts as a productivity boost that lowers shipping prices and expands retail supply, potentially more than offsetting the direct price effect of the tariff on consumers.

In our baseline calibration matched to March 2025 data, an 18% tariff on Asian goods increases consumer welfare by 1.3% of income, generates 0.9% of GDP in tariff revenue, and lowers the retail prices of imported goods by 3%. However, this result is highly sensitive to the underlying congestion regime and the degree of retail market power. If the congestion externality is increased by 50%—mimicking a severely bottlenecked environment—tariffs become welfare-reducing, costing the economy 0.5% of output. Similarly, if retailers wield greater market power (e.g., raising the retail markup from 25% to 50%), the tariff pass-through to consumer prices dominates the decongestion effect, leaving consumers worse off. Ultimately, a global 10% tariff applied uniformly across all origins is welfare-superior to an 18% tariff levied solely on Asian goods, delivering equivalent revenue with a sharper reduction in retail prices.

Related literature. This paper connects to four main strands of literature. First, foundational work studies the global shipping market, emphasizing sluggish capacity responses due to long shipbuilding lead times (Stopford, 2008, Kalouptsidi, 2014, Greenwood and Hanson, 2015, Dunn and Leibovici, 2023). Relatedly, growing research characterizes how search frictions, transportation rigidities, and market structure shape trade costs and supply chain dynamics (Brancaccio et al., 2020, 2024, 2025, Ganapati et al., 2024). We depart from this literature by focusing squarely on the *intensive* margin of shipping supply—how existing fleets are dynamically deployed, loaded, and operated—demonstrating that this margin dominates during acute disruptions.

Second, we build on research exploring the endogenous determinants of international shipping costs and their role in shaping trade patterns (Limão and Venables, 2001, Hummels and Skiba, 2004, Coşar and Demir, 2018, Asturias, 2020, Wong, 2022). By explicitly modeling route-specific congestion externalities, we provide a mechanism for how transportation costs fluctuate endogenously in response to macroeconomic shocks and trade policy.

Third, we contribute to the literature on the macroeconomic effects of recent supply chain disruptions (Alessandria et al., 2023, Bai et al., 2024), including their inflationary impacts (Carrière-Swallow et al., 2023, Isaacson and Rubinton, 2023), the Red Sea crisis (Notteboom et al., 2024), and environmental speed adjustments (Lugovskyy et al., 2025). We advance this literature by integrating granular vessel micro-data into a structural general equilibrium model to quantify the welfare costs of specific disruptions and evaluate counterfactual trade policies.

Finally, our results speak to the economics of trade policy and port pricing amid transportation frictions. While empirical work documents the macroeconomic fallout and supply chain reconfiguration caused by recent tariff escalations (Amiti et al., 2019, Fajgelbaum et al., 2020), we demonstrate that tariffs can inadvertently act as a Pigouvian corrective to shipping congestion externalities. This mechanism connects our findings to the transportation literature on optimal port pricing (Strandenes and Marlow, 2000, De Borger et al., 2011). By bridging these fields, our framework provides a rigorous basis for evaluating how unilateral trade policies and port fees interact with global chokepoints and the strategic pricing of shipping monopolies.

The remainder of the paper proceeds as follows. Sections 2 and 3 detail the construction of our dataset and present empirical facts on potential and effective shipping supply. Section 4 develops the general equilibrium model, which is calibrated and simulated over time in Section 5. Section 6 quantifies the aggregate costs of recent shipping disruptions, including the mitigating effects of military interventions and port infrastructure. Section 8 evaluates counterfactual tax and trade policies. Section 9 concludes. The supplemental appendices contain additional results, figures, and analytical derivations.

2. U.S.-BOUND POTENTIAL SHIPPING SUPPLY

We begin by quantifying the evolution of potential shipping supply to the U.S. using high-frequency satellite data on ship movements. Potential supply refers to the shipping services that could be delivered in the absence of disruptions—the theoretical upper bound assuming vessels operate at full efficiency. It is measured in metric tons or ton-miles, the latter representing the transportation of one metric ton of goods over a distance of one nautical mile (Stopford, 2008). Using vessel-tracking data matched with ship characteristics, we construct route-level measures of potential shipping supply between January 2016 and March 2025. These measures capture the structural aggregate supply of container shipping available to U.S. importers and provide the capacity frontier against which we later measure the efficiency losses from disruptions.

A critical aspect of our approach is the choice of ton-miles as the metric for shipping supply. This reliance on ton-miles is widely acknowledged in the maritime economics literature as the

most accurate method for quantifying the provision of transport services.[1] This metric captures not only the weight of the goods transported but also the distance over which they are moved. Distance is particularly important because it directly influences the time and resources required for transportation.[2]

Consequently, incorporating distance into the ton-mile metric naturally links potential supply to the speed and duration of transport. Since the rate at which vessels complete trips determines how frequently their capacity can be reused, a static measure in tons fails to capture the flow of services the fleet can provide. By defining potential supply in ton-miles based on a benchmark for maximum efficiency, we can isolate the fleet's physical carrying capacity from operational disruptions and the resulting vessel slowdowns. This is why the ton-mile metric is essential: it provides a consistent measure of the fleet's maximum service capability, independent of the transient disturbances and delays that determine effective supply.

2.1. *Data*

Our empirical analysis relies on two primary data sources. The first data source is the Automatic Identification System (AIS). Beginning in 2005, the International Maritime Organization (IMO) has mandated ships of 300 gross tonnage and above engaged in international voyages to carry an AIS transponder capable of automatically transmitting vessel information to other ships and coastal authorities. The AIS provides high-frequency signals on vessel identity (IMO ship identification number), coordinates, and speed. It updates navigational data as frequently as every two seconds and can produce more than 2,000 reports per minute per vessel. We focus on container ships since they are the main mode of transportation for manufactured goods.[3]

The second data source is the Lloyd's List vessel registry, which provides detailed ship-level characteristics, including deadweight tonnage (DWT) and ownership. We match AIS trajectories to vessel characteristics to obtain a complete picture of ship deployments to the U.S. around the world.

[1] Seminal works by Tinbergen (1934) and Koopmans (1939) established the ton-mile as the fundamental unit of market equilibrium. Modern econometric models, such as the Norbulk model by Wergeland (1981) and the standard framework by Stopford (2008), explicitly define fleet productivity and supply capacity in ton-miles to account for the spatial dimension of trade.

[2] For instance, moving 10,000 tons of cargo 5,000 nautical miles demands significantly more shipping capacity than moving the same cargo 500 nautical miles.

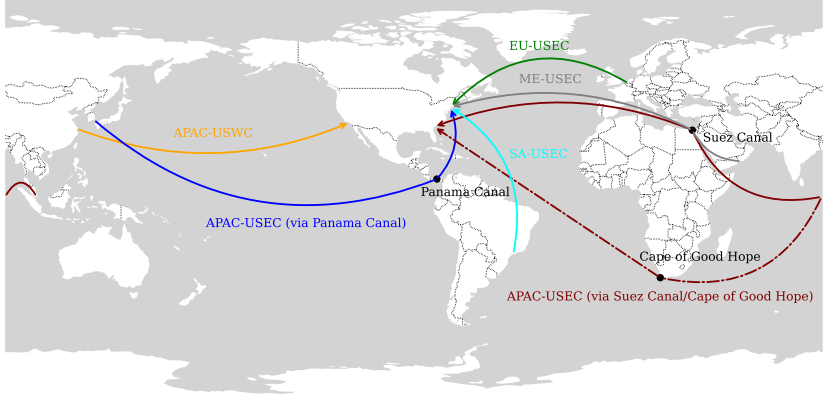
[3] Dry bulk shipping transports bulk commodities such as iron ore, coal, and grain, and oil tankers transport oil. The shares of these segments in world fleet capacity in 2024 were 43% and 28%, respectively. The remaining 30% of world fleet capacity comprises container ships and other general cargo ships (UNCTAD, 2024). In the U.S., container shipping carries more tonnage (nearly one billion short tons) and value (more than 0.7 trillion dollars) than any other transport mode, representing over 50% of U.S. trade by weight and roughly 30% by value (Bureau of Transportation Statistics, 2021). Although some high-value items, such as computer chips, are shipped by air, these products depend on other components, such as motherboards or hard drives, that are transported by container ship.

The combination of the different data sources enables us to reconstruct the full population of container-ship voyages arriving at U.S. ports, matched to ship-level characteristics, starting from January 2016—when AIS data became comprehensive enough to cover the entire globe—through March 2025. In our benchmark analysis, we work with data at a weekly frequency unless otherwise stated.

2.2. *Routes and trips*

We classify vessel trips into six major U.S.-bound trade routes, reflecting geographical origin, destination, and shipping path. The six routes are: (1) Asia-Pacific to the U.S. West Coast (APAC–USWC); (2) Asia-Pacific to the U.S. East Coast (APAC–USEC) via the Panama Canal; (3) Asia-Pacific to the U.S. East Coast via the Suez Canal or the Cape of Good Hope; (4) Europe to the U.S. East Coast (EU–USEC); (5) the Middle East to the U.S. East Coast (ME–USEC); and (6) South America to the U.S. East Coast (SA–USEC).[4] Figure 2.1 plots these six trade routes on a world map. Together, these routes represent roughly 80–90 percent of all U.S. containerized maritime imports, ensuring that focusing on them captures the bulk of U.S.-bound maritime shipping dynamics.

FIGURE 2.1.—Major U.S.-bound trade routes



Note: The figure illustrates the approximate trajectories of the six major trade routes that carry the vast majority of U.S.-bound containerized maritime imports.

Unlike dry bulk vessels or tankers, container ships typically operate on fixed service loops connecting predetermined sets of origin and destination ports.[5] To distinguish U.S. inbound

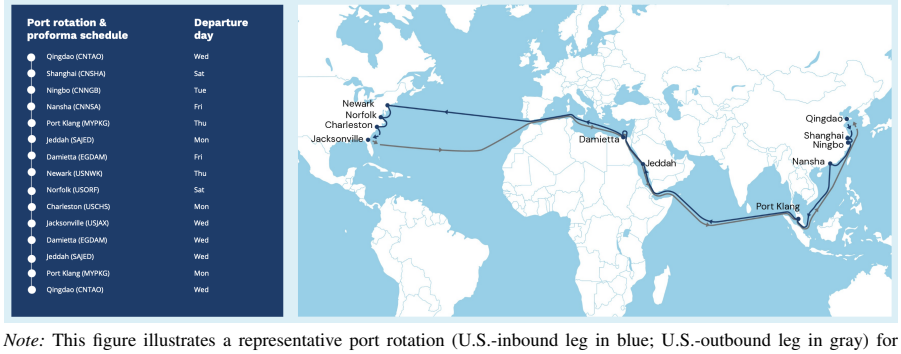
[4]For the third route, we combine the Suez Canal and Cape of Good Hope paths because the latter primarily serves as a substitute for the former, utilized during disruptions.

[5]As Brancaccio et al. (2020, p.2) explain: "The transportation sector … can be split into two categories: those that operate on fixed itineraries, much like buses, and those that operate on flexible routes, much like taxis. Container ships … belong to the first group."

from outbound trips, we define a trip as the journey that begins when a vessel departs its last port in the foreign region of origin—Asia-Pacific, Europe, the Middle East, or South America—and ends upon its arrival at the first port on either the U.S. East Coast or West Coast, possibly after several intermediate port calls.[6] Consequently, when a vessel's itinerary includes stops in multiple foreign regions, we record a separate trip for each region. This granularity enables us to focus on shipping dynamics along the intercontinental legs of vessels' service loops, while minimizing the influence of domestic and within-region movements on the measurement of shipping services provided to the U.S.[7]

Figure 2.2 illustrates this dynamic using a representative round trip between Asia-Pacific and the U.S. East Coast via the Suez Canal. During the voyage, the vessel visits multiple ports with recorded departures on weekdays. Specifically, the ship departs from Port Klang, Malaysia (Asia-Pacific) and later Jeddah, Saudi Arabia (Middle East) before terminating at Newark (U.S. East Coast). Consequently, this single voyage is classified as serving both the APAC–USEC via Suez route and the ME–USEC route.[8]

FIGURE 2.2.—Representative service loop: Asia-Pacific to U.S. East Coast via Suez



Note: This figure illustrates a representative port rotation (U.S.-inbound leg in blue; U.S.-outbound leg in gray) for a container service connecting the Asia-Pacific and Middle East regions to the U.S. East Coast via the Suez Canal. The route follows a fixed sequence of port calls—beginning in East Asia (Qingdao, Shanghai, Ningbo, and Nansha), continuing through Southeast Asia (Port Klang) and the Middle East (Jeddah), and stopping at Damietta in Egypt before reaching U.S. East Coast ports (Newark, Norfolk, Charleston, and Jacksonville). The vessel subsequently returns to Asia to complete the round trip. The schedule on the left reports the pro forma departure day at each port along the service loop. *Source:* SeaLead.

Table 2.1 summarizes the main destinations and origin ports in our sample, along with the routes they follow and the share of trips they represent during the period 2016-2025. The sample includes a total of 280 unique ports, each of which serves as either the first U.S. arrival port

[6] A port call refers to the arrival of a ship at a port where it docks to load and unload cargo.

[7] Extending the analysis to cover within-region legs or additional U.S.-bound routes (e.g., SA–USWC) is feasible but computationally intensive.

[8] A key limitation of AIS-based shipping data is the inability to track cargo origins and destinations, preventing precise measurement of cargo flows on individual routes. The integration of AIS records with U.S. bills of lading offers a promising avenue for overcoming this limitation; this is left for future research.

or the last foreign-origin port. The principal arrival ports in the U.S. are Newark and Savannah on the East Coast, and Los Angeles and Long Beach on the West Coast. The primary origin ports in the Asia-Pacific region are Busan in South Korea, and Shanghai, Yantian, and Ningbo-Zhoushan in China. In Europe, key origin ports include Valencia in Spain, Bremerhaven in Germany, and Le Havre in France. In the Middle East, Salalah in Oman serves as a major origin port, while in South America, Cartagena in Colombia is the primary origin port.

TABLE 2.1

KEY PORTS AND U.S.-BOUND TRADE ROUTES

Rank	Destination Port	Trips (%)	Rank	Origin Port	Trips (%)	Major Routes
1	Newark, NJ	19.6	1	Busan, South Korea	19.3	APAC-USWC, APAC-USEC (Panama)
2	Los Angeles, CA	11.4	2	Cartagena, Colombia	9.8	SA-USEC
3	Long Beach, CA	9.0	3	Shanghai, China	6.8	APAC-USWC, APAC-USEC (Panama)
4	Savannah, GA	5.3	4	Yantian, China	5.5	APAC-USWC, APAC-USEC (Panama)
5	Fort Lauderdale, FL	4.3	5	Ningbo-Zhoushan, China	4.8	APAC-USWC, APAC-USEC (Panama)
6	Seattle, WA	4.0	6	Valencia, Spain	4.6	EU-USEC
7	Tacoma, WA	3.9	7	Bremerhaven, Germany	3.5	EU-USEC
8	Houston, TX	3.8	8	Le Havre, France	3.0	EU-USEC
9	Miami, FL	3.6	9	Colombo, Sri Lanka	2.6	APAC-USEC (Suez/Cape)
10	Philadelphia, PA	2.7	10	Tokyo, Japan	2.4	APAC-USWC, APAC-USEC (Panama)
11	Charleston, SC	2.7	11	Yokohama, Japan	2.2	APAC-USWC
12	New York, NY	1.6	12	Kaohsiung, Taiwan	1.9	APAC-USWC, APAC-USEC (Panama)
13	Norfolk, VA	1.4	13	Santa Marta, Colombia	1.8	SA-USEC
14	Oakland, CA	1.3	14	Singapore, Singapore	1.7	APAC-USEC (Suez/Cape)
15	Portsmouth, VA	1.2	15	Point Lisas, Trinidad & Tobago	1.5	SA-USEC
16	Boston, MA	0.9	16	Antwerp, Belgium	1.5	EU-USEC
17	Chester, PA	0.9	17	Mundra, India	1.5	APAC-USEC (Suez/Cape)
18	Palm Beach, FL	0.6	18	St Georges, Grenada	1.4	SA-USEC
19	Mobile, AL	0.6	19	Melbourne, Australia	1.3	APAC-USEC (Panama), APAC-USWC
20	New Orleans, LA	0.4	20	Xiamen, China	1.3	APAC-USWC

Note: The table summarizes key ports along the major U.S.-bound routes. The third column shows the percentage of total container ship trips to each destination port listed in the second column during the sample period 2016-2025. Similarly, the sixth column presents the percentage of total trips originating from each origin port listed in the fifth column during the same period. The final column highlights the major routes on which trips depart from the respective origin ports and arrive at the U.S.

2.3. *Potential shipping supply*

We characterize potential shipping supply using two parallel metrics. First, the potential shipping supply in *metric tons* corresponds to the total DWT of container ships along a route. DWT represents the maximum weight of cargo a container ship can carry, serving as a proxy for the vessel's physical shipping capacity.[9] The potential supply in tons is defined as the sum

[9]We use DWT as the measure of shipping capacity because it reflects the weight of cargo a ship can carry, which is integral to calculating ton-miles. In contrast, Dunn and Leibovici (2023) measure shipping capacity using the total number of container ships and their capacity in TEUs, which focuses on the volume of cargo carried by the ships.

of the shipping capacity of all container ships i operating on route r during week t:

$$\texttt{Potential Supply}^{\text{tons}}_{r,t} = \sum_{i \in \boldsymbol{\mathcal{I}}_t} \mathbf{1}_{i,r,t} \times \texttt{DWT}_i, \tag{2.1}$$

where $\boldsymbol{\mathcal{I}}_t$ denotes the set of active container ships in week t (defined as vessels recording at least one AIS signal), and $\mathbf{1}_{i,r,t}$ is an indicator variable equal to one if ship i operates on route r in week t, and zero otherwise.

Reflecting the importance of distance discussed earlier, we define the potential shipping supply in *ton-miles* as the product of total DWT and the potential distance vessels could travel in one week, assuming they operate at the maximum speed observed over the sample period ($\boldsymbol{\mathcal{T}}$):

$$\begin{aligned} &\texttt{Potential Supply}^{\text{ton-miles}}_{r,t} \\ &= \texttt{Potential Supply}^{\text{tons}}_{r,t} \times \underbrace{\left(\max_{t \in \boldsymbol{\mathcal{T}}} \left\{ \overline{\texttt{Speed}}_{r,t} \right\} \times 24\,\text{hours} \times 7\,\text{days} \right)}_{\text{potential distance}}, \end{aligned} \tag{2.2}$$

where $\overline{\texttt{Speed}}_{r,t}$ is the DWT-weighted average vessel speed along route r for a given week t:

$$\overline{\texttt{Speed}}_{r,t} = \sum_{i \in \boldsymbol{\mathcal{I}}_t} \left(\frac{\mathbf{1}_{i,r,t} \times \texttt{DWT}_i}{\sum_{i \in \boldsymbol{\mathcal{I}}_t} \mathbf{1}_{i,r,t} \times \texttt{DWT}_i} \right) \times \texttt{Speed}_{i,t}. \tag{2.3}$$

Here, $\texttt{Speed}_{i,t}$ represents the average speed of vessel i in week t, calculated as the arithmetic mean of the vessel's AIS speed measurements. By using the maximum observed speed, we establish a technological upper bound for delivery speed, ensuring that our measure of potential supply reflects the fleet's feasible carrying capacity independent of transient operational slowdowns.

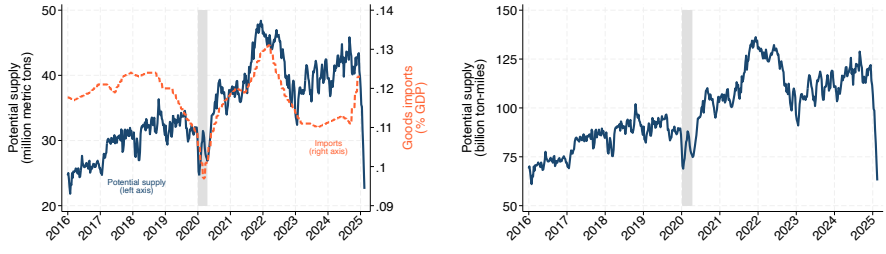
2.4. *Evolution of U.S.-bound potential shipping supply*

Aggregate trends. We now examine the evolution of aggregate U.S.-bound potential shipping supply. To do so, we calculate the number of container ships serving each U.S.-bound route and the corresponding potential supply in both tons and ton-miles—using Equations (2.1) and (2.2)—and aggregate these measures across all routes. We employ this simple aggregation to ensure direct comparability with the aggregate U.S.-bound effective shipping supply, which is

calculated later in the section by summing the effective supply for each individual U.S.-bound route after accounting for various shipping disruptions.[10]

Panel 2.3a plots the aggregate potential supply in tons. From early 2016 onward, the total DWT of U.S.-bound ships increased steadily, averaging approximately 30 million metric tons immediately prior to the COVID-19 pandemic. Following the onset of the pandemic, potential supply surged by more than 60 percent, reaching 48 million metric tons in January 2022. This sharp expansion reflects both the entry of new firms and the redeployment of vessels from other regions to capitalize on historically high freight rates on American routes.[11] However, starting in mid-2022, supply dynamics shifted from expansion to the management of volatility and contingencies arising from the pandemic. Total DWT contracted sharply from its peak, reverting to near pre-pandemic levels by early 2023 as import demand normalized. This decline proved temporary, however, as potential supply rebounded and remained elevated relative to the 2016-2019 baseline toward the end of 2024, indicating that shipping capacity had stabilized at a structurally higher level. Finally, starting in early 2025, potential supply plunged significantly, foreshadowing the U.S.-China trade war.

FIGURE 2.3.—U.S.-bound potential shipping supply, 2016-2025



(a) Potential supply (tons) (b) Potential supply (ton-miles)

Note: Panel 2.3a shows the aggregate potential shipping supply in million metric tons (left axis) and U.S. goods imports as a share of GDP (right axis). Panel 2.3b plots the potential supply in billion ton-miles. The shaded area indicates recessions.

Panel 2.3b presents the potential shipping supply in ton-miles. Because this metric relies on a constant reference speed—specifically, the maximum DWT-weighted average vessel speed observed along each route—its dynamics follow a trajectory identical to that of potential supply in tons. Potential supply averaged slightly more than 80 billion ton-miles prior to the pandemic,

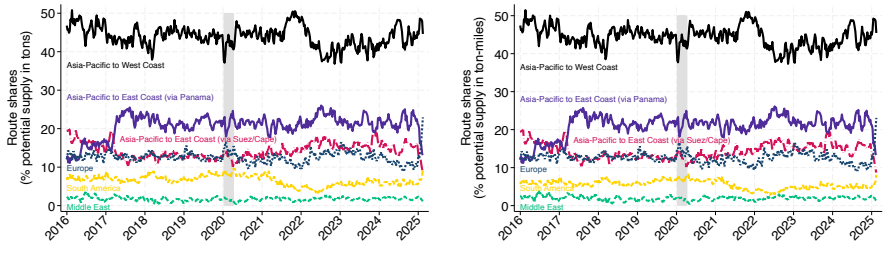
[10] We acknowledge that simply aggregating vessel DWT and ton-miles across routes may overstate the potential supply because a single vessel can serve multiple routes (as noted in Section 2.2). To address this issue, we present the aggregate total DWT and potential ton-miles using the set of unique container ships operating on U.S.-bound routes in Figure A.1 of Appendix A. Despite slight differences in magnitude, the dynamics of the potential shipping supply remain essentially the same as those presented in Figure 2.3.

[11] Africa and Latin America and the Caribbean were most affected by this redeployment, losing 12.4 percent and 13.5 percent of their respective direct liner shipping connections between late 2020 and mid-2022 (UNCTAD, 2022).

surged to a peak of 135 billion ton-miles in early 2022, and stabilized at approximately 110 billion ton-miles in 2023-2024, before plummeting to below 70 billion ton-miles by the end of the sample period. These fluctuations in aggregate capacity were mirrored by changes in the number of container ships serving U.S. ports, which followed a comparable cycle of expansion, stabilization, and contraction.[12]

Variation by route. The expansion of shipping supply was uneven across routes. The largest increase occurred on the APAC–USWC route, which absorbed the majority of new capacity after 2020. This route was the primary target for new market entrants and the main beneficiary of incumbent firms redeploying vessels from other regions—in particular, Africa, Latin America, and the Caribbean.[13] As shown in Panel 2.4a, this surge altered the composition of U.S.-bound shipping capacity, heavily skewing potential supply toward the West Coast.

FIGURE 2.4.—U.S.-bound potential shipping supply across routes, 2016-2025



(a) Potential supply (tons) (b) Potential supply (ton-miles)

Note: Panel 2.4a shows the share of U.S.-bound potential shipping supply in metric tons accounted for by each route. Panel 2.4b plots the corresponding shares in ton-miles. The shaded area indicates recessions.

Potential supply in ton-miles followed a virtually identical trajectory (Panel 2.4b). Since the reference speed for each route is held constant, variations in potential ton-miles are driven exclusively by changes in deployed tonnage. Consequently, the APAC–USWC route was the primary driver of the aggregate expansion in potential ton-miles, reflecting the massive injection of physical capacity onto this trade lane.

Although less visible in the plots, potential shipping supply from Asia-Pacific to the East Coast (via either Panama or Suez/Cape) also expanded, but the increase materialized gradually,

[12]We present the time series for the number of U.S.-bound container ships in Figure A.2 of Appendix A. The weekly number rose from approximately 360 in the pre-pandemic period to a peak of 550 in early 2022, before correcting in 2023.

[13]See UNCTAD (2022). By the end of 2021, the APAC–USWC route accounted for roughly half of the total potential supply in tons deployed on U.S.-bound routes—an increase of approximately 6 percentage points from early-2020 levels.

peaking toward the end of 2022.[14] Similar patterns emerged on the EU–USEC and ME–USEC routes. In contrast, the SA–USEC route experienced a prolonged and substantial decline in shipping capacity from early 2021 to mid-2022, as Latin America and the Caribbean lost connectivity when shipping lines reassigned vessels to the Asia–U.S. routes.

The preference for the APAC–USWC route reflects its shorter sailing distance. Before the pandemic, shipments from Asia-Pacific to the West Coast averaged 2.2 weeks, compared with approximately four weeks for shipments from Asia to the East Coast (and slightly longer when transiting through the Panama Canal rather than Suez).[15] This shorter duration allowed carriers to maximize the turnover of their fleet, incentivizing the concentration of potential supply on the West Coast during the period of peak demand.

3. Disruptions and Effective Shipping Supply

While potential shipping capacity surged after 2020, not all of it translated into effective service. Port congestion, bottlenecks at the Panama and Suez Canals, and rerouting around conflict zones severely constrained the supply available to U.S. importers. These disruptions operated through two primary channels: directly removing capacity from the market by stalling vessels at ports or canals, and reducing fleet efficiency by forcing ships to travel longer distances or sail at suboptimal speeds.

To quantify the actual provision of shipping services, we define effective shipping supply as the residual capacity remaining after accounting for these operational frictions. Formally, we express effective supply in ton-miles as:

$$\begin{aligned}\texttt{Effective Supply}_{r,t}^{\text{ton-miles}} = \texttt{Potential Supply}_{r,t}^{\text{ton-miles}} \\ - \texttt{Port Congestion}_{r,t}^{\text{ton-miles}} - \texttt{Canal Congestion}_{r,t}^{\text{ton-miles}} \\ - \texttt{Rerouting}_{r,t}^{\text{ton-miles}} - \texttt{Vessel Slowdown}_{r,t}^{\text{ton-miles}}.\end{aligned} \tag{3.1}$$

In this framework, effective supply represents the flow of shipping services that actually cleared the market. The negative terms on the right-hand side represent distinct "wedges" of lost capacity. In the remainder of this section, we define and quantify each of these disruption factors in turn, before aggregating them to construct the final measure of effective supply.

[14] This delayed adjustment reflects both operational and economic frictions: rerouting vessels to the East Coast required longer sailing distances, higher fuel costs, and more time to reposition fleets. Carriers therefore concentrated new and redeployed capacity first on the shorter and more profitable APAC–USWC route (Notteboom et al., 2022).

[15] For shipments originating in Europe, the Middle East, and South America, the pre-pandemic average durations were roughly 1.7, 2.9, and 1.3 weeks, respectively.

3.1. *Port congestion*

We develop a measure of port congestion based on AIS records of vessel speed and port anchorage duration. Port congestion occurs when ships must wait in the anchorage area of a port until a berth becomes available for docking (Bai et al., 2024). In an ideal scenario, ships proceed directly to a berth upon a port call. In practice, however, disruptions —ranging from labor shortages and inland transport delays to surges in import demand— force vessels to queue at anchor, effectively reducing the actual supply of shipping capacity.

To quantify this disruption, we measure the total ton-miles lost due to anchorage delays for U.S.-bound voyages on each route at a weekly frequency. First, we map the geographical boundaries of berth and anchorage areas for all container ports worldwide.[16] Next, for each port call, we calculate the total duration the vessel spends in the identified anchorage area. We attribute the full duration of this wait to the week in which the port call began. Let $\texttt{Port Waiting Time}_{i,p,r,t}$ denote the total hours vessel i spends in anchorage at port p during a port call initiated in week t while on a trip along route r.

To convert this waiting time into foregone nautical miles, we assume that in the absence of congestion, the vessel would have been traveling at the route's average operating speed. We therefore multiply the anchorage duration by the DWT-weighted average speed of all vessels on route r in week t —captured by $\overline{\texttt{Speed}}_{r,t}$ in Equation (2.3)— and then by the vessel's deadweight tonnage, yielding our measure of port congestion in ton-miles:

$$\begin{aligned}&\texttt{Port Congestion}^{\text{ton-miles}}_{r,t} \\ &= \sum_{i \in \boldsymbol{\mathcal{I}}_t} \mathbf{1}_{i,r,t} \times \underbrace{\texttt{DWT}_i}_{\text{tonnage}} \times \underbrace{\left(\overline{\texttt{Speed}}_{r,t} \times \sum_{p \in \boldsymbol{\mathcal{P}}_{i,r,t}} \texttt{Port Waiting Time}_{i,p,r,t} \right)}_{\text{foregone distance}},\end{aligned} \tag{3.2}$$

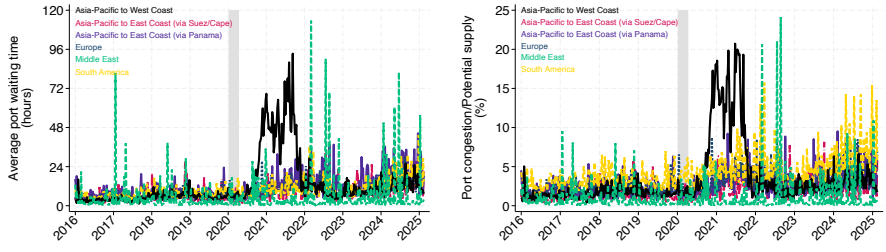
where $\boldsymbol{\mathcal{P}}_{i,r,t}$ denotes the set of port calls initiated by vessel i along route r in week t, and $\boldsymbol{\mathcal{I}}_t$ is the set of active container ships in week t.

Panel 3.1a shows the average waiting time spent at port anchorages. Across all routes, ships spent an average of roughly 6 hours at anchor prior to the pandemic. Driven by a surge in consumer demand and pandemic-related labor shortages at the Ports of Los Angeles and Long Beach, average waiting times along the APAC–USWC route exceeded 60 hours throughout the summer and fall of 2021. As bottlenecks intensified on the West Coast while nationwide demand remained elevated, shipping companies redirected capacity toward East Coast

[16] We use AIS data along with the IMA-DBSCAN (Iterative Multi-Attribute Density-Based Spatial Clustering of Applications with Noise) algorithm to accomplish this task. See Bai et al. (2023) for further details.

ports. This reallocation produced a distinct substitution pattern: congestion began to ease on the APAC–USWC route while simultaneously intensifying on the East Coast. The ME–USEC route, in particular, experienced severe delays, with average anchorage times peaking above 80 hours in specific weeks.

FIGURE 3.1.—Port congestion across routes, 2016-2025



(a) Average port waiting time (b) Port congestion/Potential supply

Note: Panel 3.1a shows the DWT-weighted average port waiting time, while Panel 3.1b plots port congestion, measured as a fraction of potential shipping supply in ton-miles, for each U.S.-bound route. The shaded area indicates recessions.

To evaluate the impact of port congestion on potential supply, Panel 3.1b plots our measure of port congestion as a fraction of potential supply in ton-miles. As shown, port congestion reduced shipping capacity along the APAC–USWC route by as much as one-fifth of the potential capacity deployed on that route in 2021, indicating substantial efficiency losses. The impact was similarly severe on the East Coast; specifically, congestion on the ME–USEC route spiked to absorb nearly a quarter of potential supply during the peak of the bottlenecks in late 2022.

3.2. *Canal congestion*

Similar to port congestion, bottlenecks at the Suez and Panama Canals can restrict shipping supply. We quantify these disruptions by monitoring vessel movements within the canal zones, identifying periods where ships are effectively stalled and delayed. This allows us to calculate the aggregate ton-miles lost due to queuing at these critical chokepoints.

First, we delineate the geographical boundaries of the Suez and Panama Canals using polygons. Within these boundaries, we identify all vessel transits and extract the sequence of AIS signals broadcast by each vessel. For every pair of consecutive AIS signals, we calculate the time elapsed, the distance traveled, and the resulting speed of the vessel over that interval.

To measure congestion, we isolate specific intervals where a vessel is effectively stationary or moving significantly below normal transit speeds due to canal bottlenecks. Specifically, we filter for intervals where the vessel's speed is one knot or less. For these delayed intervals, we calculate the foregone distance —the distance the vessel would have traveled if it had been

moving at the route's benchmark speed, minus the distance it actually traveled. The benchmark speed, $\overline{\texttt{Speed}}_{r,t}$, is defined as the DWT-weighted average speed of all vessels on route r in week t. Note that, in the calculation of port congestion (Equation (3.2)), we do not subtract the distance the vessel actually traveled while in port anchorages since vessels are mostly stationary with a speed of zero; however, in the canal calculation, we account for the fact that "waiting" vessels may still move slowly through the canal in queues.

The total canal congestion is obtained by multiplying this foregone distance by the vessel's deadweight tonnage and summing across all valid intervals for all ships on the route:

$$\texttt{Canal Congestion}_{r,t}^{\text{ton-miles}} \tag{3.3}$$
$$= \sum_{i \in \mathcal{I}_t} \mathbf{1}_{i,r,t} \times \underbrace{\texttt{DWT}_i}_{\text{tonnage}} \times \underbrace{\left[\sum_{k \in \mathcal{K}_{i,r,t}} \mathbf{1}_{\texttt{Speed}_{i,k} \leq 1} \times \left(\overline{\texttt{Speed}}_{r,t} - \texttt{Speed}_{i,k} \right) \times \tau_{i,k} \right]}_{\text{foregone distance}},$$

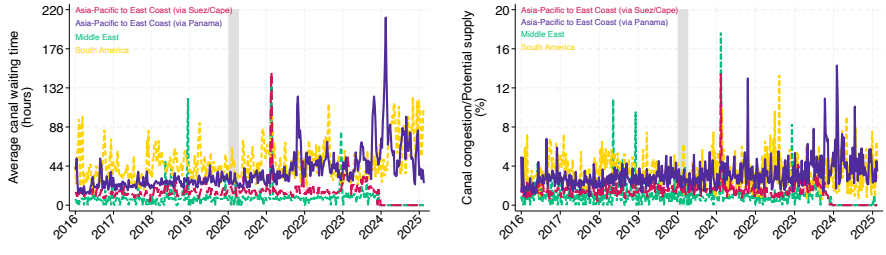
where $\mathcal{K}_{i,r,t}$ represents the set of time intervals between consecutive AIS signals for vessel i while within the boundaries of the Suez or Panama Canal during a trip along route r in week t. For each interval k, $\tau_{i,k}$ denotes the duration in hours, and $\texttt{Speed}_{i,k}$ denotes the vessel's observed speed. The indicator function $\mathbf{1}_{\texttt{Speed}_{i,k} \leq 1}$ ensures that we only aggregate foregone ton-miles during periods where the vessel was effectively stalled.

Panel 3.2a shows the average waiting time at the Suez and Panama Canals for routes from Asia-Pacific, the Middle East, and South America to the U.S. East Coast.[17] In the pre-pandemic period, ships spent modest time queuing at the Suez and Panama canals, averaging 11 and 34 hours, respectively. Since then, congestion patterns at the two bottlenecks have diverged. The Suez Canal experienced two notable but short-lived spikes: one in March 2021, corresponding to the blockage caused by the container ship *Ever Given*, and another in January 2023, when the bulk carrier *M/V Glory* ran aground due to technical failure (though it was quickly refloated, causing only minor delays). Additionally, since the beginning of 2024, geopolitical unrest in the Red Sea has led many shipping companies to divert vessels to the longer route around the Cape of Good Hope (see Figure 3.3 below). This rerouting reduced traffic through the Suez Canal, effectively dropping waiting times to zero. Conversely, average waiting times at the Panama Canal have been on an upward trajectory since 2023, particularly for the APAC–USEC route. This trend reflects reduced transit capacity caused by severe drought conditions and aggravated by the onset of El Niño.

[17] Delays at these chokepoints are not relevant for the APAC-USWC and EU-USEC routes, as these services rely on direct trans-Pacific or trans-Atlantic connections.

Panel 3.2b plots canal congestion as a fraction of potential shipping supply (in ton-miles) across different routes. As shown, congestion at the Suez Canal accounted for less than two percent of the potential capacity deployed on the APAC–USEC (via Suez/Cape) and ME–USEC routes for most of the sample period —with the exception of several short-lived spikes— until most recently, when the number dropped to zero as the Red Sea crisis escalated. In contrast, the capacity loss from the 2023–24 drought and El Niño at the Panama Canal was more sustained, absorbing more than four percent of potential supply on the APAC–USEC and SA–USEC routes.

FIGURE 3.2.—Canal congestion across routes, 2016-2025



(a) Average canal waiting time (b) Canal congestion/Potential supply

Note: Panel 3.2a shows the DWT-weighted average canal waiting time, while Panel 3.2b plots our measure of canal congestion as a fraction of potential supply (in ton-miles) for each U.S.-bound route. The shaded area indicates recessions.

3.3. *Rerouting*

We now focus on rerouting episodes that forced vessels to divert from their planned course to a longer and/or costlier alternative to reach U.S. ports. Often in response to changing market conditions or major external events such as the Red Sea crisis in 2024, these route diversions can add significant costs to the provision of shipping services.

Using AIS tracking data, we first group trips taken by container ships along each U.S.-bound route according to their origin-destination (o-d) port pairs. We specifically focus on trade routes that historically exhibit multiple routing options (e.g., both Suez and Cape of Good Hope).[18] Under normal operating conditions, vessels typically traverse the shortest available path to minimize fuel consumption and transit time. Therefore, for each o-d pair, we identify the trip with the shortest travel distance and use the shipping trajectory of the corresponding vessel as the benchmark. Let $\texttt{Min Distance}_{o,d,r}$ represent the shortest trip distance between origin o and destination d along route r.

[18]This ensures that the measured deviations reflect significant strategic rerouting decisions rather than minor navigational adjustments on a single fixed route.

Accordingly, we classify a trip j as rerouted if it deviates from the benchmark trajectory. Let $\texttt{Trip Distance}_{i,j,o,d,r}$ denote vessel i's trip j distance from origin o to destination d along route r, measured in nautical miles. To account for the fact that trips span varying durations, we calculate the intensity of the deviation as a rate. The additional nautical miles accumulated per hour of travel is given by:

$$\texttt{Extra NM/Hour}_{i,j,o,d,r} \equiv \frac{\max\left(0, \texttt{Trip Distance}_{i,j,o,d,r} - \texttt{Min Distance}_{o,d,r}\right)}{\texttt{Trip Duration}_{i,j,o,d,r}},$$

where $\texttt{Trip Duration}_{i,j,o,d,r}$ is the trip duration in hours. We then derive the implied foregone distance over a week by scaling this rate by the duration of a week in hours:

$$\texttt{Weekly Extra NM}_{i,j,o,d,r} \equiv \texttt{Extra NM/Hour}_{i,j,o,d,r} \times 24\,\text{hours} \times 7\,\text{days}.$$

Consequently, our aggregated weekly measure of rerouting in ton-miles is given by:

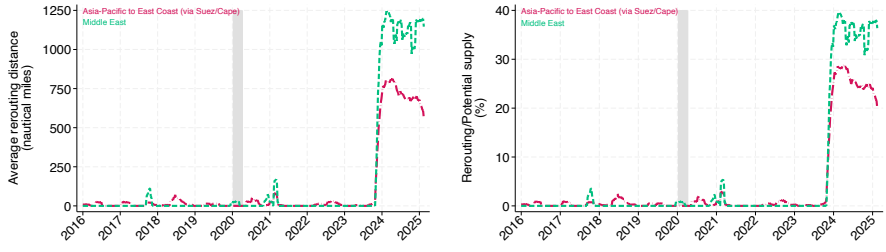
$$\texttt{Rerouting}^{\text{ton-miles}}_{r,t} = \sum_{o\in\boldsymbol{\mathcal{O}}_r}\sum_{d\in\boldsymbol{\mathcal{D}}_r}\sum_{j\in\boldsymbol{\mathcal{J}}_{o,d,r,t}}\sum_{i\in\boldsymbol{\mathcal{I}}_t}\mathbf{1}_{i,j} \times \underbrace{\texttt{DWT}_i}_{\text{tonnage}} \times \underbrace{\texttt{Weekly Extra NM}_{i,j,o,d,r}}_{\text{foregone distance}}, \quad (3.4)$$

where $\boldsymbol{\mathcal{O}}_r$ and $\boldsymbol{\mathcal{D}}_r$ are the sets of origin and destination ports along trade route r. $\boldsymbol{\mathcal{J}}_{o,d,r,t}$ represents the set of rerouted trips between origin o and destination d in route r that overlap with week t, and $\boldsymbol{\mathcal{I}}_t$ is the set of active vessels in week t. $\mathbf{1}_{i,j}$ is an indicator equal to 1 if vessel i performed trip j.

Panel 3.3a illustrates the average additional distance in nautical miles incurred by vessels rerouting on trade lanes that typically traverse the Suez Canal. While the March 2021 Suez blockage caused negligible route deviations, the Red Sea crisis beginning in early 2024 precipitated a sustained structural shift in routing behavior. The strategic diversion of vessels around the Cape of Good Hope added between 800 and 1,200 nautical miles to voyages from the Asia-Pacific and Middle East to the U.S. East Coast, significantly increasing both fuel consumption and transit duration.

To quantify the supply-side implications of these longer voyages, Panel 3.3b reports the share of potential supply absorbed by vessel rerouting. The extensive diversions observed in early 2024 effectively consumed a substantial portion of the capacity deployed on the APAC–USEC and ME–USEC routes, accounting for approximately 25 percent and 36 percent of potential supply, respectively.

FIGURE 3.3.—Vessel rerouting, 2016-2025



(a) Average rerouting distance (b) Rerouting/Potential supply

Note: Panel 3.3a shows the DWT-weighted average excess nautical miles traveled relative to the shortest navigable distance for the APAC–USEC (via Suez/Cape) and ME–USEC routes. Panel 3.3b plots the corresponding shares of potential supply (in ton-miles) absorbed by vessel rerouting. The shaded area indicates recessions.

3.4. *Vessel slowdown*

Finally, we account for reductions in shipping supply driven by adjustments in vessel speed. Even when vessels are not stationary at anchor or diverting to longer routes, they may operate below their maximum potential speed —a practice often referred to as "slow steaming"— to economize on fuel or manage arrival times at congested ports.

To quantify this disruption, we measure the gap between the realized fleet speed and the route's technological potential. Using the DWT-weighted average speed $\overline{\texttt{Speed}}_{r,t}$ (as defined in Equation (2.3)), we set the reference speed as the maximum average speed observed on route r over the entire sample period $\mathcal{T}$. The total capacity lost due to vessel slowdown is then calculated as the product of the aggregate deployed tonnage and the distance foregone by sailing below this maximum speed:

$$\begin{aligned}&\texttt{Vessel Slowdown}^{\text{ton-miles}}_{r,t} \\ &= \texttt{Potential Supply}^{\text{tons}}_{r,t} \times \underbrace{\left[\left(\max_{t\in\mathcal{T}}\left\{\overline{\texttt{Speed}}_{r,t}\right\} - \overline{\texttt{Speed}}_{r,t}\right) \times 24\,\text{hours} \times 7\,\text{days}\right]}_{\text{foregone distance}},\end{aligned} \tag{3.5}$$

where $\texttt{Potential Supply}^{\text{tons}}_{r,t}$ denotes the total deadweight tonnage of active vessels on the route (Equation (2.1)). The term in brackets captures the nautical miles lost per week due to operational deceleration.

Panel 3.4a plots the evolution of average vessel speed across the six U.S.-bound routes. The data reveal a structural decline in operating speeds, most pronounced on the major east-west trade lanes. Prior to the pandemic (2016–2019), vessels on the APAC–USWC route averaged approximately 16 knots. This figure dropped sharply during the pandemic, bottoming out near 10 knots in 2022. This sharp deceleration was largely driven by the implementation of a new

virtual queuing system at the Ports of Los Angeles and Long Beach in late 2021.[19] Designed to mitigate safety risks and pollution from congested ships, this system allocated queue positions based on departure time, effectively eliminating the "hurry up and wait" incentive and encouraging vessels to slow steam across the Pacific.

The trend extends beyond the West Coast: average speeds on the EU–USEC route and the APAC-USEC route (via Panama) have also drifted downward, falling from pre-pandemic averages of 14.2 and 15.5 knots, respectively, to approximately 13.5 and 14.5 knots in the recent period. This broad-based deceleration is sustained by rising fuel prices in 2022 and new environmental regulations, such as the IMO's Carbon Intensity Indicator.[20] Although speeds have recovered slightly since mid-2023, they remain structurally lower than pre-pandemic levels across these key corridors.

The deceleration has significant economic implications. Panel 3.4b reports the share of potential supply absorbed by vessel slowdown. On the APAC–USWC route, slow steaming accounted for only about 6 percent of potential capacity prior to the pandemic. However, during the height of the supply chain crisis, it absorbed nearly 40 percent of the potential capacity, acting as a massive supply sink. This efficiency loss is not unique to the Pacific; the EU–USEC route, which operates with a higher baseline of friction, saw the share of capacity absorbed by slowdown rise from roughly 15 percent pre-pandemic to 20 percent more recently.

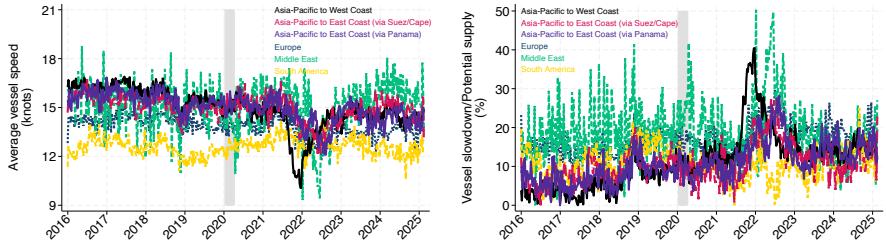
We also observe significant volatility on the ME–USEC route, where the slowdown metric averaged 19 percent but frequently spiked above 30 percent. This instability reflects the "lumpiness" of a trade lane served by a very small fleet —fewer than 10 vessels for the majority of the sample period. With such a small sample size, the operational decisions of individual ships —or delays at regional chokepoints— can disproportionately skew the aggregate measure.

Despite these regional variations, the overarching trend is clear. Across the major U.S.-bound corridors, vessel slowdown continues to absorb a substantial share of potential capacity in the post-crisis period (2023–2025) —ranging from approximately 14 percent on the APAC-USWC and APAC-USEC via Panama routes to nearly 19 percent on the EU-USEC route. This persistent drag suggests that speed adjustments have transitioned from a temporary operational response to a semi-permanent feature of the container shipping industry.

[19] See https://mxsocal.org/assets/pdf/web-container-vessel-queuing-release-final-and-executive-summary.pdf (accessed Dec 17, 2025) for further details.

[20] The implementation of IMO 2023 (EEXI/CII) regulations has forced many older vessels to permanently reduce sailing speeds to meet carbon intensity targets.

FIGURE 3.4.—Vessel slowdown across routes, 2016-2025



(a) Average vessel speed (b) Vessel slowdown/Potential supply

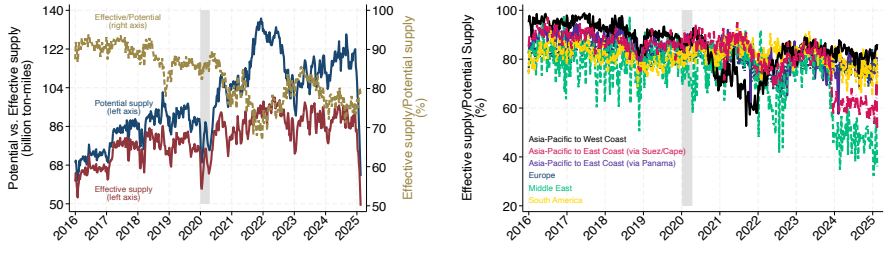
Note: Panel 3.4a shows the DWT-weighted average speed (in knots), while Panel 3.4b plots the capacity absorbed by vessel slowdown as a fraction of potential supply (in ton-miles) for each U.S.-bound route. The shaded area indicates recessions.

3.5. *Evolution of U.S.-bound effective shipping supply*

Subtracting the capacity absorbed by the four disruption factors —port congestion, canal bottlenecks, vessel rerouting, and speed adjustments— from potential supply yields our primary measure of effective shipping supply. This metric captures the net capacity actually available to the shipping of goods to America.

Aggregate trends. Panel 3.5a presents the aggregate potential versus effective shipping supply (in ton-miles) across all U.S.-bound routes. The gap between the two series represents the "efficiency wedge" —the total capacity lost to supply chain disruptions. To better evaluate the magnitude of this friction, we also plot the ratio of effective to potential supply.

FIGURE 3.5.—U.S.-bound effective shipping supply, 2016-2025



(a) Aggregate trends (b) Effective supply/Potential supply

Note: Panel 3.5a plots the aggregate potential and effective shipping supply in billion ton-miles (left axis) and the ratio of effective to potential supply (right axis) across all U.S.-bound routes. Panel 3.5b displays the ratio of effective to potential supply for each individual route. The shaded area indicates recessions.

The figure reveals a striking divergence beginning in late 2020. Prior to the pandemic (2016–2019), the U.S.-bound shipping network operated with high efficiency: approximately 89 percent of the fleet's potential capacity was successfully translated into effective service, with the remaining 11 percent accounting for normal operational friction. However, this rela-

tionship collapsed during the global supply chain disruption. While carriers aggressively deployed new tonnage —driving potential supply to record highs— effective supply stagnated. At the peak of the disruption (2021–2022), the aggregate efficiency of the U.S.-bound fleet fell below 70 percent. In other words, nearly one-third of the deployed capacity was effectively "deleted" from the market, absorbed by ships waiting at anchor, steaming slowly, or diverting around maritime bottlenecks.

Notably, the network has not returned to its pre-pandemic efficiency. In the recent period (2023–2025), aggregate efficiency has averaged roughly 79 percent, suggesting that the market has entered a new regime where logistical frictions —particularly vessel slowdown and rerouting— absorb a structurally higher share of shipping capacity.

Variation by route. The aggregate decline in efficiency masks significant heterogeneity across trade lanes. Panel 3.5b plots the ratio of effective to potential supply for each of the six U.S.-bound shipping routes.

The APAC–USWC route was the epicenter of the pandemic-era collapse. Despite being historically the most efficient corridor (converting over 92 percent of potential capacity into effective supply pre-pandemic), the route saw its efficiency plummet to a low of 53 percent in late 2021. This indicates that at the height of the supply chain crisis, nearly half of the capacity dedicated to the trans-Pacific trade was absorbed by port congestion and speed adjustments. While this route has since recovered to approximately 83 percent efficiency, it remains well below its historical norm.

In contrast, the recent deterioration in industry-wide efficiency is driven largely by routes affected by geopolitical instability. The efficiency of the Middle East and Asia-Pacific routes to the U.S. East Coast (via Suez/Cape) has deteriorated sharply since late 2023, dropping to 48 percent and 61 percent, respectively. This decline is mechanical rather than operational: the diversion of vessels around the Cape of Good Hope drastically inflates "potential" ton-miles (due to longer distances) without delivering additional cargo, severely depressing the ratio of effective service to deployed capacity.

4. A MODEL OF THE SHIPPING MARKET WITH MULTIPLE ROUTES

The evidence in Sections 2 and 3 highlights two distinct but complementary forces in U.S.-bound shipping. On one hand, shipping firms endogenously expanded and reallocated potential capacity. On the other hand, exogenous disruptions related to port congestion, canal bottlenecks, and security issues, absorbed large shares of this capacity, sharply reducing the effective supply of shipping services that reached U.S. ports. Together, these patterns suggest that the shipping market is a central intermediary and that the choices and constraints of shipping firms can actively shape import flows.

To interpret these patterns and quantify their implications, we now develop a multi-route general equilibrium model that embeds the two forces that shape U.S.-bound shipping: (i) the endogenous allocation of capacity across routes by profit-maximizing shipping firms; and (ii) exogenous disruptions that reduce the delivery of shipping services. By nesting these mechanisms in a tractable general equilibrium framework, the model allows us to quantify how shocks transmit through the shipping sector to trade flows and prices, as well as to evaluate counterfactuals that are central to trade policy.

4.1. *Overview*

Consider an economy with consumers, producers, retailers, and shipping firms. In addition to domestically-produced goods, consumers enjoy foreign goods that have to be shipped from one of the four ports of origin $o \in \mathcal{O} = \{A, E, M, S\}$ (standing for Asia, Europe, the Middle East, and South America) to one of the two arrival ports $a \in \mathcal{A} = \{E, W\}$ (standing for the East and West coasts of the United States). Imported goods from different regions are imperfect substitutes, but consumers are indifferent about the routes goods produced in the same region took to arrive in the U.S.

Shipping firms operate a fleet of container vessels and compete across multiple U.S. bound routes $r \in \mathcal{R} = \{$*Asia to West Coast*, *Asia to East Coast via Panama Canal*, *Asia to East Coast via Suez Canal*, *Europe to East Coast*, *Middle East to East Coast*, *South America to East Coast*$\}$. In line with the empirical evidence, there is only one route and one arrival port for goods produced in Europe, the Middle East, or South America. Goods from Asia come in three different variants: they are either delivered to the East or West coast ports; and if delivered to the East coast, they can be routed through the Panama canal or the Suez canal. Shipping firms decide how to allocate vessel capacity, what sailing speeds to adopt, and how intensively to load ships. They take the manufactured goods produced in one of the four regions to one of the destination ports along a route r. Once ships arrive at their destination, retailers purchase the goods and resell them to consumers. Retailers' sourcing decisions depend on route-specific shipping prices and idiosyncratic preferences. Time is discrete.

4.2. *Goods producers*

Domestic. There is a representative firm that produces domestic goods d using a linear technology in labor with productivity z_d. The firm hires domestic labor, l_d, at the wage rate w and sells the goods directly to consumers at price p_d. The domestic firm's maximization problem requires that

$$p_d z_d = w. \tag{4.1}$$

Foreign. There are foreign firms producing goods to be exported in each origin region. These firms are willing to supply any amount of goods demanded at the price $\overline{p}_o$ (in dollars) for goods with origin in region $o \in \mathcal{O}$. The foreign producers sell their goods to retailers, but for simplicity we let the shipping firms act as intermediaries. The producers are indifferent about the routes shipping firms take and therefore do not price discriminate them (though that is an easy extension).

4.3. *Shipping firms*

Shipping market. There is a continuum of monopolistically competitive shipping firms of measure N. Each shipping firm is endowed with total capacity κ that can be optimally allocated among different routes or stay idle. The capacity allocated to each route r is given by κ_r and idle capacity (or capacity allocated to unmodeled routes) is $\overline{\kappa}$.[21] The capacity constraint of a shipping firm can be expressed as

$$\kappa = \sum_{r \in \mathcal{R}} \kappa_r + \overline{\kappa}. \tag{4.2}$$

Shipping technology. Along each route r, shipping firms choose the average speed needed to operate their ships, s, and the amount of goods they want to transport in them or loading, ℓ, in order to produce the shipping service q_r.

The technology to produce the shipping service is a function of the number of trips made along the route, $n_r(s)$, and the amount of goods transported per trip, $\ell\kappa_r$, according to

$$\underbrace{q_r}_{\text{effective supply}} = z_r \underbrace{n_r(s)\,\ell\kappa_r}_{\text{potential supply}}. \tag{4.3}$$

Here, z_r is a firm and route specific productivity term, influenced by disruptions related to congestion, the weather, strength of waves or storms, or the presence of pirates. It corresponds to the impact of shipping disruptions on shipping supply presented in Sections 2 and 3. Hence, a fall in z_r corresponds to an increase in shipping disruptions. The shipping productivity has an exogenous component, denoted x_r, and an endogenous component driven by a congestion externality, $g(K_r)$, that is increasing in the market capacity allocated to route r, K_r. The shipping productivity is given by

$$z_r = \frac{x_r}{g(K_r)}. \tag{4.4}$$

[21] Note that idle capacity only plays a role in counterfactual experiments as it puts an upper bound on how much capacity shipping firms can reallocate to U.S.-bound routes. As new ships take on average three years to build, this can represent a binding constraint in any given period.

In turn, the number of trips made within a period evolves according to

$$n_r(s) = A_r s^{\alpha}, \tag{4.5}$$

where A_r is a route-specific efficiency term translating nautical miles per hour into number of trips and $\alpha > 0$ is a parameter. The average speed of ships is equivalent to the ratio of the distance traveled along route r, d_r, to the time traveled within the period, τ, i.e., $s \equiv d_r/\tau$.[22] The loading of ships, $\ell \in [0, 1]$, is the fraction of the capacity allocated to the route, κ_r, used to transport goods. If $\ell = 0$, ships are traveling empty; if $\ell = 1$, ships are at full capacity.

Congestion. The congestion factor disrupting route r depends on the aggregate capacity deployed along the route by all the N-competing shipping firms and reads

$$g(K_r) = \left(\int_0^N \kappa_r(j) dj \right)^{\phi}. \tag{4.6}$$

The higher is the aggregate capacity traveling along a route, the more congested, and therefore disruptive, the route is.

Shipping costs. The cost of shipping goods includes the value of the goods shipped and the expenses related with transporting them. The transportation cost per trip is $\overline{p}_n$, which is assumed to be the same across all routes. The longer is the distance, the fewer number of trips a shipping firm makes and the costlier it is to transport goods (e.g., it requires more fuel). The total cost of shipping along route r is

$$tc_r = \overline{p}_n (n_r(s))^{\zeta} + \overline{p}_o (\ell \kappa_r)^{\nu}. \tag{4.7}$$

The cost exponents are such that $\zeta, \nu \geq 1$ and $1/\zeta + 1/\nu = 1$. This restriction ensures the total cost function is homogeneous of degree 1 in the shipping service output.[23] The total cost of shipping is convex in the number of trips made and the quantity of goods transported. This captures the fact that there are diminishing marginal returns to or higher adjustment costs in scaling up sailing speeds (e.g., the engine might require more maintenance or ships might require more specialized sailors) or the amount of goods to load ships (e.g., cranes and specialized workers needed to stack containers on top of each other become more expensive).

The optimal choices of sailing speed and loading, s_r and ℓ_r, satisfy the firm's cost minimization problem, equation (4.7), taking as given the capacity allocated to the route, κ_r, and

[22] Here, the distance along route r is exogenous and common to all shipping firms. Hence, increases in speed reduce the time traveled between origin and arrival ports.

[23] Note that the exponents $1/\zeta$ and $1/\nu$ in the cost function are isomorphic to having the exponents ζ and ν in the production technology.

subject to its shipping service technological constraint, equation (4.3), as well as the loading constraint $\ell \in [0,1]$. When the optimal load is interior, i.e., $\ell_r < 1$, the solution to the firm's problem yields the marginal cost of shipping through route r as

$$mc_r = \frac{g(K_r)}{x_r}\left[\frac{\overline{p}_n}{1/\zeta}\right]^{1/\zeta}\left[\frac{\overline{p}_o}{1/\nu}\right]^{1/\nu}, \tag{4.8}$$

The marginal cost of shipping goods is increasing in shipping disruptions, congestion, the transportation price, and the price of goods at the origin port. When the ship is fully loaded, the marginal cost is also increasing in capacity.[24]

Profits per route. A shipping firm maximizes its profits along route r by choosing the price of its shipping services, p, taking the retailers' demand for its services, $\mathtt{y}_r(p)$, as given. The shipping firm's profit maximization problem for route r reads

$$\pi_r = \max_p (p - mc_r)\, q_r, \tag{4.9}$$

subject to the supply of shipping services meeting its demand, i.e., $q_r = \mathtt{y}_r(p)$.

The solution to the shipping firm's problem yields a route-specific price, p_r, equivalent to a markup over the firm's marginal cost given by

$$p_r = m_r mc_r. \tag{4.10}$$

In turn, the shipping firm's markup depends on retailers' price elasticity of demand for its manufactured goods shipped through the route, $\xi_r \equiv -(\partial \mathtt{y}_r(p_r)/\partial p_r)(p_r/\mathtt{y}_r(p_r))$, according to

$$m_r = \frac{\xi_r}{\xi_r - 1}. \tag{4.11}$$

The more inelastic is the retailers' demand for goods shipped through route r (i.e., the lower is ξ_r), the higher is the shipping firm's markup.

Optimal capacity per route. The capacity allocated to each route r is chosen to maximize the shipping firm's aggregate profit, π. The aggregate profit corresponds to the sum of profits per route across all routes net of the cost of deploying ships across routes, encapsulated by the quadratic cost on capacity adjustment priced at $\overline{p}_\kappa$. The shipping firm's aggregate profit is given

[24] When the optimal load is at the boundary $\ell_r = 1$, the marginal cost of shipping through route r is given by $mc_r = \frac{g(K_r)}{x_r}\left[\frac{\overline{p}_n}{1/\zeta}\right]^{1/\zeta}\left[\frac{\overline{p}_o}{1/\nu} + \frac{\mu_r}{\kappa_r^\nu}\right]^{1/\nu}$, where $\mu_r > 0$ is the Lagrange multiplier on the load's upper bound constraint. An expression can be obtained for the Lagrange multiplier as a function of capacity, number of trips, and input prices, according to $\mu_r = \zeta \overline{p}_n n_r (s_r)^\zeta - \nu \overline{p}_o \kappa_r^\nu$.

by

$$\pi = \max_{\{\kappa_r\}_{r\in\mathcal{R}}} \left\{ \sum_r \pi_r - \overline{p}_\kappa \sum_r \frac{\kappa_r^2}{2} \right\}. \tag{4.12}$$

subject to the capacity constraint (4.2). The shipping firm's optimal capacity per route is obtained by replacing the Lagrange multiplier on the capacity constraint in the shipping firm's first-order condition to problem (4.12). The shipping firm does not internalize the effect of its capacity choice on congestion and therefore output.

The optimal capacity per route equates the marginal benefit of additional capacity to its marginal cost. Increasing capacity in one route raises the route's profit per ton traveled relative to the firm's average profits. However, it also increases the cost of deploying capacity to that route relative to its average. The more congested a route is, the lower is the profit per ton traveled from that route, and the more likely the firm is to reallocate capacity along the other routes. The first-order condition of the profit maximization problem when the optimal loading of ships is interior, i.e., $\ell_r < 1$, yields the following expression

$$\underbrace{\frac{(p_r - mc_r)\, x_r n_r(s_r)\ell_r}{g(K_r)}}_{\text{profit per ton traveled along route } r} - \underbrace{\frac{1}{|\mathcal{R}|}\sum_h \frac{(p_h - mc_h)\, x_h n_h(s_h)\ell_h}{g(K_h)}}_{\text{average profit per ton traveled}} = \overline{p}_\kappa \left[\kappa_r - \underbrace{\frac{1}{|\mathcal{R}|}(\kappa - \overline{\kappa})}_{\text{average capacity per route}} \right] \tag{4.13}$$

where $|\mathcal{R}|$ is the number of routes (i.e., 6). The left-hand side of equation (4.13) represents the marginal benefit of reallocating capacity to route r expressed in terms of the route's profit per ton traveled relative to the firm's average profit per ton traveled. The right-hand side is the marginal cost of reallocating capacity, which corresponds to cost of deployment from route r relative to the average cost of deployment.

Note that the firm faces an additional marginal cost pressure from the loading constraint when $\ell_r = 1$. If its ship is fully loaded, adding capacity reduces the firm's marginal cost of shipping along route r relative to its average marginal cost. The reason is that the shipping firm can now fully load a bigger ship, which increases the profit from operating along route r relative to the other routes.[25]

Entrants in the shipping market. Potential shipping firms consider entering the shipping market as long as they can make profits. If a shipping firm decides to enter, it gets the expected profits from operating in the market, or $\left(\int_0^N \pi(j)dj\right)/N$. Not entering the shipping market delivers a profit of zero. The free-entry condition determines the number of shipping firms, N.

[25] The first-order condition of the profit maximization problem when the optimal load choice along route r is at the upper bound, i.e., $\ell_r = 1$, is $\frac{(p_r - mc_r)x_r n_r(s_r)\ell_r}{g(K_r)} - \frac{1}{|\mathcal{R}|}\sum_h \frac{(p_h - mc_h)x_h n_h(s_h)\ell_h}{g(K_h)} = \overline{p}_\kappa \left[\kappa_r - \frac{1}{|\mathcal{R}|}(\kappa - \overline{\kappa})\right] + \frac{\partial mc_r}{\partial \kappa_r} q_r - \frac{1}{|\mathcal{R}|}\sum_h \frac{\partial mc_h}{\partial \kappa_h} q_h$. Here, $\partial mc_h/\partial \kappa_h = -\left(mc_h/\kappa_h\right)\mu_h/\left[\nu \overline{p}_o \kappa_h^\nu + \mu_h\right] < 0$ when $\ell_h = 1$.

4.4. *Retailers*

There is a measure $\mathcal{I}$ of identical retailers, who source goods from different regions and routes. Retailers purchase manufactured goods from a shipping firm j operating route r at the price $p_r(j)$ and resell them to consumers at the final price p_o for $o \in \mathcal{O}$. The final price only depends on the origin of the goods as consumers are indifferent about the arrival port they were delivered to or the route goods took to arrive at their destination.

Technology. The output of retailers sourcing goods from route r is produced according to a decreasing returns to scale technology that aggregates all services produced by shipping firms operating along the route, with $1/(1-\sigma)$ as the elasticity of substitution, or

$$y_r = \left[\chi_r \left(\int_0^N y_r(j)^\sigma dj \right)^{1/\sigma} \right]^\theta , \tag{4.14}$$

where χ_r is the productivity of retailers from specializing in manufactured goods delivered along route r and $\theta \in (0,1)$ is the returns to scale from dealing with shipping firms, common across all routes.

Profits per route. Retailers' profit from each route r is given by

$$\Pi_r = \max_{\{y_r(j)\}} \left\{ p_o \chi_r^\theta \left(\int_0^N y_r(j)^\sigma dj \right)^{\theta/\sigma} - \int_0^N p_r(j) y_r(j) dj - f \right\}, \tag{4.15}$$

where $f > 0$ denotes the fixed costs of operating in the retail sector. As $\theta < 1$, retailers can make profits on some routes.

Optimal sourcing decision. We make retailers' sourcing decision endogenous, which allows shipping disruptions to have both an intensive and an extensive margin. As a result, shipping disruptions alter both the quantity demanded by retailers and the distribution of retailers across routes. This is achieved by adding idiosyncratic taste shocks retailers have for goods sourced from different routes. Retailers thus choose which route r they want to source their goods from according to the following discrete choice problem

$$\Pi = \max_{r \in \mathcal{R}} \{ \Pi_r + \epsilon_r \},$$

where ϵ_r are taste shocks for goods sourced from route r, assumed to be mean zero Type I extreme value with scale parameter $\lambda > 0$.

The optimal sourcing decision for goods from route r is governed by the following expression

$$o_r = \frac{e^{\lambda \Pi_r}}{\sum_{x \in \mathcal{R}} e^{\lambda \Pi_x}}. \tag{4.16}$$

More profitable routes are more likely to have a larger number of retailers sourcing from them.

Retailers' demand for shipping services. It transpires that the total demand for manufactured goods sourced from route r and transported by a shipping firm j, $\mathtt{y}_r(j)$, corresponds to the product of the quantity demanded by each retailer conditional on sourcing goods from route r, given by $y_r(j)$, and the number of retailers sourcing goods from route r. The latter is given by the probability a retailer sources goods from route r, o_r, summed across all retailers, $\mathcal{I}$. The total demand for shipping services provided by a shipping firm j operating along route r is then

$$\mathtt{y}_r(j) \equiv y_r(j) o_r \mathcal{I} = \left[\frac{\theta \chi_r^{\sigma} p_o y_r^{(1-\sigma/\theta)}}{p_r(j)} \right]^{1/(1-\sigma)} o_r \mathcal{I}, \tag{4.17}$$

where the last term after the equal sign is obtained from replacing $y_r(j)$ with the solution to the retailer's problem (4.15).

Entrants in the retail market. Potential retailers consider entering the retail market. If a firm enters the retail market, its expected profit is $\sum_{r \in \mathcal{R}} o_r \Pi_r$. If the firm decides not to enter the retail market, it gets a profit of zero. As long as profits can be made, potential entrants will join the retail sector. The free-entry condition determines the measure of retailers, $\mathcal{I}$.

4.5. *Consumers*

There is a unit measure of consumers, endowed with one unit of time. Consumers supply their unit of time inelastically in exchange for the wage rate w and receive profits Λ accrued from the portfolio of retail and shipping firms they own. Consumers purchase domestically-produced goods, d, at price p_d as well as imported goods from Asia, Europe, the Middle East, and South America, c_o for $o \in \mathcal{O}$, sold by retailers at price p_o. The budget constraint of a consumer is given by

$$\sum_{o \in \mathcal{O}} p_o c_o + p_d d = w + \Lambda. \tag{4.18}$$

Goods from different regions are imperfect substitutes, with $1/(1-\rho)$ as the elasticity of substitution between them. The bundle of imported goods can be written as

$$c = \left(\sum_{o \in \mathcal{O}} \gamma_o c_o^{\rho} \right)^{1/\rho}, \tag{4.19}$$

with γ_o denoting an origin-specific utility weight such that $\sum_{o \in \mathcal{O}} \gamma_o = 1$. Goods from the same region but sourced from different routes are perfect substitutes.

A consumer derives utility from domestic goods and the bundle of imported goods, with their elasticity of substitution given by $1/(1-\varrho)$. The consumer's problem reads

$$u(c_A, c_E, c_M, c_S, d) = \max_{c_A, c_E, c_M, c_S, d} \left[\gamma_d d^{\varrho} + (1-\gamma_d) c^{\varrho} \right]^{1/\varrho} \tag{4.20}$$

subject to the budget constraint (4.18) and the bundle of imported goods (4.19).

4.6. *Equilibrium*

Definition (**EQUILIBRIUM**)**.** An equilibrium consists of a solution for: (1) the domestic goods price and the domestic firms' labor demand, $\{p_d, l_d\}$; (2) a shipping firm's profit, output, number of trips, sailing speed, price, markup, load, and capacity along each route $r \in \mathcal{R}$, $\{\pi_r(j), q_r(j), n_r(j), s_r(j), p_r(j), m_r(j), \ell_r(j), \kappa_r(j)\}$, as well as total profits, $\pi(j)$, for all firms $j \in [0, N]$; (3) retailers' demand for goods shipped by each shipping firm j, $\mathrm{y}_r(j)$, output, y_r, corresponding profits, Π_r, and optimal sourcing decision o_r for each route $r \in \mathcal{R}$; (4) consumers' demand for domestically-produced goods, d, and imported goods from each region $o \in \mathcal{O}$, c_o; (5) the wage rate, w; (6) retail prices of goods from each region $o \in \mathcal{O}$, p_o; (7) the measure of shipping firms, N; (8) the measure of retailers, $\mathcal{I}$; (9) the aggregate profits, Λ. These allocations are determined such that

1. The domestic firms' problem satisfies (4.1) and the labor demanded by producers of domestic goods is given by

$$l_d = 1 - \frac{1}{w} \int_0^N \sum_{r \in \mathcal{R}} \left\{ \zeta \overline{p}_n n_r(j)^{\zeta} - \frac{\mu_r(j)}{\nu} + \overline{p}_{\kappa} \frac{\kappa_r(j)^2}{2} \right\} dj. \tag{4.21}$$

2. Given the transportation price, $\overline{p}_n$, and goods prices at the origin port, $\overline{p}_o$, each shipping firm j maximizes its profits $\pi_r(j)$ according to (4.9), yielding a solution for $\{q_r(j), n_r(j), s_r(j), p_r(j), m_r(j), \ell_r(j)\}$ along each route r that satisfy (4.3), (4.5), (4.8), (4.10), (4.11), as well as $\ell_r(j) = \min \left\{ 1, \left(\frac{\zeta}{\nu} \frac{\overline{p}_n}{\overline{p}_o} \right)^{1/\nu} n_r(j)^{\zeta/\nu} / \kappa_r(j) \right\}$. Total profits, $\pi(j)$, and the optimal capacity per route, $\kappa_r(j)$, satisfy (4.12) and (4.13).

3. Given the prices of shipping services, $p_r(j)$, and retail prices, p_o, retailers' allocations $\{y_r, \Pi_r, o_r\}$ and $\{\mathrm{y}_r(j)\}_0^N$ satisfy equations (4.14), (4.15), (4.16), and (4.17) for each route $r \in \mathcal{R}$.
4. Given the retail price of goods, p_d and p_o, wages, w, and profits, Λ, consumer demand for domestically-produced goods, d, and imported goods, c_o, from each origin $o \in \mathcal{O}$ maximize their utility (4.20) subject to the budget constraint (4.18) and the bundle of imported goods (4.19).
5. The market between shipping firms and retailers clears in each route r so that the quantity supplied by shipping firms equates the quantity demanded by retailers (4.17), or

$$\int_0^N q_r(j)dj = o_r \mathcal{I} \left[\theta \chi_r^\sigma \, p_o y_r^{(1-\sigma/\theta)}\right]^{1/(1-\sigma)} \int_0^N p_r(j)^{1/(\sigma-1)} dj.$$

6. The market between retailers and consumers clears according to

$$\begin{aligned} c_A &= (o_{AEP} y_{AEP} + o_{AES} y_{AES} + o_{AW} y_{AW})\,\mathcal{I} \\ c_j &= o_{jE} y_{jE} \mathcal{I} \qquad \text{for } j = \{E, M, S\}, \end{aligned}$$

   which determines the retail prices of consumer goods, p_o, from each origin $o \in \mathcal{O}$.
7. The free-entry condition for the shipping market holds according to

$$\int_0^N \pi(j)dj = 0,$$

   which determines the number of shipping firms, N.
8. The free-entry condition for the retail market holds according to

$$\sum_{r \in \mathcal{R}} o_r \Pi_r = 0,$$

   which determines the measure of retailers, $\mathcal{I}$.
9. Entry costs in the retail market are rebated to consumers according to

$$f\mathcal{I} = \Lambda. \tag{4.22}$$

4.7. *Unpacking the impact of shipping disruptions*

Our framework allows us to derive closed-form expressions of the first-order impact of shipping disruptions on aggregate output and consumer welfare akin to Hulten (1978)'s theorem

(see Baqaee and Farhi (2019)). Proposition 4.1 shows how shipping disruptions along a specific route transmit to aggregate output and consumers. The first-order impact of the disruptions depends on how important the route is in aggregate output (equivalent to the route's Domar weight) and includes amplifying or dampening effects through the retail sector via changes in retail output and sourcing decisions. The remaining effects on aggregate output operate through general equilibrium effects that affect incentives to enter the retail and shipping markets.

Let $X_r \equiv \left[\int_0^N x_r(j)^{\sigma/(1-\sigma)} dj\right]^{(1-\sigma)/\sigma}$ denote the aggregate exogenous component of route-r shipping productivity. A fall in X_r corresponds to an increase in the exogenous component of shipping disruptions along route r. It is easy to deduce that the route-r disruptions including the effect of congestion are given by $Z_r \equiv X_r/g(K_r)$, where $Z_r \equiv \left[\int_0^N z_r(j)^{\sigma/(1-\sigma)}\right]^{(1-\sigma)/\sigma}$. The impact of shipping disruptions on aggregate output discussed in the proposition below can equivalently be expressed with X_r or Z_r.

PROPOSITION 4.1: (IMPACT OF SHIPPING DISRUPTIONS ON AGGREGATE OUTPUT) The first-order impact of route-r shipping disruptions on aggregate output is given by

$$\frac{\partial Y}{\partial X_r}\frac{X_r}{Y} \approx \sum_{h\in\mathcal{R}} \underbrace{\left(\begin{array}{c}\text{Route } h\text{'s share in}\\ \text{aggregate output}\end{array}\right)}_{\text{Domar weight}} \times \left(\underbrace{\frac{\partial y_h}{\partial X_r}\frac{X_r}{y_h}}_{\text{intensive margin}} + \underbrace{\frac{\partial o_h}{\partial X_r}\frac{X_r}{o_h}}_{\text{extensive margin}}\right),$$

where the route h's share in aggregate output $\equiv p_s y_h o_h \mathcal{I}/(w+\Lambda)$. Here, p_s is the retail price of goods transported via route h. It is straightforward to show the first-order impact on output of the route-specific congestion externality, $g(K_r)$, or total disruptions, Z_r.

PROOF: See Appendix B.1.1. *Q.E.D.*

Propositions B.1 and B.2 in Appendix B.1 discuss how shipping disruptions affect retailers' output and their sourcing decisions in partial equilibrium. In Section 6, the model is used to compute the route-specific Domar weights as well as the elasticity of retailers' output and sourcing decisions in response to a shipping productivity shock along each route taking into account their general equilibrium effects.

5. TAKING THE MODEL TO DATA

In this section, we calibrate the model to U.S. data to quantitatively match the shipping trends documented in Section 2.[26] Our empirical strategy proceeds in two steps. First, we calibrate

[26]Throughout this section, weekly data is time-aggregated to a monthly frequency.

the model to match a pre-disruption steady state based on data from February 2016. Second, we simulate the model to trace the dynamic evolution of key macroeconomic and shipping aggregates from March 2016 through March 2025.

Parameters. The framework features 41 parameters: 7 consumer preference parameters, $\{\rho, \varrho, \gamma_d, \gamma_o\}$ for $o \in \mathcal{O}$; 10 parameters governing the retailers' problem, $\{\chi_r, \theta, \sigma, f, \lambda\}$ for $r \in \mathcal{R}$; 17 parameters characterizing the shipping market, $\{x_r, A_r, \phi, \alpha, \zeta, \nu, \overline{\kappa}\}$ for $r \in \mathcal{R}$; the price of redeploying capacity, $\overline{p}_\kappa$; the price of transportation, $\overline{p}_n$; 4 prices of foreign goods, $\overline{p}_o$ for $o \in \mathcal{O}$; and the productivity of domestic goods producers, z_d. The aggregate wage is normalized to one as the numeraire.

Our calibration strategy divides these parameters into three distinct groups. The first group consists of parameters that either have direct empirical counterparts or can be normalized. A second set of parameters is backed out directly from the theoretical equilibrium conditions to match specific data targets exactly. The remaining parameters are calibrated jointly to minimize the difference between the model-implied moments and their respective empirical targets. The full set of estimated parameters is summarized in Table 5.1. Finally, Table 5.2 contrasts the targeted model moments against the data as of February 2016.

5.1. *Exogenous and externally estimated parameters*

Consumer elasticity of substitution. There is a vast literature estimating trade elasticities. A robust finding is that the elasticity of substitution across goods from different foreign countries is higher than the elasticity between domestic and foreign goods; consumers are more willing to substitute among alternative import sources than to substitute away from domestic varieties. Feenstra et al. (2018) estimate these parameters using U.S. data from 1992 to 2007. They find a "micro-Armington" elasticity (between foreign sources) ranging from 3.22 to 4.05, and a "macro-Armington" elasticity (between domestic and foreign sources) of approximately 2 for most sectors. In line with these estimates, we set the substitution parameter between imported goods to $\rho = 0.75$ (implying an elasticity of substitution of 4) and the parameter between foreign and domestically produced goods to $\varrho = 0.5$ (implying an elasticity of 2).

Retail technology and sourcing. Retailer productivity parameters across most routes can be normalized to one, with the exception of those originating in Asia. Because goods from the same origin region are perfect substitutes, the productivities of two Asian routes must be calibrated internally to match observed shipping supply shares. Consequently, we normalize $\chi_{AEP} = \chi_{EE} = \chi_{ME} = \chi_{SE} = 1$ and jointly estimate χ_{AES} and χ_{AW}.

The price elasticity of retailers' demand for shipping services is given by $\xi_r = 1/(1-\sigma)$, which implies an average markup for shipping firms of $1/\sigma$. We target a shipping firm markup of 25%, pinning down the underlying elasticity of substitution at $\sigma = 0.8$. Similarly, the

marginal cost for retailers conditional on sourcing goods from a particular route is θp_o, yielding a retail markup of $1/\theta$. We set $\theta = 0.8$ to match a targeted retail markup of 25%. Finally, we normalize the scale parameter of the mean-zero Gumbel shock for retailers' sourcing decisions to $\lambda = 1$, where higher values of λ correspond to a greater variance in retailers' idiosyncratic taste shocks.

Shipping technology and costs. We estimate the elasticity of the number of trips with respect to sailing speed, denoted by α, directly from the data. Using satellite-based AIS data from January 2016 through March 2025, we compute the capacity-weighted average number of trips per ship along route r in month t as:

$$\overline{\texttt{Number of Trips}}_{r,t} = \sum_{i \in \boldsymbol{\mathcal{I}}_t} \left(\frac{\mathbf{1}_{i,r,t} \times \texttt{DWT}_i}{\sum_{i \in \boldsymbol{\mathcal{I}}_t} \mathbf{1}_{i,r,t} \times \texttt{DWT}_i} \right) \times \texttt{Number of Trips}_{i,r,t},$$

where $\texttt{Number of Trips}_{i,r,t}$ represents the total trips completed by vessel i on route r in month t. We also construct the capacity-weighted average sailing speed following equation (2.3) at a monthly frequency. To recover α, we regress the natural logarithm of the average number of trips on the natural logarithm of the average sailing speed. Table B.1 in Appendix B.2.1 reports the full estimation results. For our baseline calibration, we set $\alpha = 0.036$, which corresponds to our preferred specification controlling for route, year, and month fixed effects.

We also assume that shipping costs are increasing and strictly convex in both the number of trips and the quantity of goods transported per trip. Due to a lack of granular firm-level data to estimate these cost elasticities directly, we impose a standard quadratic cost structure. Specifically, we set the elasticity with respect to the number of trips to $\zeta = 2$. The theoretical restriction on the cost parameters, $1/\zeta + 1/\nu = 1$, then symmetrically pins down the elasticity with respect to the transported quantity at $\nu = 2$.

Congestion. The exponent on the congestion factor, ϕ, is calibrated by estimating the elasticity of total congestion time with respect to the total number of port calls. Using the vessel-level AIS data and the IMA-DBSCAN algorithm described in Section 3.1, we construct a comprehensive monthly panel of total port calls and total congestion times for major global container ports. Specifically, we compute the total number of hours container ships wait in a port's anchorage area before docking at a berth, and regress the natural logarithm of this total congestion time on the natural logarithm of the total number of port calls. Table B.2 in Appendix B.2.1 presents the results. Our preferred specification, which controls for unobserved heterogeneity via port, year, and month fixed effects, yields a highly significant estimated elasticity of 1.809. This point estimate directly informs our calibrated value of $\phi = 1.809$.

Domestic producers. We normalize the productivity of domestic producers to $z_d = 1$. Because the aggregate wage is our chosen numeraire, this normalization pins down the unit price of domestically produced goods to one.

TABLE 5.1

PARAMETER VALUES

Parameter	Description	Value	Identification
Consumer preferences			
ϱ	Elast. of sub. between imported and domestic goods	0.500	Feenstra et al. (2018)
ρ	Elast. of sub. among imported goods	0.750	Feenstra et al. (2018)
γ_d	Cons. weight, domestic goods	0.955	Total import share
γ_o	Cons. weight, Asia, Europe, Middle East, South America	0.368, 0.359 0.093, 0.180	Regional import shares
Retail market			
χ_r	Retail prod., Asia to East coast via Panama/Suez/to West Coast	1.000, 1.082, 1.229	Potential shipping supply,
	Europe, Middle East, South America to East Coast	1.000, 1.000, 1.000	normalization
θ	Returns to scale	0.800	Retail markup
σ	Elast. of sub. between shipped goods	0.800	Shipping markup
f	Entry cost in retail market	0.024	Number of retail firms
λ	Scale parameter in optimal shipping route	1.000	Normalization
Shipping market			
x_r	Route prod., Asia to East coast via Panama/Suez/to West Coast	13.974, 19.120, 36.212	Shipping disruptions
	Europe, Middle East, South America to East Coast	17.831, 6.385, 9.812	
A_r	Speed eff., Asia to East coast via Panama/Suez/to West Coast	0.879, 1.117, 1.706	Average speed
	Europe, Middle East, South America to East Coast	1.120, 0.320, 0.660	
ϕ	Congestion exponent	1.809	Congestion time
α	Exponent on speed	0.036	Elast. trip number wrt speed
ζ	Exponent on number of trips	2.000	Exogenous
ν	Exponent on quantity transported	2.000	
$\overline{\kappa}$	Idle capacity	1.078	Non-US shipping supply
$\overline{p}_\kappa$	Redeployment price	0.008	Number of shipping firms
$\overline{p}_n$	Transportation price ($\times 100$)	0.014	Average number of trips
Producers			
z_d	Productivity of domestic firms	1.000	Normalization
$\overline{p}_o$	Origin prices, Asia, Europe, Middle East, South America	0.016, 0.035 0.011, 0.013	Potential shipping supply

5.2. *Internally calibrated parameters*

Import shares. We calibrate the consumption weights on domestically produced and imported goods, $\{\gamma_d, \gamma_A, \gamma_E, \gamma_M, \gamma_S\}$, to match the total goods import share of output from the BEA, as well as each region's share of U.S. merchandise trade from the Census Bureau, as of February 2016.[27] Regional import shares correspond to the ratio of containerized vessel values from a specific region to the total from all four origin regions. In February 2016, the aggregate import share of output was 11.8%, with the composition originating from Asia (8.7%), Europe (2.2%), the Middle East (0.2%), and South America (0.8%).

[27]BEA data is available here, and Census Bureau trade data is available here. Countries are assigned to regions following the World Bank's classification (link).

Given equilibrium prices and consumer elasticities of substitution, we back out the values of γ_d and $\{\gamma_o\}_{o\in\mathcal{O}}$ to exactly match these four targets, subject to the constraint $\sum_{o\in\mathcal{O}}\gamma_o = 1$. Solving the consumer's problem in (4.20) yields the expenditure share on domestic goods, $\omega_d \equiv p_d d/(w+\Lambda)$, as:

$$\omega_d = \gamma_d^{1/(1-\varrho)}\left(\frac{p_d}{P^{\text{total}}}\right)^{\varrho/(\varrho-1)},$$

and the expenditure share on imported goods from region $o\in\mathcal{O}$, $\omega_o \equiv p_o c_o/(w+\Lambda)$, as:

$$\omega_o = \gamma_o^{1/(1-\rho)}\left(\frac{p_o}{P^{\text{imp}}}\right)^{\rho/(\rho-1)}(1-\omega_d).$$

Here, $P^{\text{total}} \equiv \left[\gamma_d^{1/(1-\varrho)}p_d^{\varrho/(\varrho-1)} + (1-\gamma_d)^{1/(1-\varrho)}\left(P^{\text{imp}}\right)^{\varrho/(\varrho-1)}\right]^{(\varrho-1)/\varrho}$ denotes the economy-wide ideal price index, and $P^{\text{imp}} \equiv \left(\sum_{o\in\mathcal{O}}\gamma_o^{1/(1-\rho)}p_o^{\rho/(\rho-1)}\right)^{(\rho-1)/\rho}$ is the ideal price index for imported goods.

Shipping disruptions. Route-specific shipping productivity, z_r, maps directly to the ratio of effective to potential shipping supply discussed in Section 3 and presented in Figure 3.5b. Given the endogenous congestion externality, $g(K_r)$, we back out the route-specific exogenous component of shipping productivity, $\{x_r\}_{r\in\mathcal{R}}$, to exactly match the empirical ratio of effective to potential supply.

Potential shipping supply. We calibrate the origin prices of goods, $\{\overline{p}_A, \overline{p}_E, \overline{p}_M, \overline{p}_S\}$, alongside retailer productivities for sourcing from Asia to the East Coast (via the Suez) and the West Coast, χ_{AES} and χ_{AW}, to match the potential shipping supply (in DWT) by route as of February 2016 (see Section 2 and Figure 2.3a). The theoretical counterpart to potential supply is $\int_0^N n_r(j)\ell_r(j)\kappa_r(j)dj$. Given the cost elasticities (α,ν,ζ), speed efficiencies (A_r), sailing speeds (s_r), and the mass of shipping firms (N), these origin prices and productivities ensure the model matches the observed tonnages perfectly.

Average sailing speeds. We identify the speed efficiency shifters, $\{A_r\}_{r\in\mathcal{R}}$, using the average sailing speed of vessels on each route. This target is derived according to equation (2.3) using February 2016 satellite data (presented in Figure 3.4a). Given the targeted sailing speed s_r and the optimal number of trips n_r, we uniquely identify A_r to clear this moment.

Average number of trips. We calibrate the price per trip, $\overline{p}_n$, such that the model's average number of trips matches the empirical average in the AIS data. The theoretical average is defined as:

$$\overline{n} = \frac{\sum_{r\in\mathcal{R}}\int_0^N n_r(j)dj}{N|\mathcal{R}|}.$$

Empirically, in February 2016, a vessel completed an average of 1.066 trips per month, given that ships must also undertake a return voyage to their origin regions.

Idle capacity. We calibrate idle capacity, $\overline{\kappa}$, to match the fraction of global capacity allocated to U.S.-bound routes. In the model, this share is given by:

$$\frac{\int_0^N \sum_{r\in\mathcal{R}} \ell_r(j)\kappa_r(j)dj}{\int_0^N \sum_{r\in\mathcal{R}} \ell_r(j)\kappa_r(j)dj + N\psi\overline{\kappa}},$$

where $\psi = 0.8$ is an assumed load factor adjustment for non-U.S.-bound ships. Empirically, we use AIS data to track the global fleet. The target is the ratio of U.S.-bound potential supply (inbound and outbound) to total global potential supply. In February 2016, about 60% of the world's total DWT was allocated to non-U.S.-bound routes, perfectly identifying $\overline{\kappa}$.

Number of retail and shipping firms. We set the retail entry cost, f, to normalize the measure of retailers, $\mathcal{I}$, to one. Finally, we calibrate the capacity redeployment price, $\overline{p}_\kappa$, to match the average number of shipping firms, N, operating across U.S.-bound routes. In February 2016, this averaged 33 firms.

5.3. *Tracing the evolution of U.S.-bound shipping between 2016 and 2025*

The model is now simulated to trace the evolution of our measure of shipping disruptions, import shares across regions, route-specific potential shipping supply, average sailing speeds, non-U.S.-bound capacity, and number of firms between March 2016 and March 2025. This is achieved by solving for the values of the exogenous shipping disruptions, speed efficiencies, idle capacity, redeployment price, retail productivities, retail entry cost, and origin prices, $\left\{\{x_{r_t}\}_{r\in\mathcal{R}}, \{A_{r_t}\}_{r\in\mathcal{R}}, \overline{\kappa}_t, \overline{p}_{\kappa_t}, \{\chi_{r_t}\}_{r\in\mathcal{R}}, f_t, \{\overline{p}_{o_t}\}_{o\in\mathcal{O}}\right\}$. In particular, the algorithm solves for the values that minimize the distance between the model-implied aggregates and the targeted data at each point in time between March 2016 and March 2025. All the other parameters are held constant over time. These simulations are the baseline for the counterfactual experiments we explore in Section 6 when assessing the impact of shipping disruptions.

Figure B.1 in Appendix B.2.1 presents the evolution of the targeted time series, Figure B.2 displays the underlying exogenous variables necessary to match the data, and Figure B.3 shows the evolution of other aggregates of interest.

The model matches the evolution of the targeted series perfectly. The exogenous component of shipping productivity, x_r, increases notably between 2021 and 2023 to counteract the increase in congestion, $g(K_r)$. The increase in congestion was driven by a decline in idle capac-

TABLE 5.2

TARGETED MOMENTS: DATA VS. MODEL (FEBRUARY 2016)

Moment	Model	Data	Source
Import shares of output, ω_o			
Total	0.118	0.118	BEA
Asia	0.087	0.087	Census
Europe	0.022	0.022	Census
Middle East	0.002	0.002	Census
South America	0.008	0.008	Census
Shipping disruptions (effective/potential supply), z_r			
Asia to East coast via Panama Canal	0.849	0.849	AIS
Asia to East coast via Suez Canal	0.882	0.882	AIS
Asia to West coast	0.953	0.953	AIS
Europe to East coast	0.823	0.823	AIS
Middle East to East coast	0.821	0.821	AIS
South America to East coast	0.797	0.797	AIS
Potential shipping supply (in DWT), $N q_r / z_r$			
Total	24.143	24.143	AIS
Asia to East coast via Panama Canal	2.921	2.921	AIS
Asia to East coast via Suez Canal	4.714	4.714	AIS
Asia to West coast	11.056	11.056	AIS
Europe to East coast	3.202	3.202	AIS
Middle East to East coast	0.478	0.478	AIS
South America to East coast	1.773	1.773	AIS
Sailing speeds, s_r			
Asia to East coast via Panama Canal	15.433	15.433	AIS
Asia to East coast via Suez Canal	15.325	15.325	AIS
Asia to West coast	16.264	16.264	AIS
Europe to East coast	14.018	14.018	AIS
Middle East to East coast	15.824	15.824	AIS
South America to East coast	12.149	12.149	AIS
Other targets			
Average number of trips	1.066	1.066	AIS
Non-U.S.-bound capacity (% of world capacity)	0.598	0.598	AIS
Number of shipping firms	33.0	33.0	AIS
Number of retail firms	1.0	1.0	Normalization

ity, $\overline{\kappa}$, and thus an increase in capacity allocated to U.S.-bound routes, K_r. The 2022 shipping disruptions added delays of about three days along the Asian routes and pushed loading factors of container ships departing from Asia up relative to other other routes. Yet, these disruptions did not significantly reduced the number of trips taken by ships in line with the empirical evidence. Retail productivity and entry costs, χ_r and f, fell during the Covid-19 pandemic and recovered swiftly after, which help explain the changes in the import share of goods from Asia.

6. THE MACROECONOMIC IMPACT OF SHIPPING DISRUPTIONS

With the calibrated model in hand, we revisit Proposition 4.1 and compute the impact of route-specific shipping disruptions on aggregate output. We then focus on two specific disruption events and study their macroeconomic effects. The first event relates to the months that preceded the post-pandemic boom of late 2021. Our measured disruptions during that period disproportionately affected the Asia to West Coast route. The second episode studies the rerouting away from the Suez Canal due to Houthi attacks in the Red Sea in early 2024. These

disruptions significantly impacted the Asia to East Coast route via the Suez Canal and the Middle East to East Coast route. In both cases, counterfactual economies without the measured disruptions are simulated and compared to our baseline economy. The difference in outcomes allows us to quantify the macroeconomic impact of these these events.

Finally, we study the impact of the U.S. Navy and other allies presence in the Red Sea in 2024, when destroyers were deployed to counteract the Houthi attacks on container ships. A counterfactual economy is constructed in which shipping disruptions would have continued to persist throughout March 2025.

6.1. *Revisiting Proposition 4.1 on the impact of shipping disruptions on aggregate output*

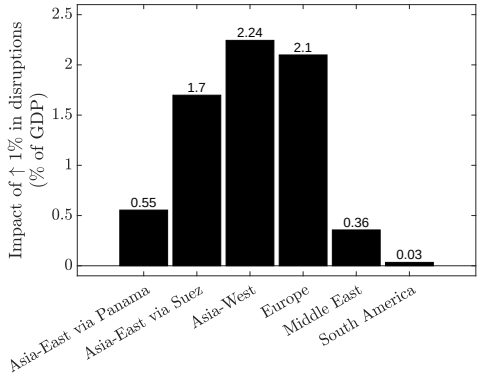
The model matched to February 2016 data is now used to numerically estimate the elasticity of aggregate output in response to a shipping productivity shock along each route taking into account the general equilibrium effects. Figure 6.1a shows that elasticity for the six routes. For instance, a 1% increase in the exogenous component of shipping disruptions, X_r, along the Asia to East Coast route via the Suez Canal reduces output by 1.7%, while a shock along the route that crosses the Panama Canal decreases output by 0.6%.

Figure 6.1b shows each route's share of U.S. aggregate output (akin to the route's Domar weight) as of February 2016. For instance, the Asia to West Coast route accounted for nearly 5% of aggregate output, while the Asia to the East Coast route via the Suez canal and the Europe to East Coast route represent about 2% of aggregate output each. The sum of the route weight corresponds to the total import share. To understand why disruptions are more or less detrimental than what the route's Domar weight would suggest, we look at the response of retailers' output and sourcing decisions to a shipping shock.

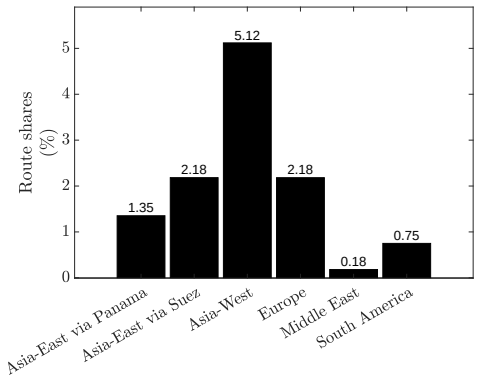
Figure 6.2a shows the impact of a negative route-specific disruption shock on retail output, $-(\partial y_h/\partial X_r)(X_r/y_h)$. Disruptions along a particular route tend to reduce retail output from that same route (diagonal cells in the matrix) and to increase output on goods sourced from other routes (off-diagonal cells). For instance, a 1% disruption shock tends to reduce retail output from the same route by about 0.8 to 1.5%. There are also spillover effects from other routes that can amplify or dampen the impact disruptions on retail output. For instance, 1% disruption shock along the Asia to East Coast route via the Panama Canal increases retail output of goods from other routes by 0.1%. In contrast, disruptions along the routes originating in Europe or the Middle East tend have very little spillovers.

The elasticity of retail output to disruptions depends on how retail prices and congestion react to disruptions as shows Proposition B.1 in Appendix B.1. Figures B.4a and B.4b in Appendix B.2.2 display the effect of disruptions on retail prices and congestion. Shipping disruptions increase the retail price consumers pay and have a stronger impact on the price of goods from

FIGURE 6.1.—The impact of shipping disruptions on aggregate output



(a) Elasticity of output to disruptions, $\frac{\partial Y}{\partial X_r}\frac{X_r}{Y}$



(b) Route shares in aggregate output

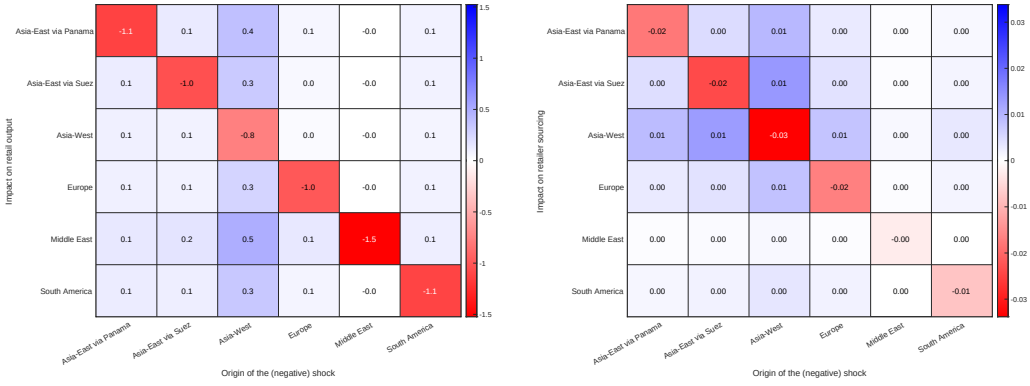
Note: Panel (a) shows the elasticity of aggregate output to shipping disruptions, $\frac{\partial Y}{\partial X_r}\frac{X_r}{Y}$, taking into account the general equilibrium effects. Panel (b) shows each route's share in aggregate output (equivalent to their Domar weight).

the same region of the shock. For instance, a 1% disruption shock tends to raise retail prices of goods from the same region by about 0.05% to 0.4%. Similarly, disruptions tend to reduce congestion along the affected route, diverting ships to competing U.S.-bound routes or leaving them idle, reducing congestion altogether.

Figure 6.2b displays the impact of shipping disruptions on retailers' sourcing decision, $-(\partial o_h/\partial X_r)(X_r/o_h)$. Disruptions lead to a reallocation of retailers to goods transported along different routes. For instance, a 1% increase in disruptions tends to reduce the fraction of retailers sourcing goods from the affected route by about 0.02%, driving them to source goods originating from other routes.

As the proof of 4.1 shows, shipping disruptions also impact aggregate output through the reallocation of consumption toward domestically-produced goods. For instance, a 1% disruption shock increases demand for domestic goods between 0.02% to 1.4%, depending on which route it originates from. Shipping disruptions also reduce incentives to enter the retail market. A 1% disruption shock reduces the number of active retail firms between 0.03% to 1.7%.

FIGURE 6.2.—Intensive and extensive margins of shipping disruptions



(a) Intensive margin: quantity choice

(b) Extensive margin: sourcing choice

Note: Panel (a) displays the elasticity of retail output from goods transported along route h to disruptions along route r, $-(\partial y_h/\partial X_r)(X_r/y_h)$. Panel (b) displays the elasticity of retailers' choice of sourcing goods from route h to disruptions along route r, $-(\partial o_h/\partial X_r)(X_r/o_h)$.

6.2. *Port congestion in the Summer and Fall of 2021*

The summer and fall of 2021 saw a record number of ships waiting at the ports of Los Angeles and Long Beach. This unprecedented strain put massive pressure on the shipping sector, in particular along the Asia to West Coast route. Although port congestion only became news in the summer of 2021, our micro-level estimate of disruptions started signaling a fall in effective shipping supply as early as January 2021, reaching its lowest value by the end of 2021. Shipping productivity along the Asia to West Coast route fell 20 percentage points between November 2020 and November 2021.

To study the aggregate impact of the 2021 shipping disruptions along the Asia to West Coast route, we build a counterfactual economy in which shipping disruptions along that route are absent while preserving all the other parameter values at their baseline levels. In particular, we solve for the values of x_{AW} in each month that keep the shipping productivity, z_{AW}, at its value as of February 2016. We then contrast that counterfactual economy with the baseline economy simulated over time to match the main aggregates. Figure B.5 in Appendix B.2.3 provides the time series evolution.

Our measure of shipping disruptions in February 2016 was 0.953, which was more than 1.5 times larger than the lowest value of z_{AW} at the end 2021. The higher level of z_{AW} is not entirely driven by the exogenous shipping productivity, x_{AW} as the congestion externality also increases. Shipping firms find it optimal to reallocate ships from other Asian routes to the Asia to West Coast route. In contrast, the capacity allocated to Europe, the Middle East, and South America is practically unchanged and more ships stay idle. The increase in capacity allocated

to the Asia to West Coast route drives firms to increase the number of voyages along that route. Instead of 1.7 trips per month at end of 2021, shipping firms would do 2.5 trips. That increase comes at the expense of fewer trips per month along the other Asian routes. The U.S.-bound potential shipping supply increased from 48 million metric tons at the end of 2021 to 57 million metric tons. The effective shipping supply increased in a similar fashion from 34 to 53 million metric tons.

Imports rise thanks the increase in U.S.-bound shipping supply. The import share of GDP increases from less than 12.9% to 14.6% at the end of 2021. That increase is entirely driven by more imports of Asian goods. Sourcing goods from the Asia to West Coast route became more profitable leading more retailers to specialize on these goods. The boost in imports is driven by a 16% decline in the retail price of Asian goods in November 2021. The aggregate price index falls by much less as most goods consumed are produced domestically. The price index falls by 1.7% in November 2021 relative to the baseline economy.

Panel (a) of Figure 6.3 plots the welfare impact of the shipping disruptions related with the West Coast port congestion in 2021. The welfare impact corresponds to the value of $\varepsilon_{\text{ev}_t}$ that solves the following equation for each month t

$$(1+\varepsilon_{\text{ev}_t})u(c_{A_t}^{\text{Baseline}}, c_{E_t}^{\text{Baseline}}, c_{M_t}^{\text{Baseline}}, c_{S_t}^{\text{Baseline}}, d_t^{\text{Baseline}}) = u(c_{A_t}^{\text{Exp}}, c_{E_t}^{\text{Exp}}, c_{M_t}^{\text{Exp}}, c_{S_t}^{\text{Exp}}, d_t^{\text{Exp}}), \quad (6.1)$$

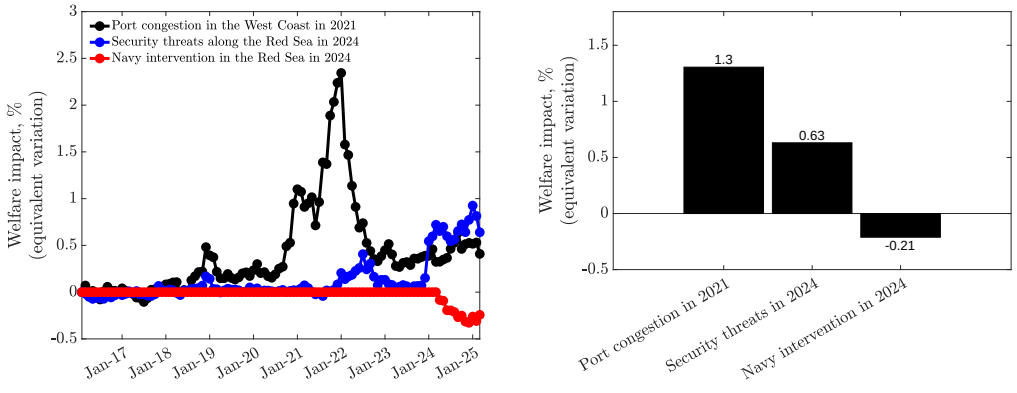
where the left-hand side corresponds to the utility in the baseline economy and the right-hand side to the utility in the counterfactual economy. Given equation (4.20), ε_{ev} measures the change in a consumer's income, at the prices obtained in the baseline economy, that are equivalent to the utility the consumer gets in the counterfactual economy without shipping disruptions. As the utility is higher in a world with lower shipping disruptions, consumers would pay a positive amount to live in the counterfactual economy. For instance, at the peak of our measured shipping disruptions along the Asia to West Coast route in December 2021, consumers would be willing to pay 2.2% of their income in that month to avoid the impact of shipping disruptions.

Panel (b) of Figure 6.3 shows the discounted welfare impact of shipping disruptions measured as the value ε_{ev} that solves the equation

$$(1+\varepsilon_{\text{ev}})\sum_{\tau=t}^{T}\beta^{\tau-t}u(c_{A_t}^{\text{Baseline}}, c_{E_t}^{\text{Baseline}}, c_{M_t}^{\text{Baseline}}, c_{S_t}^{\text{Baseline}}, d_t^{\text{Baseline}}) = \sum_{\tau=t}^{T}\beta^{\tau-t}u(c_{A_t}^{\text{Exp}}, c_{E_t}^{\text{Exp}}, c_{M_t}^{\text{Exp}}, c_{S_t}^{\text{Exp}}, d_t^{\text{Exp}}), \quad (6.2)$$

where β is the consumer's discount factor assumed to be 0.96. The average welfare impact of the shipping disruptions from port congestion for the year of 2021 is 1.3% of GDP.

FIGURE 6.3.—Welfare impact of shipping disruptions



(a) Time-varying equivalent variation (b) Average equivalent variation

Note: Panel (a) shows the welfare impact of shipping disruptions, measured as in equation (6.1), that affected the Asia to West Coast route in the Summer and Fall of 2021 (in black) and the Asia to East Coast route via the Suez Canal and the Middle East to the East Coast due to security threats along the Red Sea in early 2024 (in blue). The red curve measures the welfare impact of the Navy intervention following the Houthi attacks in 2024. Panel (b) shows the average welfare impact of shipping disruptions, measured as in equation (6.2) with a discount factor of 0.96.

6.3. *Security threats in the Red Sea in early 2024*

Attacks on container vessels in the Red Sea began in late 2023 and intensified throughout 2024, forcing shipping companies to reroute vessels away from the Suez Canal to the Cape of Good Hope in order to reach the U.S. ports. We showed in Section 3.3 that this added between 800 to 1,200 nautical miles to the journeys passing through the Suez Canal, corresponding to about 4 to 5 additional days of travel in our sample. Our micro-level estimate of shipping disruptions along the routes from Asia to the East Coast via the Suez Canal and from the Middle East to the East Coast, z_{AS} and z_{ME}, fell from by 21 and 31 percentage points between March 2023 and March 2024.

To study the aggregate impact of the Houthi attacks in the Red Sea in early 2024, we build a counterfactual economy in which shipping disruptions along the Asia to the East Coast via the Suez Canal and from the Middle East to the East Coast routes are absent. That is achieved by solving for the values of x_{AS} and x_{ME} in each month that keep the shipping productivities, z_{AS} and z_{ME}, at their values as of February 2016. Figures B.6 and B.7 in Appendix B.2.4 contrast the counterfactual economy with the baseline economy for each route.

Our micro-level measure of shipping productivity in February 2016 was 0.88 and 0.82 for the routes from Asia via the Suez Canal and from the Middle East to the East Coast. These values are more than 25 percentage points higher than what was measured for 2024. Without the shipping disruptions from the security threats, congestion increases mostly in the route from Asia via the Suez Canal. The increase in congestion is driven by a reallocation of ships from

other Asian routes to the one via the Suez Canal as idle capacity stays about the same as in the baseline economy. Shipping firms increase the number of trips from 1 to about 1.6 a month along the Suez Canal and double the number of trips from the Middle East. Despite the change in the composition of shipping supply away from goods transported along the Asia to the West Coast and to the East via the Panama Canal, the total U.S.-bound potential shipping supply increases modestly from 42 million metric tons to 46 in May 2024.

The import share of GDP in May 2024 rises in the counterfactual economy from 11.2 to 11.8% of GDP driven by more imported goods from Asia and the Middle East. The increase in imports was driven by a fall in the retail price of goods from Asia and the Middle East of 7% and 22% in May 2024 relative to the baseline economy. The retail price of goods from Europe and South American stay practically unchanged. The aggregate price index falls by 0.6% in May 2024 relative to the baseline economy.

Figure 6.3 above plots the welfare impact of the shipping disruptions related with the Houthis attacks in the Red Sea in 2024. As was the case with the port congestion of 2021, consumers would be better off without the security threats in the Red Sea. The welfare cost of the security threats in the Red Sea between March 2024 and March 2025 amounted to 0.6% of GDP. The shipping disruptions in the Summer and Fall of 2021 were considerably more detrimental than the attacks in the Red Sea in early 2024 in part because of the U.S. Navy protection in the Red Sea, which is analyzed next.

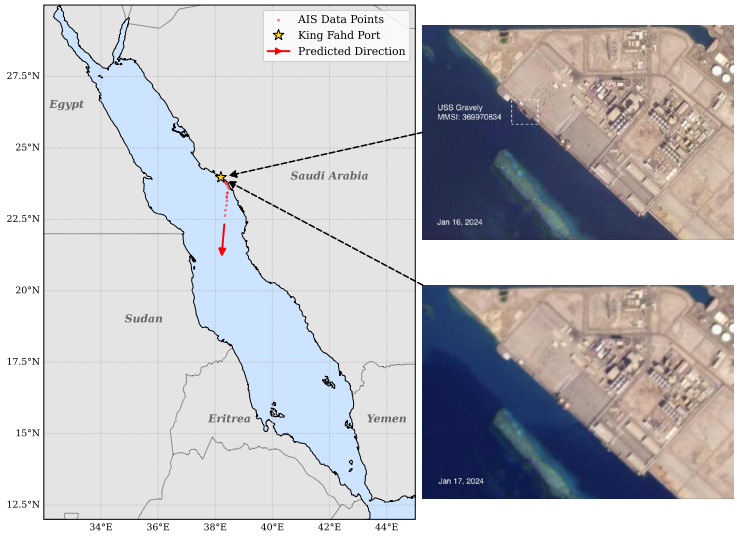
6.4. *The value of Navy's intervention*

Houthis began targeting ships in the Red Sea and the Gulf of Aden in late 2023 and early 2024 using drones and anti-ship cruise missiles against commercial vessels. In response to these attacks, the U.S. Navy and other allies deployed destroyers to patrol the Red Sea and actively shoot down incoming Houthi missiles and drones. To illustrate the tangible and highly mobilized nature of these operations, Figure 6.4 maps the movements of the USS Gravely in the Red Sea on January 17, 2024.[28] This visual evidence captures the destroyer's active patrol routes, underscoring the instrumental military presence required to safeguard this critical shipping corridor. The broader campaign was successful in reducing the Houthi attacks on U.S. vessels, culminating in a ceasefire in May 2025.

The model is now used to provide an estimate of the value of military intervention. We construct a counterfactual economy in which shipping disruptions along routes from Asia to

[28]The USS Gravely played a prominent role in Operation Prosperity Guardian, frequently engaging Houthi anti-ship ballistic missiles and unmanned aerial vehicles to protect critical commercial shipping lanes. Additional figures detailing the USS Gravely's earlier deployment at NSA Bahrain on December 13, 2023, and its subsequent presence at the Port of Duqm in Oman on March 8, 2024, are provided in Appendix A.

FIGURE 6.4.—USS Gravely Operations in the Red Sea (January 17, 2024)



Note: The figure illustrates the movement of the Arleigh Burke-class guided-missile destroyer USS Gravely (DDG 107) utilizing AIS data. Because AIS transmissions for U.S. Navy ships are typically disabled during active military operations for security reasons, the available data are limited and primarily concentrated around periods when the ship was departing for operations or docking afterward. Satellite images are included alongside the map as an external validation to confirm that the USS Gravely was indeed present at the dock of the respective port prior to its departure.

the East Coast via the Suez Canal and from the Middle East to the East Coast would continue to grow throughout 2024 and early 2025. The shipping productivities, z_{AS} and z_{ME}, reached their lowest values in March 2024, dropping 4.5 and 6.1% relative to the previous month. We assume that they keep falling at the same rate until March 2025. Figures B.8 and B.9 in Appendix B.2.5 display these time paths.[29] We then compare this counterfactual economy with the simulated baseline economy.

Figure 6.3 shows the welfare impact of shipping disruptions if the attacks on container ships would have worsened and lasted longer. As consumer welfare is lower without Navy's protection, consumers are now worse off relative to the baseline economy. The value of Navy's support between March 2024 and March 2025 amounted to 0.2% of GDP. The support was not enough to compensate for the entire disruptions as most of the damages started a few months earlier in January 2024.

7. IMPROVING PORT INFRASTRUCTURE

Improvements in port infrastructure have emerged as a first-order priority to overcome shipping disruptions. Recent investments have targeted reductions in turnaround times, the expan-

[29] As before, they are computed by solving for the values of the exogenous component of shipping productivity, x_{AS} and x_{ME}, that deliver the paths of z_{AS} and z_{ME}.

sion of physical capacity, and better inland connectivity. These port upgrades are likely to matter quantitatively as they alleviate congestion, smooth vessel scheduling, and effectively raise the utilization of existing shipping infrastructure. To address these issues, we add the shifter ε_k in the congestion externality in equation (4.6), i.e. $g(K_r) \equiv \varepsilon_k \left(\int_0^N \kappa_r(j) dj \right)^{\phi}$, and reduce its value to analyze the general equilibrium effect of port infrastructure improvements that alleviate congestion. We construct a counterfactual economy in which ports along all routes improve by the same factor and thus set $\varepsilon_k = 0.9$. Table 7.1 contrasts the outcomes from this counterfactual economy with the baseline economy matched to March 2025 aggregates.

Improvements in port infrastructure reduce congestion and lead to an increase in the productivity of shipping firms, allowing them to deliver more goods faster. The effective shipping supply increases by 8% across all routes. Although ε_k falls by 10% relative to the baseline, the congestion factor falls by less than 3%. The reduction in congestion leads firms to reallocate ships that were idle to U.S.-bound routes, with the total share of idle supply decreasing by 1.4%. The fall in congestion also encourages more shipping firms to enter the U.S.-bound routes, with the number of shipping firms increasing by 3.7%. As the productivity of shipping firms increases, the price of shipping services falls. As a result, retailers demand more imported goods, which they sell at a lower price to consumers. The import share of output increases by 4.8% relative to the baseline and retail prices of imported goods from all regions fall by 5.2%. Consumers are better off with port upgrades that decongest shipping routes. They would need an additional 0.733% of their monthly income in the baseline economy to make them as well as in the economy with improvements in port infrastructure. The lower is the congestion externality, the larger are the welfare gains from port improvements.

TABLE 7.1

THE IMPACT OF PORT INFRASTRUCTURE IMPROVEMENTS

		Baseline (1)	$\downarrow \varepsilon_k$ (2)	$\Delta\%$ (3)
Shipping market				
Q_r	Effective shipping supply (in DWT), *Total*	18.942	20.457	8.0
	Asia-East Coast via Panama	2.620	2.831	8.0
	Asia-East Coast via Suez	1.229	1.328	8.1
	Asia-West Coast	9.478	10.234	8.0
	Europe to East Coast	3.852	4.160	8.0
	Middle East to East Coast	0.146	0.158	8.1
	South America to East Coast	1.616	1.746	8.0
N	Number of shipping firms	36.000	37.341	3.7
$N\overline{\kappa}/K$	Idle capacity share	0.754	0.743	-1.4
$g(K_r)$	Congestion factor, *Asia-East Coast via Panama*	35.109	34.134	-2.8
	Asia-East Coast via Suez	28.074	27.297	-2.8
	Asia-West Coast	76.507	74.325	-2.9
	Europe to East Coast	53.651	52.142	-2.8
	Middle East to East Coast	15.958	15.512	-2.8
	South America to East Coast	28.179	27.394	-2.8
n_r	Number of trips/month, *Asia-East Coast via Panama*	0.956	0.962	0.6
	Asia-East Coast via Suez	0.771	0.776	0.6
	Asia-West Coast	1.767	1.777	0.6
	Europe to East Coast	1.359	1.367	0.6
	Middle East to East Coast	0.343	0.346	0.6
	South America to East Coast	0.774	0.779	0.6
p_r	Shipping prices, *Asia-East Coast via Panama*	0.004	0.004	-2.8
	Asia-East Coast via Suez	0.006	0.006	-2.8
	Asia-West Coast	0.004	0.004	-2.9
	Europe to East Coast	0.006	0.006	-2.8
	Middle East to East Coast	0.010	0.010	-2.8
	South America to East Coast	0.005	0.005	-2.8
$N\pi_r$	Shipping profits, *Asia-East Coast via Panama*	0.002	0.002	5.0
	Asia-East Coast via Suez	0.002	0.002	5.1
	Asia-West Coast	0.008	0.008	4.9
	Europe to East Coast	0.005	0.005	5.0
	Middle East to East Coast	0.000	0.000	5.1
	South America to East Coast	0.002	0.002	5.0
Retail market				
$\mathcal{I}$	Measure of retailers	1.000	1.181	18.1
o_r	Specialization, *Asia to East Coast via Panama*	0.166	0.166	0.1
	Asia to East Coast via Suez	0.165	0.165	0.1
	Asia to West Coast	0.173	0.172	-0.4
	Europe to East Coast	0.169	0.169	-0.1
	Middle East to East Coast	0.163	0.164	0.2
	South America to East Coast	0.165	0.165	0.1
ω_o	Import share of output, *Total*	0.113	0.118	4.8
	Asia	0.073	0.076	4.8
	Europe	0.029	0.030	4.8
	Middle East	0.002	0.002	5.0
	South America	0.009	0.010	4.9
P^{tot}/p_d	Retail price (rel. to domestic goods), *All goods*	0.972	0.966	-0.6
P^{imp}/p_d	*Imported goods*	0.017	0.016	-5.2
p_o/p_d	*Asia*	0.005	0.005	-5.2
	Europe	0.007	0.007	-5.2
	Middle East	0.003	0.003	-5.2
	South America	0.004	0.004	-5.2
Welfare				
	Equivalent variation (% of income)		0.733	

Note: The experiment is based on the model calibrated to March 2025 data.

8. TAX POLICY: PORT FEES AND TARIFFS

Motivated by the escalation of the trade war in 2025, we now append a government to this economy to study the role of tariffs and port fees. The 2025 tariffs have led to a substantial increase in the U.S. average effective tariff rate, applied widely across many trading partners. Although some of these duties have been eliminated for agricultural products, the average effective tariff rate was nearly 18% as of October 2025—the highest level since 1934. In October 2025, the U.S. government also started imposing fees on Chinese-built and Chinese-owned vessels. The fee for non-Chinese operators of Chinese-built ships was set to $18 per net ton (or $120 per container) per voyage, while the fee on Chinese-operated ships was $50 per net ton per voyage, both up to a cap of 5 voyages per vessel per year. The fees were later suspended in November 2025 for a year following China's retaliatory fees.

8.1. *The shipping market with tax policy*

To study the impact of tax policies when the shipping market is a key sector shaping the allocation of goods, we now introduce port fees and tariffs in our framework. Let $\mathfrak{f}_o$ denote region-specific port fees and τ_o the region-specific tariff rate on goods originating from region o. The port fees are levied on shipping firms, raising their marginal cost of shipping along route r (equation (4.8)) according to

$$mc_r = \frac{g(K_r)}{x_r}\left[\frac{\overline{p}_n}{1/\zeta}\right]^{1/\zeta}\left[\frac{(\overline{p}_o + \mathfrak{f}_o)}{1/\nu}\right]^{1/\nu}. \tag{8.1}$$

Hence, increases in port fees are passed on to retailers through higher prices of shipping services. Tariffs on the other hand are imposed on retailers. They affect their profit from sourcing goods from route r (equation (4.15)), which is now given by

$$\Pi_r = \max_{\{y_r(j)\}}\left\{p_o\chi_r^{\theta}\left(\int_0^N y_r(j)^{\sigma}dj\right)^{\theta/\sigma} - (1+\tau_o)\int_0^N p_r(j)y_r(j)dj - f\right\}, \tag{8.2}$$

and their demand for imported goods from a shipping firm (equation (4.17)), which is now given by

$$\mathrm{y}_r(j) = o_r\left[\frac{\theta\chi_r^{\sigma}\, p_o y_r^{(1-\sigma/\theta)}}{(1+\tau_o)p_r(j)}\right]^{1/(1-\sigma)}\mathcal{I}. \tag{8.3}$$

Raising tariffs reduces retailers' demand for imported goods as well their profits, ultimately impacting their sourcing decisions.

The government collects the revenue from port fees and tariffs, and rebates it lump sum to consumers, where total revenue T is defined as

$$T = \sum_{o=\{A,E,M,S\}} \sum_{r=\mathcal{R}_o} \left[\int_0^N \mathfrak{f}_o(\ell_r(j)\kappa_r(j))^\nu dj + o_r \mathcal{I} \tau_o \int_0^N p_r(j) y_r(j) dj \right], \quad (8.4)$$

Adding these tax policy instruments also alters the labor market clearing condition.[30]

Tariffs are not necessarily detrimental in this framework. Propositions B.3, B.4, and B.5 in Appendix B.1.4 show why. Tariffs can work like a Pigouvian tax if they can reduce shipping congestion by more than the increase in retail prices. An increase in tariffs on a particular region decreases congestion along routes originating in that same region, as $\frac{\partial g(K_h)}{\partial \tau_o} \frac{\tau_o}{g(K_h)} \leq 0$ (for route h originating in region o), and potentially lead to an increase in congestion on routes originating in other regions. A fall in congestion works as a productivity boost for shipping firms allowing them to supply more goods in a shorter amount of time and at cheaper prices. A fall in the price of shipping services lead to an increase in retail demand, which in turn translates into an increase in retail output, as $\frac{\partial y_h}{\partial p_h(j)} \frac{p_h(j)}{y_h} \leq 0$.

An increase in tariffs on a particular region also puts upward pressure on the retail price of goods from that region as they increase the marginal cost of retailers. If the tariff increase drives the price of shipping services up, then it can lead to an increase in retail prices. If instead the fall in the price of shipping services from reduced congestion dominates the tariff increase, the retail price of goods might eventually fall. As a result, consumers might be better off when tariffs are introduced. Which effect dominates is a quantitative question.

As the propositions show, retail market power can also amplify or dampen the impact of tariffs. If the reduction in congestion dominates the price effect so that an increase in tariffs increases output and reduces retail prices, then the more market power retail firms have (i.e., lower θ) the larger the increase in retail output and the fall in retail prices. If the price effects dominates the reduction in congestion so that an increase in tariffs reduces output and raises retail prices, then the more market power retail firms have the larger is the fall in retail output and the increase in retail prices.

8.2. *Dissecting the effect of tariffs*

We now contrast the baseline economy as of March 2025 with a counterfactual economy in which goods originating from Asia are taxed at a 18% rate. In the economy with tariffs

[30] The labor demanded by domestic firms (equation (4.21)) is now given by $l_d = 1 - \frac{1}{w} \int_0^N \sum_{r \in \mathcal{R}} \left\{ \overline{p}_n n_r(j)^\zeta + \frac{\overline{p}_o}{\nu(\overline{p}_o + \mathfrak{f}_o)} \left[\zeta \overline{p}_n n_r(j)^\zeta - \mu_r(j) \right] + \overline{p}_\kappa \frac{\kappa_r(j)^2}{2} \right\} dj$.

on Asian goods, we proceed with two experiments. First, the congestion externality is raised by 50%, i.e., $\varepsilon_k = 1.5$, which is equivalent to increasing shipping disruptions in all routes by 50%. Second, the retail markup is increased from 25% to 50%, i.e., $\theta = 1/1.5$. Table 8.1 below summarizes the results.

Baseline effect (columns (2)-(3)). Levying tariffs on goods from Asia reduces retailers' demand for goods originating in Asia. This fall in demand drives shipping firms to reduce the prices of shipping services along the routes from Asia by 7%, while the price of shipping services from other regions increased. Lower prices lead to a fall in profits from operating Asian routes (by at least 13%), forcing firms to reallocate ships to more profitable routes. As a result, shipping firms reallocate their capacity to the U.S.-bound routes from Europe, the Middle East, and South America, but also reallocate capacity away from the U.S. towards other non-U.S. routes (the idle capacity share increased by 0.3%).

As there are fewer U.S.-bound ships from Asia, congestion falls across all Asian routes. The decrease in congestion acts like a positive productivity shock. However, as capacity is reduced along these routes, the effective shipping supply from Asian routes decreases by 6.6-9.0%. The number of voyages from Asia also fell by about 8.9-9.7%. As a result, the total effective shipping supply declined by 5% from 18.9 to 18.1 million metric tons despite the increase in supply from non-Asian routes.

We now turn our attention to the retail market. The decline in shipping prices encourages retailers to increase their demand for imported goods, which leads to a slight increase in the total import share of output from 11.3% of GDP to 11.6%. Imports from Europe, the Middle East, and South America surge by 5.4-12.5%. Despite the introduction of the tariff, retail profits increased, encouraging new entrants (59.6% more retailers). Some of these profit gains are passed on to consumers, who now face lower retail prices on all imported goods. The ideal price index of imported goods falls by 3% and that of all goods falls by 0.3%.

Tariff revenues amount to 0.9% of GDP, raising consumer income. As retail prices of imported goods fell and incomes rose, real GDP went up. In this economy, tariffs made consumers better off as they led to a fall in retail prices as shipping firms readjusted their supply and prices across routes.

Shipping disruptions (columns (4)-(5)). We now analyze the economy with tariffs on goods from Asia with a more detrimental impact of congestion on shipping firms. Although capacity fell across most routes, the congestion externality increased significantly (up to 102% along the Asia to West Coast route). The total effective shipping supply almost halved to 11 million metric tons. The shipping supply fell across all routes as shipping firms reduced their capacity and the number of trips declined as it now takes more time to reach U.S. ports. To overcome more

congested routes, shipping firms increase the price of shipping services. The price increase is not enough to compensate for profit losses across most routes.

The increase in the price of shipping services, together with the tariff, pressures retailers to increase their prices, raising retail prices of all imported goods by 11.2%. The increase in retail prices leads to a fall in imports from all regions, with the import share of GDP decreasing by 9%. Tariff revenue totaled 0.8% of GDP, slighly less than in the previous experiment. Levying tariffs on Asian goods made consumers worse off, costing the economy 0.5% of output (in equivalent variation).

Retail market power (columns (6)-(7)). We now study the economy with tariffs on goods from Asia when retail firms have more market power. More retail market power implies that retailers have more leeway to pass on the tariff to consumers. Although the price of shipping services has declined, retail prices have increased. The ideal price index of imported goods increased by 17.7%. As imported goods became more expensive, consumers demand fewer imported goods. The import share declined from 11.3% to 9.8% of GDP. Although tariffs generated 0.6% of GDP in revenues, consumers are worse off. The tariffs with more retail market power had a welfare impact of 0.05% of income.

Weaker retail demand impacts the shipping sector. The effective shipping supply decreased to 14 million metric tons. Shipping firms reduce the number of trips performed in any given month and idle capacity increased, which helped reduce congestion along the Asian routes.

8.3. *Global tariffs of 10%*

We also perform another counterfactual experiment where tariffs are levied on imported goods from all regions at the rate of 10%. Table B.3 in Appendix B.2.6 contrasts that economy with the one with a 18% tariff on Asian goods only.

Imposing a lower tariff rate on all regions makes consumers better off than levying a higher tariff rate on Asian goods only. The tariff revenues as a fraction of GDP are about the same, but they deliver a sharper fall in retail prices (about 5.2% for the bundle of imported goods). The lower retail prices imply a a higher import share (from 11.3 to 11.9% of output).

8.4. *Port fees*

Port fees work in a similar fashion. However, since they are levied on shipping firms they have a weaker transmission mechanism than tariffs levied on retailers (they are rescaled by the value of the cost exponent ν). Appendix B.1.5 provides the theoretical details. Appendix B.2.7 performs a quantitative analysis of the macroeconomic impact of imposing port fees on ships departing from Asia. To obtain an estimate of port fees, $\mathfrak{f}_o$, an implied price per ton per voyage is needed. This is achieved by dividing the value of containerized shipping imports (from the

TABLE 8.1

THE IMPACT OF TARIFFS ON ASIAN GOODS

		Baseline (1)	**Tariffs** (2)	Δ% (3)	↑ ϵ_k (4)	Δ% (5)	↓ θ (6)	Δ% (7)
Shipping market								
Q_r	Effective shipping supply (in DWT), *Total*	18.942	18.059	-4.7	11.031	-41.8	13.979	-26.2
	Asia-EC via Pan.	2.620	2.409	-8.1	1.473	-43.8	1.977	-24.5
	Asia-EC via Suez	1.229	1.119	-9.0	0.684	-44.3	0.984	-19.9
	Asia-West Coast	9.478	8.854	-6.6	5.405	-43.0	6.534	-31.1
	Europe to EC	3.852	3.850	0.0	2.352	-38.9	2.974	-22.8
	Middle East to EC	0.146	0.163	11.1	0.100	-32.0	0.163	11.5
	South Am. to EC	1.616	1.665	3.0	1.018	-37.0	1.347	-16.7
N	Number of shipping firms	36.000	37.587	4.4	40.866	13.5	48.438	34.6
$N\overline{\kappa}/K$	Idle capacity share	0.754	0.757	0.3	0.761	1.0	0.762	1.0
$g(K_r)$	Congestion factor, *Asia-EC via Pan.*	35.109	32.738	-6.8	47.368	34.9	32.196	-8.3
	Asia-EC via Suez	28.074	26.240	-6.5	37.977	35.3	27.120	-3.4
	Asia-West Coast	76.507	70.914	-7.3	102.364	33.8	58.790	-23.2
	Europe to EC	53.651	57.128	6.5	82.562	53.9	52.325	-2.5
	Middle East to EC	15.958	16.315	2.2	23.596	47.9	16.365	2.6
	South Am. to EC	28.179	29.682	5.3	42.933	52.4	28.450	1.0
n_r	Number of trips/month, *Asia-EC via Pan.*	0.956	0.866	-9.4	0.781	-18.3	0.686	-28.3
	Asia-EC via Suez	0.771	0.696	-9.7	0.628	-18.5	0.585	-24.2
	Asia-West Coast	1.767	1.609	-8.9	1.448	-18.0	1.108	-37.3
	Europe to EC	1.359	1.372	1.0	1.237	-9.0	1.017	-25.2
	Middle East to EC	0.343	0.358	4.3	0.323	-5.9	0.317	-7.8
	South Am. to EC	0.774	0.789	1.9	0.712	-8.1	0.612	-20.9
p_r	Shipping prices, *Asia-EC via Pan.*	0.004	0.004	-6.8	0.006	34.9	0.004	-8.3
	Asia-EC via Suez	0.006	0.006	-6.5	0.008	35.3	0.006	-3.4
	Asia-West Coast	0.004	0.004	-7.3	0.006	33.8	0.003	-23.2
	Europe to EC	0.006	0.007	6.5	0.009	53.9	0.006	-2.5
	Middle East to EC	0.010	0.011	2.2	0.015	47.9	0.011	2.6
	South Am. to EC	0.005	0.005	5.3	0.007	52.4	0.005	1.0
$N\pi_r$	Shipping profits, *Asia-EC via Pan.*	0.002	0.002	-14.3	0.002	-24.2	0.002	-30.8
	Asia-EC via Suez	0.002	0.001	-14.9	0.001	-24.6	0.001	-22.6
	Asia-West Coast	0.008	0.007	-13.4	0.006	-23.7	0.004	-47.0
	Europe to EC	0.005	0.005	6.4	0.004	-6.0	0.004	-24.7
	Middle East to EC	0.000	0.000	13.6	0.000	0.6	0.000	14.4
	South Am. to EC	0.002	0.002	8.5	0.001	-4.1	0.001	-15.9
Retail market								
$\mathcal{I}$	Measure of retailers	1.000	1.596	59.6	2.879	187.9	3.429	242.9
o_r	Specialization, *Asia to EC via Pan.*	0.166	0.166	0.1	0.166	0.3	0.166	0.4
	Asia to EC via Suez	0.165	0.165	0.4	0.166	0.8	0.166	0.8
	Asia to West Coast	0.173	0.170	-1.2	0.169	-2.4	0.169	-2.3
	Europe to EC	0.169	0.168	-0.4	0.167	-0.8	0.168	-0.7
	Middle East to EC	0.163	0.164	0.7	0.166	1.4	0.165	1.2
	South Am. to EC	0.165	0.165	0.4	0.166	0.8	0.166	0.7
ω_o	Import share of output, *Total*	0.113	0.116	2.7	0.103	-9.0	0.098	-13.5
	Asia	0.073	0.073	0.7	0.065	-10.8	0.060	-17.4
	Europe	0.029	0.031	5.4	0.027	-6.6	0.026	-11.1
	Middle East	0.002	0.002	12.5	0.002	0.0	0.003	35.0
	South America	0.009	0.010	7.4	0.009	-4.6	0.009	-0.7
P^{tot}/p_d	Retail price (rel. to domestic goods), *All goods*	0.972	0.968	-0.3	0.983	1.1	0.989	1.7
P^{imp}/p_d	*Imported*	0.017	0.017	-3.0	0.019	11.2	0.020	17.7
p_o/p_d	*Asia*	0.005	0.005	-2.3	0.006	11.9	0.006	19.5
	Europe	0.007	0.007	-3.8	0.008	10.2	0.008	16.6
	Middle East	0.003	0.003	-5.9	0.003	7.7	0.003	1.4
	South Am.	0.004	0.004	-4.4	0.004	9.4	0.004	12.3
Government								
T/Y	Tax revenues (% of GDP)		0.894		0.792		0.611	
Welfare								
	Equivalent variation (% of income, rel. to baseline)		1.334		-0.536		-0.052	

Note: The experiment is based on the model calibrated to March 2025 data.

Census) by our measure of effective shipping supply by region. The implied price per ton per trip for ships originating from Asia corresponds to about \$5,000. Hence, a fee of \$50 per ton per voyage would represent 1% of the implied price per ton per voyage. The model counterpart for the price per ton per voyage is $\overline{p}_o$. We thus set $\mathfrak{f}_o = 0.01 \times \overline{p}_o$.

9. Conclusion

This paper has shown that disruptions in the container shipping sector had a major impact on the U.S. economy. Using vessel-level AIS records for every container ship arriving at a U.S. port from January 2016 to March 2025, we decompose the gap between potential and effective shipping supply into four wedges: port congestion, canal bottlenecks, rerouting, and slow steaming. We show that shipping disruptions absorbed a large share of the U.S.-bound potential supply.

We embed these facts in a multi-route general equilibrium model with monopolistically competitive shipping firms and endogenous congestion externalities, and use it to run three sets of counterfactuals. The welfare cost of the 2021 West Coast port congestion was 1.3% of GDP. The 2024 Houthi attacks on Red Sea shipping cost 0.6% of GDP—a smaller figure that partly reflects the mitigating role of the U.S. Navy, whose intervention we value at 0.2% of GDP. On trade policy, we show that tariffs can raise consumer welfare by decongesting shipping routes, but this result hinges critically on the severity of congestion and the degree of retail market power; under plausible alternative parameterizations, the same tariff is welfare-reducing.

References

G. Alessandria, S. Y. Khan, A. Khederlarian, C. Mix, and K. J. Ruhl. The Aggregate Effects of Global and Local Supply Chain Disruptions: 2020-2022. *Journal of International Economics*, 146:103788, 2023. [4]

M. Amiti, S. J. Redding, and D. E. Weinstein. The Impact of the 2018 Tariffs on Prices and Welfare. *Journal of Economic Perspectives*, 33(4):187–210, 2019. [4]

J. Asturias. Endogenous Transportation Costs. *European Economic Review*, 123:103366, 2020. [3]

X. Bai, Z. Ma, Y. Hou, Y. Li, and D. Yang. A Data-Driven Iterative Multi-Attribute Clustering Algorithm and Its Application in Port Congestion Estimation. *IEEE Transactions on Intelligent Transportation Systems*, 24(11): 12026–12037, 2023. [13]

X. Bai, J. Fernández-Villaverde, Y. Li, and F. Zanetti. The Causal Effects of Global Supply Chain Disruptions on Macroeconomic Outcomes: Evidence and Theory. Working Paper 32098, National Bureau of Economic Research, 2024. [4, 13]

D. R. Baqaee and E. Farhi. The Macroeconomic Impact of Microeconomic Shocks: Beyond Hulten's Theorem. *Econometrica*, 87(4):1155–1203, 2019. [31]

G. Brancaccio, M. Kalouptsidi, and T. Papageorgiou. Geography, Transportation, and Endogenous Trade Costs. *Econometrica*, 88(2):657–691, 2020. [3, 6]

G. Brancaccio, M. Kalouptsidi, and T. Papageorgiou. Investment in Infrastructure and Trade: The Case of Ports. Working Paper 32503, National Bureau of Economic Research, 2024. [3]

G. Brancaccio, M. Kalouptsidi, and T. Papageorgiou. Rigidities in Transportation and Supply Chain Disruptions. *AEA Papers and Proceedings*, 115:543–50, 5 2025. . [3]

Bureau of Transportation Statistics. On National Maritime Day and Every Day, U.S. Economy Relies on Waterborne Shipping. Data Spotlights, 2021. [5]

Y. Carrière-Swallow, P. Deb, D. Furceri, D. Jiménez, and J. D. Ostry. Shipping Costs and Inflation. *Journal of International Money and Finance*, 130:102771, 2023. [4]

A. K. Coşar and B. Demir. Shipping Inside the Box: Containerization and Trade. *Journal of International Economics*, 114:331–345, 2018. [3]

B. De Borger, S. Proost, and K. Van Dender. Port Activities, Hinterland Congestion, and Optimal Government Policies: The Role of Vertical Integration in Logistic Operations. *Journal of Transport Economics and Policy*, 45 (2):247–275, 2011. [4]

J. Dunn and F. Leibovici. Navigating the Waves of Global Shipping: Drivers and Aggregate Implications. Working Paper 2023-002, Federal Reserve Bank of St. Louis, 2023. [3, 8]

P. D. Fajgelbaum, P. K. Goldberg, P. J. Kennedy, and A. K. Khandelwal. The Return to Protectionism. *The Quarterly Journal of Economics*, 135(1):1–55, 2020. [4]

R. C. Feenstra, P. Luck, M. Obstfeld, and K. N. Russ. In Search of the Armington Elasticity. *The Review of Economics and Statistics*, 100(1):135–150, 2018. [32, 34]

S. Ganapati, W. F. Wong, and O. Ziv. Entrepôt: Hubs, Scale, and Trade Costs. *American Economic Journal: Macroeconomics*, 16(4):239–78, 10 2024. . [3]

R. Greenwood and S. G. Hanson. Waves in Ship Prices and Investment. *The Quarterly Journal of Economics*, 130 (1):55–109, 2015. [3]

C. R. Hulten. Growth Accounting With Intermediate Inputs. *The Review of Economic Studies*, 45(3):511–518, 1978. [30]

D. Hummels and A. Skiba. Shipping the Good Apples Out? An Empirical Confirmation of the Alchian-Allen Conjecture. *Journal of Political Economy*, 112(6):1384–1402, 2004. [3]

M. Isaacson and H. Rubinton. Shipping Prices and Import Price Inflation. *Federal Reserve Bank of St. Louis Review*, 105(4):274–288, 2023. [4]

M. Kalouptsidi. Time to Build and Fluctuations in Bulk Shipping. *American Economic Review*, 104(2):564–608, 2014. [3]

T. C. Koopmans. *Tanker Freight Rates and Tankship Building: An Analysis of Cyclical Fluctuations*. De Erven F. Bohn N.V., Haarlem, 1939. [5]

N. Limão and A. J. Venables. Infrastructure, Geographical Disadvantage, Transport Costs, and Trade. *The World Bank Economic Review*, 15(3):451–479, 2001. [3]

V. Lugovskyy, A. Skiba, and D. Terner. Unintended Consequences of Environmental Regulation of Maritime Shipping: Carbon Leakage to Air Shipping. *Journal of International Economics*, 155:104081, 2025. ISSN 0022-1996. . [4]

T. Notteboom, A. Pallis, and J.-P. Rodrigue. *Port Economics, Management and Policy*. Routledge, London, 1 edition, 2022. [12]

T. Notteboom, H. Haralambides, and K. Cullinane. The Red Sea Crisis: Ramifications for Vessel Operations, Shipping Networks, and Maritime Supply Chains. *Maritime Economics & Logistics*, 26(1):1–20, 2024. [4]

M. Stopford. *Maritime Economics*. Routledge, London, 3 edition, 2008. [3, 4, 5]

S. P. Strandenes and P. B. Marlow. Port Pricing and Competitiveness in Short Sea Shipping. *International Journal of Transport Economics*, 27(3):315–334, 2000. [4]

J. Tinbergen. Scheepsruimte en Vrachten. *De Nederlandsche Conjunctuur*, 3:23–35, 1934. [5]

UNCTAD. Review of Maritime Transport 2022. United Nations Conference on Trade and Development, 2022. [10, 11]

UNCTAD. Review of Maritime Transport 2024. United Nations Conference on Trade and Development, 2024. [5]

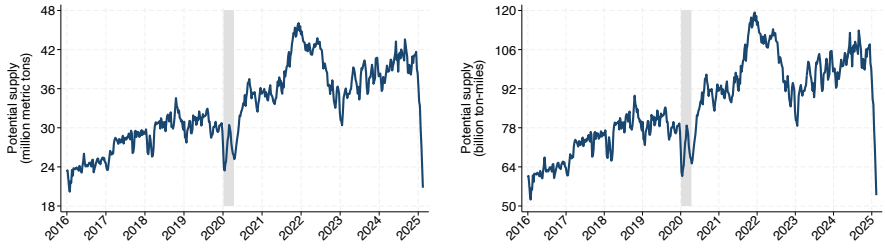
T. Wergeland. Norbulk: A Simulation Model of Bulk Market Freight Rates. Working Paper 12, Norwegian School of Economics and Business Administration, Bergen, 1981. [5]

W. F. Wong. The Round Trip Effect: Endogenous Transport Costs and International Trade. *American Economic Journal: Applied Economics*, 14(4):127–166, 2022. [3]

ONLINE APPENDIX

A: EMPIRICS

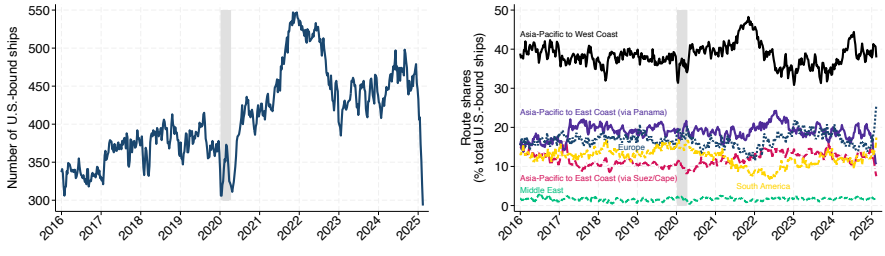
FIGURE A.1.—Potential supply from unique container ships on U.S.-bound routes, 2016-2025



(a) Potential supply (tons) (b) Potential supply (ton-miles)

Note: This figure plots aggregate potential shipping supply in million metric tons (Panel A.1a) and billion ton-miles (Panel A.1b). Estimates are derived from the set of unique container ships operating on U.S.-bound routes. Shaded areas indicate recessions.

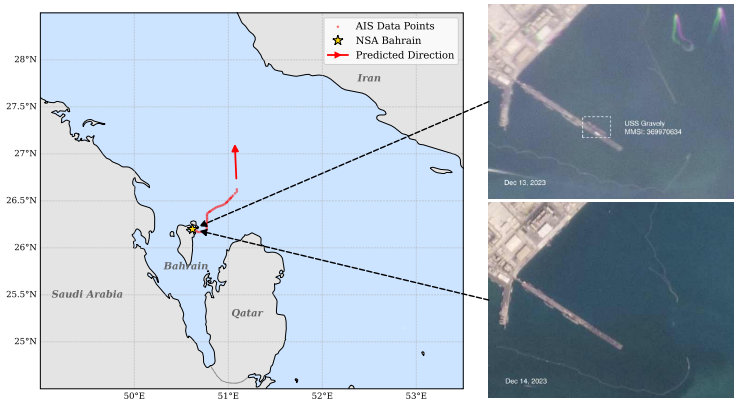
FIGURE A.2.—U.S.-bound container ships, 2016-2025



(a) Total Quantity (b) Route Shares

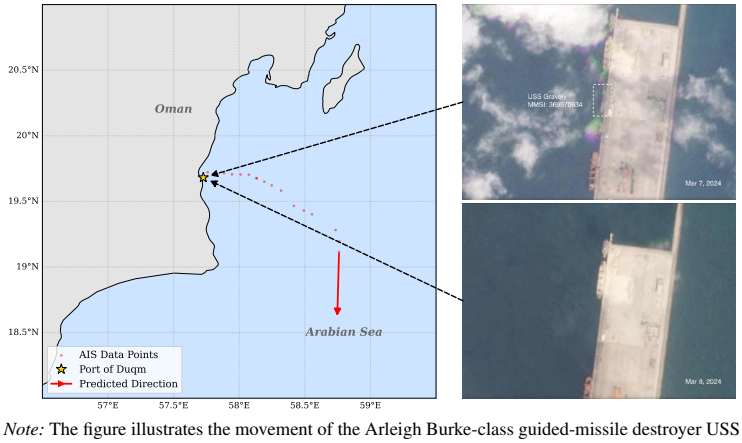
Note: Panel A.2a plots the total number of container ships operating on U.S.-bound routes. Panel A.2b shows the share of ships by specific route. Shaded areas indicate recessions.

FIGURE A.3.—USS Gravely near NSA Bahrain (December 13, 2023)



Note: The figure illustrates the movement of the Arleigh Burke-class guided-missile destroyer USS Gravely (DDG 107) near Naval Support Activity (NSA) Bahrain utilizing AIS data.

FIGURE A.4.—USS Gravely near the Port of Duqm, Oman (March 8, 2024)



Note: The figure illustrates the movement of the Arleigh Burke-class guided-missile destroyer USS Gravely (DDG 107) near the Port of Duqm in Oman utilizing AIS data.

B: MODEL

B.1. *Proofs and additional theoretical results*

B.1.1. *Proof of Proposition 4.1 (Impact of shipping disruptions on aggregate output)*

Real aggregate output in this economy is equivalent to aggregate consumption, $Y \equiv \left[\gamma_d d^{\varrho} + (1-\gamma_d)c^{\varrho}\right]^{1/\varrho}$. Applying the chain rule, the elasticity of aggregate output to route-r aggregate shipping productivity, $\left(\partial Y/\partial X_r\right)/\left(X_r/Y\right)$, where the route-$r$ aggregate productivity is defined as $X_r \equiv \left[\int_0^N x_r(j)^{\sigma/(1-\sigma)}dj\right]^{(1-\sigma)/\sigma}$, is given by

$$\frac{\partial Y}{\partial X_r}\frac{X_r}{Y} = \left(\frac{\partial Y}{\partial d}\frac{d}{Y}\right)\left(\frac{\partial d}{\partial X_r}\frac{X_r}{d}\right) + \left(\frac{\partial Y}{\partial c}\frac{c}{Y}\right)\left\{\sum_{o\in\{A,E,M,S\}}\left(\frac{\partial c}{\partial c_o}\frac{c_o}{c}\right)\right. \tag{B.1}$$

$$\left.\times\sum_{h|o}\omega_h\left[\left(\frac{\partial y_h}{\partial X_r}\frac{X_r}{y_h}\right) + \left(\frac{\partial o_h}{\partial X_r}\frac{X_r}{o_h}\right) + \left(\frac{\partial \mathcal{I}}{\partial X_r}\frac{X_r}{\mathcal{I}}\right)\right]\right\},$$

where $\omega_h \equiv o_h y_h/c_o$ is the share of route h goods in the consumption of goods from region o. As there is only one route for goods from Europe, the Middle East, and South America to arrive to the U.S., $\omega_h = 1$ for $o \in \{E, M, S\}$.

From the consumer's first-order conditions, it is straightforward to deduce that

$$\frac{\partial Y}{\partial d}\frac{d}{Y} = \frac{p_d d}{w+\Lambda} \equiv \text{Domestic share in aggregate output},$$

$$\frac{\partial Y}{\partial c}\frac{c}{Y} = \frac{P^{\text{imp}}c}{w+\Lambda} \equiv \text{Total import share in aggregate output},$$

and

$$\frac{\partial c}{\partial c_o}\frac{c_o}{c} = \frac{p_o c_o}{P^{\text{imp}}c} \equiv \text{Region } o\text{'s import share of total imports},$$

where $P^{\text{imp}} \equiv \left(\sum_{o\in\mathcal{O}}\gamma_o^{1/(1-\rho)}p_o^{\rho/(\rho-1)}\right)^{(\rho-1)/\rho}$ is the imported goods price index. The route's Domar weight is then simply given by

$$\text{Route } h\text{'s share in aggregate output} \equiv \frac{\partial Y}{\partial c}\frac{c}{Y} \times \frac{\partial c}{\partial c_o}\frac{c_o}{c} \times \frac{o_h y_h \mathcal{I}}{c_o}$$

The impact of shipping disruptions along route r on the consumption of and spending on domestic goods depend on how the shipping disruptions affect the labor demanded by producers

of domestic goods through general equilibrium effects. This in turn depends on how shipping profits and entry are affected by the disruptions. Similarly, the impact of shipping disruptions on the number of retailers depends on the free-entry condition in the retail sector.

B.1.2. *Proposition B.1 (Impact of shipping disruptions on retailers' output and sales)*

PROPOSITION B.1: (IMPACT OF SHIPPING DISRUPTIONS ON RETAILERS' OUTPUT AND SALES) A one percent increase in shipping productivity along route r raises retailers' output and sales from that same route by

$$\frac{\partial p_o y_r}{\partial X_r}\frac{X_r}{p_o y_r} = \frac{\partial y_r}{\partial X_r}\frac{X_r}{y_r} \approx \frac{\theta}{1-\theta} > 0.$$

In contrast, a one percent increase in shipping productivity along route r has no effect on retailers' output and sales from other routes, i.e.,

$$\frac{\partial p_{\hat{o}} y_h}{\partial X_r}\frac{X_r}{p_{\hat{o}} y_h} = \frac{\partial y_h}{\partial X_r}\frac{X_r}{y_h} \approx 0.$$

PROOF: Start with retailers' demand for the shipping service provided by firm j along route r conditional on their optimal choice of specialization

$$y_r(j) = \left[\frac{\sigma\theta\chi_r^{\sigma}\, p_o y_r^{(1-\sigma/\theta)} x_r(j)}{g(K_r)\left(\frac{\overline{p}_n}{1/\zeta}\right)^{1/\zeta}\left(\frac{\overline{p}_o}{1/\nu}\right)^{1/\nu}}\right]^{1/(1-\sigma)},$$

where the price of the shipping services was replaced by the firm's markup and marginal cost and, for simplicity, an interior solution for the shipping firm's optimal loading was assumed. Exponentiate both sides, aggregate over all shipping firms, and rearrange to obtain retailers' supply conditional on their optimal choice of specialization, or

$$y_r = \left[\frac{\sigma\theta\chi_r\, p_o X_r}{g(K_r)\left(\frac{\overline{p}_n}{1/\zeta}\right)^{1/\zeta}\left(\frac{\overline{p}_o}{1/\nu}\right)^{1/\nu}}\right]^{\theta/(1-\theta)}$$

as well as their sales

$$p_o y_r = \left[\frac{\sigma\theta\chi_r p_o^{1/\theta} X_r}{g(K_r)\left(\frac{\overline{p}_n}{1/\zeta}\right)^{1/\zeta}\left(\frac{\overline{p}_o}{1/\nu}\right)^{1/\nu}} \right]^{\theta/(1-\theta)}.$$

The impact of shipping disruptions on retailers' output of goods from the disrupted route is given by

$$\frac{\partial y_r}{\partial X_r}\frac{X_r}{y_r} = \frac{\theta}{1-\theta}\left(1 + \frac{\partial p_o}{\partial X_r}\frac{X_r}{p_o} - \frac{\partial g(K_r)}{\partial X_r}\frac{X_r}{g(K_r)}\right),$$

and on retailers' output of goods from different routes is

$$\frac{\partial y_h}{\partial X_r}\frac{X_r}{y_h} = \frac{\theta}{1-\theta}\left(\frac{\partial p_{\hat{o}}}{\partial X_r}\frac{X_r}{p_{\hat{o}}} - \frac{\partial g(K_h)}{\partial X_r}\frac{X_r}{g(K_h)}\right),$$

where $p_{\hat{o}}$ is the retail price of the goods associated with route $h \neq r$. As long as $(\partial p_o/\partial X_r)(X_r/p_o) - (\partial g(K_r)/\partial X_r)(X_r/g(K_r)) \approx 0$ and $(\partial p_{\hat{o}}/\partial X_r)(X_r/p_{\hat{o}}) - (\partial g(K_h)/\partial X_r)(X_r/g(K_h)) \approx 0$, then $(\partial y_r/\partial Z_r)(Z_r/y_r) \approx \theta/(1-\theta)$ and $(\partial y_h/\partial Z_r)(Z_r/y_h) \approx 0$.

Q.E.D.

B.1.3. *Proposition B.2 (Impact of shipping disruptions on retail sourcing)*

PROPOSITION B.2: (IMPACT OF SHIPPING DISRUPTIONS ON RETAIL SOURCING) A one percent increase in shipping productivity along route r raises the share of retailers sourcing goods from that same route by

$$\frac{\partial o_r}{\partial X_r}\frac{X_r}{o_r} \approx \lambda\frac{\theta}{1-\theta}(\Pi_r + f) > 0,$$

where retailers' profit from selling goods transported along route r (net of the fixed cost) is $\Pi_r + f = (1-\theta)\left[\frac{\sigma\theta\chi_r p_o^{1/\theta} X_r}{g(K_r)\left(\frac{w}{1/\zeta}\right)^{1/\zeta}\left(\frac{\overline{p}_o}{1/\nu}\right)^{1/\nu}}\right]^{\theta/(1-\theta)}$. A one percent increase in shipping productivity along route r decreases the share of retailers sourcing goods from other routes according to

$$\frac{\partial o_h}{\partial X_r}\frac{X_r}{o_h} \approx -o_r\lambda\frac{\theta}{1-\theta}(\Pi_r + f) < 0,$$

where the optimal sourcing choice, o_r, is given by equation (4.16).

PROOF: Using retailers' first-order conditions, the profit from producing goods from route r conditional on their sourcing decision is

$$\Pi_r = (1-\theta)\left[\frac{\sigma\theta\chi_r p_o^{1/\theta} X_r}{g(K_r)\left(\frac{\overline{p}_n}{1/\zeta}\right)^{1/\zeta}\left(\frac{\overline{p}_o}{1/\nu}\right)^{1/\nu}}\right]^{\theta/(1-\theta)} - f.$$

The impact of route-r shipping disruptions on retailers' sourcing choice of goods transported along route h is given by

$$\begin{aligned}\frac{\partial o_h}{\partial X_r}\frac{X_r}{o_h} &= \lambda X_r\left(\frac{\partial \Pi_h}{\partial X_r} - \sum_\kappa o_\kappa \frac{\partial \Pi_\kappa}{\partial X_r}\right)\\ &= \lambda(1-\theta)X_r\left(\frac{\partial p_{\tilde{o}} y_h}{\partial X_r} - \sum_\kappa o_\kappa \frac{\partial p_{\tilde{o}} y_\kappa}{\partial X_r}\right)\end{aligned}$$

Ceteris paribus, the first-order effect of shipping disruptions on the share of retailers sourcing goods from route r is

$$\frac{\partial o_r}{\partial X_r}\frac{X_r}{o_r} \approx \lambda\theta p_o y_r = \lambda\frac{\theta}{1-\theta}(\Pi_r + f),$$

and the first-order effect of shipping disruptions on the share of retailers sourcing goods from routes $\kappa \neq r$ is given by

$$\frac{\partial o_\kappa}{\partial X_r}\frac{X_r}{o_\kappa} = -o_r\lambda\theta p_o y_r = -o_r\lambda\frac{\theta}{1-\theta}(\Pi_r + f),$$

where o_r is given by equation (4.16). Note that the weighted sum of these elasticities is such that $\sum_h o_h\left(\frac{\partial o_h}{\partial X_r}\frac{X_r}{o_h}\right) = 0$.

Q.E.D.

B.1.4. *The impact of tariffs on aggregate output*

PROPOSITION B.3: (IMPACT OF TARIFFS ON AGGREGATE OUTPUT) The elasticity of aggregate output to tariffs on goods from region $o \in \mathcal{O}$ is given by

$$\frac{\partial Y}{\partial \tau_o}\frac{\tau_o}{Y} = \left(\substack{\text{Domestic share in}\\ \text{aggregate output}}\right)\left(\frac{\partial d}{\partial \tau_o}\frac{\tau_o}{d}\right) + \sum_{h\in\mathcal{R}}\left(\substack{\text{Route } h\text{'s share in}\\ \text{aggregate output}}\right)\times\left(\frac{\partial y_h}{\partial \tau_o}\frac{\tau_o}{y_h} + \frac{\partial o_h}{\partial \tau_o}\frac{\tau_o}{o_h} + \frac{\partial \mathcal{I}}{\partial \tau_o}\frac{\tau_o}{\mathcal{I}}\right),$$

where $\left(\substack{\text{Domestic share in}\\ \text{aggregate output}}\right) = p_d d/(w+\Lambda+T)$ and $\left(\substack{\text{Route } h\text{'s share in}\\ \text{aggregate output}}\right) = o_h y_h \mathcal{I}/(w+\Lambda+T)$.

PROOF: Straightforward from the proof of Proposition B.1.1. *Q.E.D.*

PROPOSITION B.4: (IMPACT OF TARIFFS ON RETAILERS' OUTPUT AND SALES) The elasticity of retail output to tariffs is

$$\frac{\partial y_h}{\partial \tau_o}\frac{\tau_o}{y_h} = \begin{cases} -\frac{\theta}{1-\theta}\left(\frac{\tau_o}{1+\tau_o} + \frac{\partial g(K_h)}{\partial \tau_o}\frac{\tau_o}{g(K_h)} - \frac{\partial p_o}{\partial \tau_o}\frac{\tau_o}{p_o}\right) & \text{if route } h\text{'s origin} = o \\ -\frac{\theta}{1-\theta}\left(\frac{\partial g(K_h)}{\partial \tau_o}\frac{\tau_o}{g(K_h)} - \frac{\partial p_{\hat{o}}}{\partial \tau_o}\frac{\tau_o}{p_{\hat{o}}}\right) & \text{if route } h\text{'s origin} \neq o, \end{cases}$$

where $p_{\hat{o}}$ is the retail price of the goods associated with route h when the region of origin is not o.

PROOF: Retail output of goods sourced from route h with port fees, $\mathfrak{f}_o$, and tariffs, τ_o, is now given by

$$y_h = \left[\frac{\sigma\theta\chi_h\, p_o X_h}{(1+\tau_o)g(K_h)\left(\frac{\overline{p}_n}{1/\zeta}\right)^{1/\zeta}\left(\frac{\overline{p}_o + \mathfrak{f}_o}{1/\nu}\right)^{1/\nu}}\right]^{\theta/(1-\theta)}$$

XXX

Q.E.D.

Hence, an increase in tariffs does not necessarily reduce retail output. The impact depends on how it affects retail prices and congestion across all routes. An increase in tariffs on region o puts upward pressure on the retail price of goods from that same region, i.e., $\frac{\partial p_o}{\partial \tau_o}\frac{\tau_o}{p_o} \geq 0$. An increase in retail prices encourages retailers to supply more goods. An increase in retail prices encourages retailers to supply more goods as $\frac{\partial y_h}{\partial p_o}\frac{p_o}{y_h} > 0$.

An increase in tariffs on a particular region should decrease congestion along routes originating in that same region as $\frac{\partial g(K_h)}{\partial \tau_o}\frac{\tau_o}{g(K_h)} \leq 0$ and potentially lead to an increase in congestion on routes originating in other regions. A fall in congestion works like a productivity boost for shipping firms allowing them to supply more goods in a shorter amount of time and at cheaper prices. This in turn should lead to an increase in retail output as $\frac{\partial y_h}{\partial p_h(j)}\frac{p_h(j)}{y_h} > 0$.

PROPOSITION B.5: (IMPACT OF TARIFFS ON RETAIL SOURCING) The elasticity of retailers' sourcing decision to tariffs is given by

$$\frac{\partial o_h}{\partial \tau_o}\frac{\tau_o}{o_h} = \lambda(1-\theta)\tau_o\left(\frac{\partial p_{\tilde{o}} y_h}{\partial \tau_o} - \sum_{\kappa} o_\kappa \frac{\partial p_{\tilde{o}} y_\kappa}{\partial \tau_o}\right).$$

PROOF: Retail profit from sourcing goods from route h is

$$\Pi_h = (1-\theta)\left[\frac{\sigma\theta\chi_h p_o^{1/\theta} X_h}{(1+\tau_o)g(K_h)\left(\frac{\overline{p}_n}{1/\zeta}\right)^{1/\zeta}\left(\frac{\overline{p}_o+\mathfrak{f}_o}{1/\nu}\right)^{1/\nu}}\right]^{\theta/(1-\theta)} - f.$$

Q.E.D.

The higher is

B.1.5. *The impact of port fees on aggregate output*

PROPOSITION B.6: (IMPACT OF PORT FEES ON AGGREGATE OUTPUT) The first-order impact of port fees on Asian ships on aggregate output is

$$\frac{\partial Y}{\partial \mathfrak{f}_A}\frac{\mathfrak{f}_A}{Y} = -\left(\begin{smallmatrix}\text{Asia import share}\\ \text{of output}\end{smallmatrix}\right) \times \left(\frac{\theta}{1-\theta}\right)\frac{\mathfrak{f}_A}{\nu(\overline{p}_A+\mathfrak{f}_A)}\left[1+\lambda(1-\theta)D\right],$$

where $D \equiv D(o_{AP}, o_{AS}, o_{AW}, \omega_{AP}, \omega_{AS}, \omega_{AW}, p_A c_A)$.

PROOF: The first-order impact of a tariff on Asian goods is given by

$$\frac{\partial Y}{\partial \mathfrak{f}_A}\frac{\mathfrak{f}_A}{Y} = \left(\frac{p_A c_A}{w+\Lambda+T}\right)\left\{\sum_{h\in\{AP,AS,AW\}}\omega_h\left[\left(\frac{\partial p_A y_h}{\partial \mathfrak{f}_A}\frac{\mathfrak{f}_A}{p_A y_h}\right)+\left(\frac{\partial o_h}{\partial \mathfrak{f}_A}\frac{\mathfrak{f}_A}{o_h}\right)\right]\right\}, \quad \text{(B.2)}$$

where the elasticity of retail sales to port fees is

$$\frac{\partial p_A y_h}{\partial \mathfrak{f}_A}\frac{\mathfrak{f}_A}{p_A y_h} = -\left(\frac{\theta}{1-\theta}\right)\left(\frac{\mathfrak{f}_A}{\nu(\overline{p}_A+\mathfrak{f}_A)}\right),$$

and the elasticity of retail specialization to port fees is

$$\begin{aligned}\frac{\partial o_h}{\partial \mathfrak{f}_A}\frac{\mathfrak{f}_A}{o_h} &= \lambda(1-\theta)p_A y_h\left(\frac{\partial p_A y_h}{\partial \tau_A}\frac{\tau_A}{p_A y_h} - o_h\sum_{\kappa\neq h}\frac{\omega_\kappa}{\omega_h}\frac{\partial p_A y_\kappa}{\partial \tau_A}\frac{\tau_A}{p_A y_\kappa}\right)\\ &= -\lambda\theta\left(\frac{\mathfrak{f}_A}{\nu(\overline{p}_A+\mathfrak{f}_A)}\right)\left(\frac{\omega_h}{o_h}-(1-\omega_h)\right)p_A c_A.\end{aligned}$$

Replacing these elasticities in equation (B.2) yields the expression in the main text.

Q.E.D.

B.2. *Quantitative analysis*

B.2.1. *Calibration and simulation*

TABLE B.1

AVERAGE NUMBER OF TRIPS AND AVERAGE SPEED

	Log(Average Number of Trips per Vessel)		
	(1)	(2)	(3)
Log(Average Sailing Speed)	-0.854***	0.021	0.036*
	(0.056)	(0.018)	(0.020)
Route FE	No	Yes	Yes
Year FE	No	No	Yes
Month FE	No	No	Yes
Observations	582	582	582
R^2	0.354	0.959	0.961

Note: Robust standard errors in parentheses. *** p<0.01, ** p<0.05, * p<0.1.

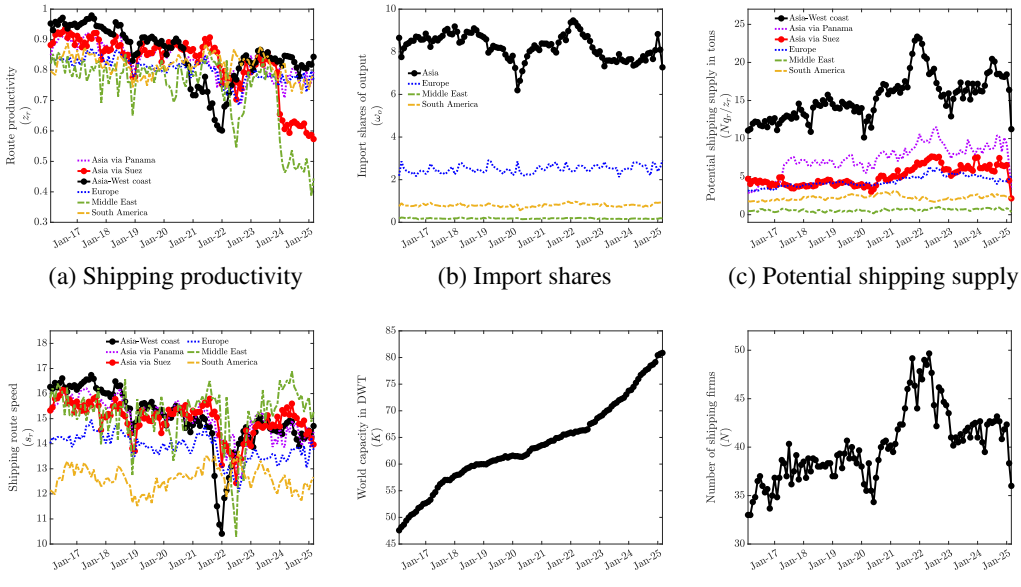
TABLE B.2

TOTAL PORT CONGESTION TIME AND TOTAL NUMBER OF PORT CALLS

	Log(Total Congestion Time)		
	(1)	(2)	(3)
Log(Total Port Calls)	0.940***	1.383***	1.809***
	(0.022)	(0.083)	(0.086)
Port FE	No	Yes	Yes
Year FE	No	No	Yes
Month FE	No	No	Yes
Observations	4,584	4,584	4,584
R^2	0.376	0.750	0.778

Note: Robust standard errors in parentheses. *** p<0.01, ** p<0.05, * p<0.1.

FIGURE B.1.—Targeted time series, 2017-2025

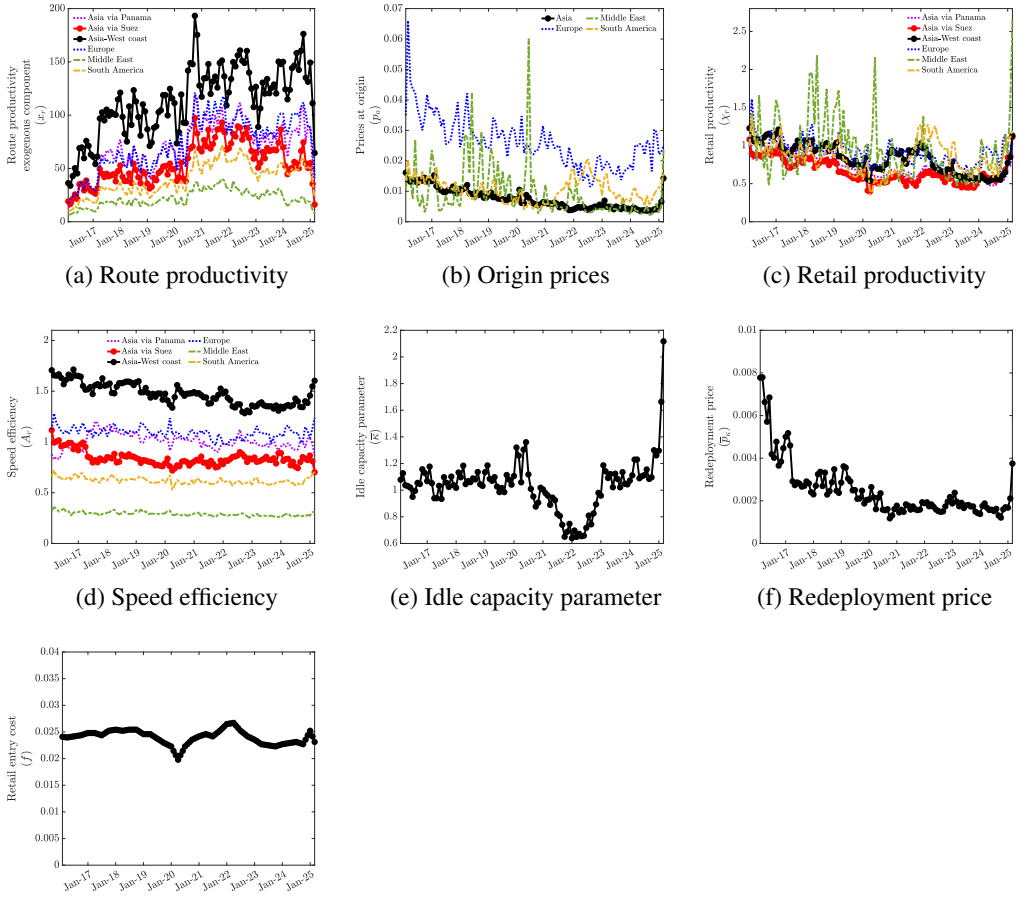


(a) Shipping productivity (b) Import shares (c) Potential shipping supply

(d) Average sailing speeds (e) Aggregate capacity (f) Number of shipping firms

Note: Panel (a) shows our measure of shipping productivity defined as the ratio of effective shipping supply to potential shipping supply for the six shipping routes. Panel (b) shows the import shares of output from Asia, Europe, the Middle East, and South America. Panel (c) shows the potential shipping supply in tons for the six shipping routes. Panel (d) shows the average sailing speeds along the six shipping routes. Panel (e) shows the world capacity in DWT. Panel (f) shows the number of shipping firms. The targeted number of retail firms is equal to one over the same period. All these model-implied time series match the data.

FIGURE B.2.—Evolution of the underlying exogenous variables, 2017-2025



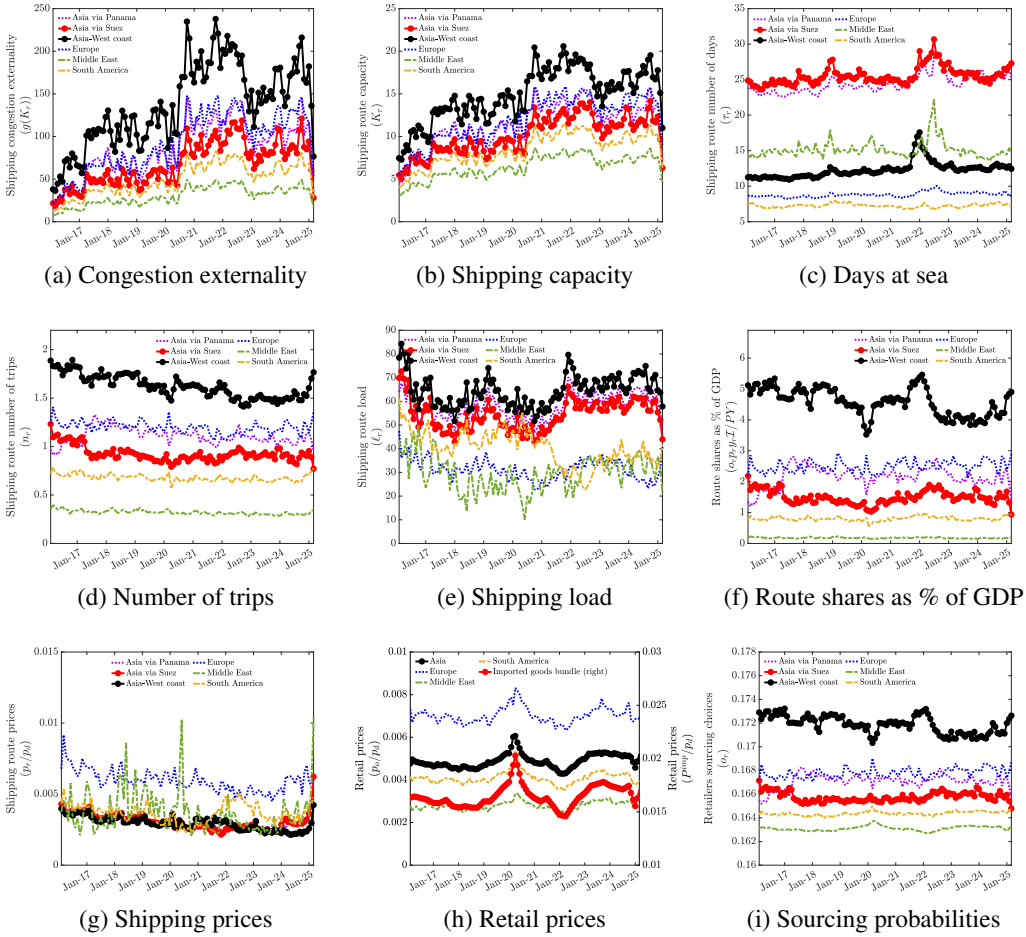
(a) Route productivity (b) Origin prices (c) Retail productivity

(d) Speed efficiency (e) Idle capacity parameter (f) Redeployment price

(g) Retail entry cost

Note: Panel (a) shows the exogenous component of the shipping productivity. Panel (b) shows the origin prices of goods produced in Asia, Europe, the Middle East, and South America. Panel (c) shows retailers' productivity. Panel (d) shows the speed efficiency. Panel (e) shows the idle capacity parameter. Panel (f) shows the price of redeployment. Panel (g) shows the entry cost in the retail market. These exogenous variables match the time series displayed in Figure B.1 together with the constraint on the number of retail firms.

FIGURE B.3.—Evolution of other endogenous variables, 2017-2025



(a) Congestion externality (b) Shipping capacity (c) Days at sea

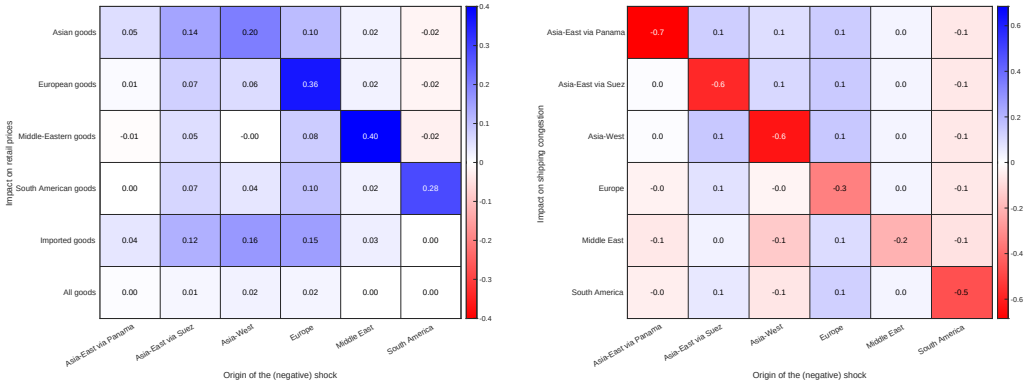
(d) Number of trips (e) Shipping load (f) Route shares as % of GDP

(g) Shipping prices (h) Retail prices (i) Sourcing probabilities

Note: Panel (a) shows the congestion externality in shipping productivity. Panel (b) shows the aggregate shipping capacity. Panel (c) shows the average number of days spent on voyages to the U.S. Panel (d) shows the average number of trips. Panel (e) shows the shipping load. Panel (f) shows the route shares as a fraction of GDP. Panel (g) shows the price of shipping services. Panel (h) shows the retail price of imported goods. Panel (i) shows the retailers' sourcing probabilities.

B.2.2. *Impact of shipping disruptions*

FIGURE B.4.—Impact of disruptions on retail prices and congestion

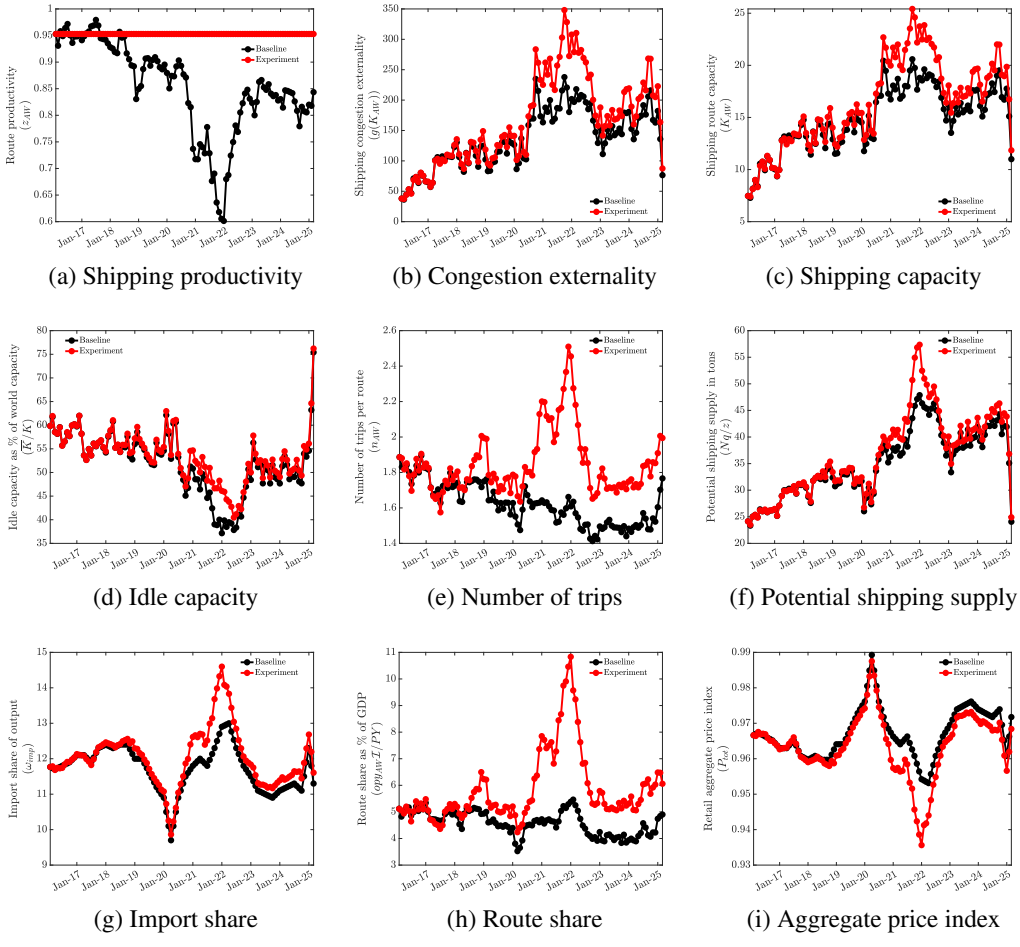


(a) Impact on retail prices (b) Impact on congestion

Note: Panel (a) displays the elasticity of retail prices from goods originating in region o to disruptions along route r, $-(\partial p_o/\partial X_r)(X_r/p_o)$. Panel (b) displays the elasticity of the congestion externality along route h to disruptions along route r, $-(\partial g(K_h)/\partial X_r)(X_r/g(K_h))$.

B.2.3. *Impact of port congestion in the Summer and Fall of 2021*

FIGURE B.5.—Evolution of selected aggregates: baseline vs. low shipping disruptions along the Asia to the West Coast route, 2017-2025



(a) Shipping productivity (b) Congestion externality (c) Shipping capacity

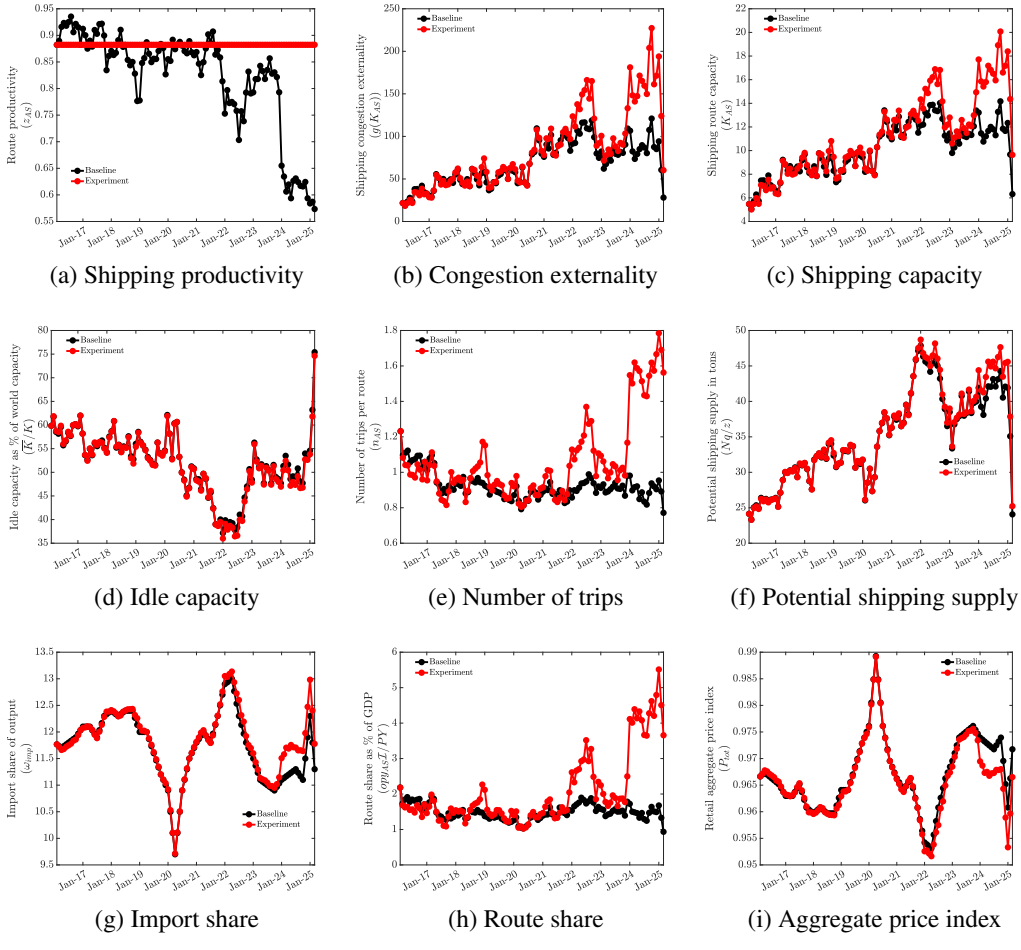
(d) Idle capacity (e) Number of trips (f) Potential shipping supply

(g) Import share (h) Route share (i) Aggregate price index

Note: Panel (a) shows the shipping productivity along the Asia to West Coast route. Panel (b) shows the congestion externality along the Asia to West Coast route. Panel (c) shows the shipping capacity allocated to the Asia to West Coast route. Panel (d) shows the idle capacity as a share of world capacity. Panel (e) shows the number of trips realized along the Asia to West Coast route. Panel (f) shows the U.S.-bound potential shipping supply. Panel (g) shows the import share of GDP. Panel (h) shows the Asia to West Coast route share of GDP. Panel (i) shows the aggregate price index.

B.2.4. *Impact of security threats in the Red Sea in early 2024*

FIGURE B.6.—Evolution of selected aggregates: baseline vs. low shipping disruptions along the Asia to the East Coast route via the Suez Canal, 2017-2025



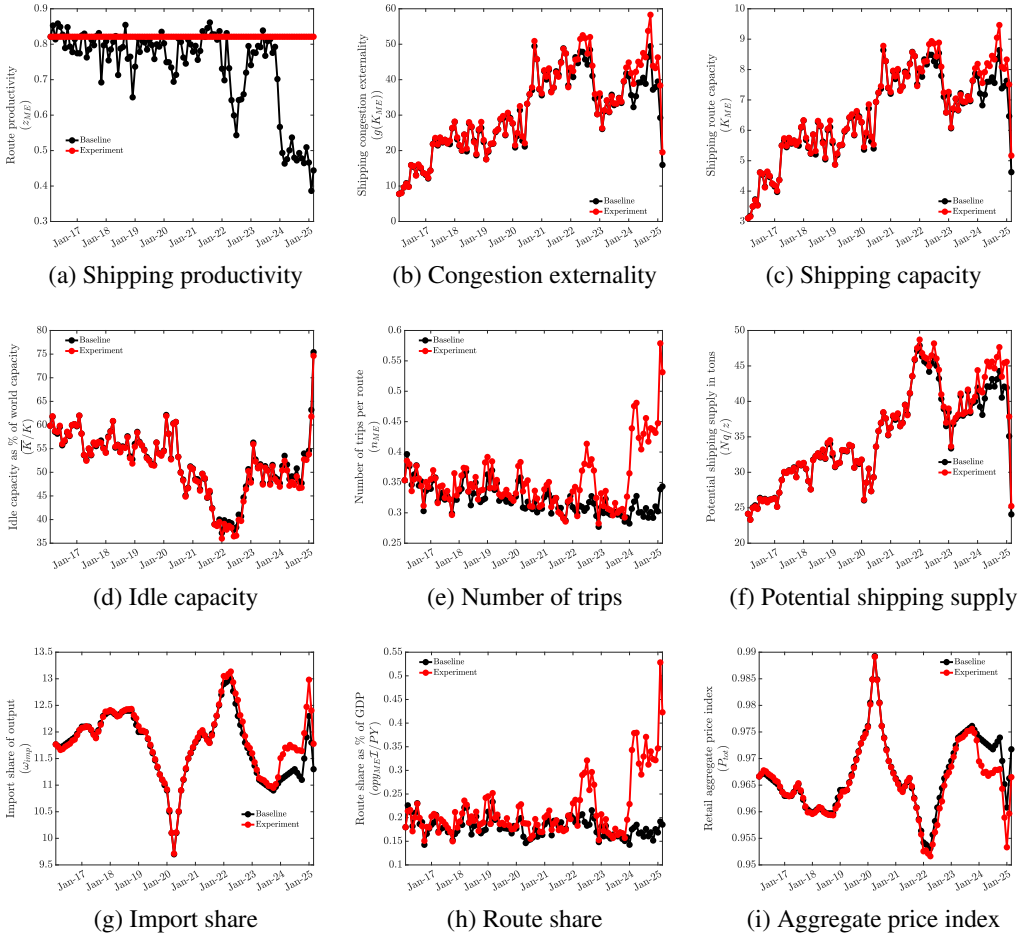
(a) Shipping productivity (b) Congestion externality (c) Shipping capacity

(d) Idle capacity (e) Number of trips (f) Potential shipping supply

(g) Import share (h) Route share (i) Aggregate price index

Note: Panel (a) shows the shipping productivity along the Asia to East Coast via the Suez Canal route. Panel (b) shows the congestion externality along the Asia to East Coast via the Suez Canal route. Panel (c) shows the shipping capacity allocated to the Asia to East Coast via the Suez Canal route. Panel (d) shows the idle capacity as a share of world capacity. Panel (e) shows the number of trips realized along the Asia to East Coast via the Suez Canal route. Panel (f) shows the U.S.-bound potential shipping supply. Panel (g) shows the import share of GDP. Panel (h) shows the Asia to East Coast via the Suez Canal route share of GDP. Panel (i) shows the aggregate price index.

FIGURE B.7.—Evolution of selected aggregates: baseline vs. low shipping disruptions along the Middle East to the East Coast route, 2017-2025



(a) Shipping productivity (b) Congestion externality (c) Shipping capacity

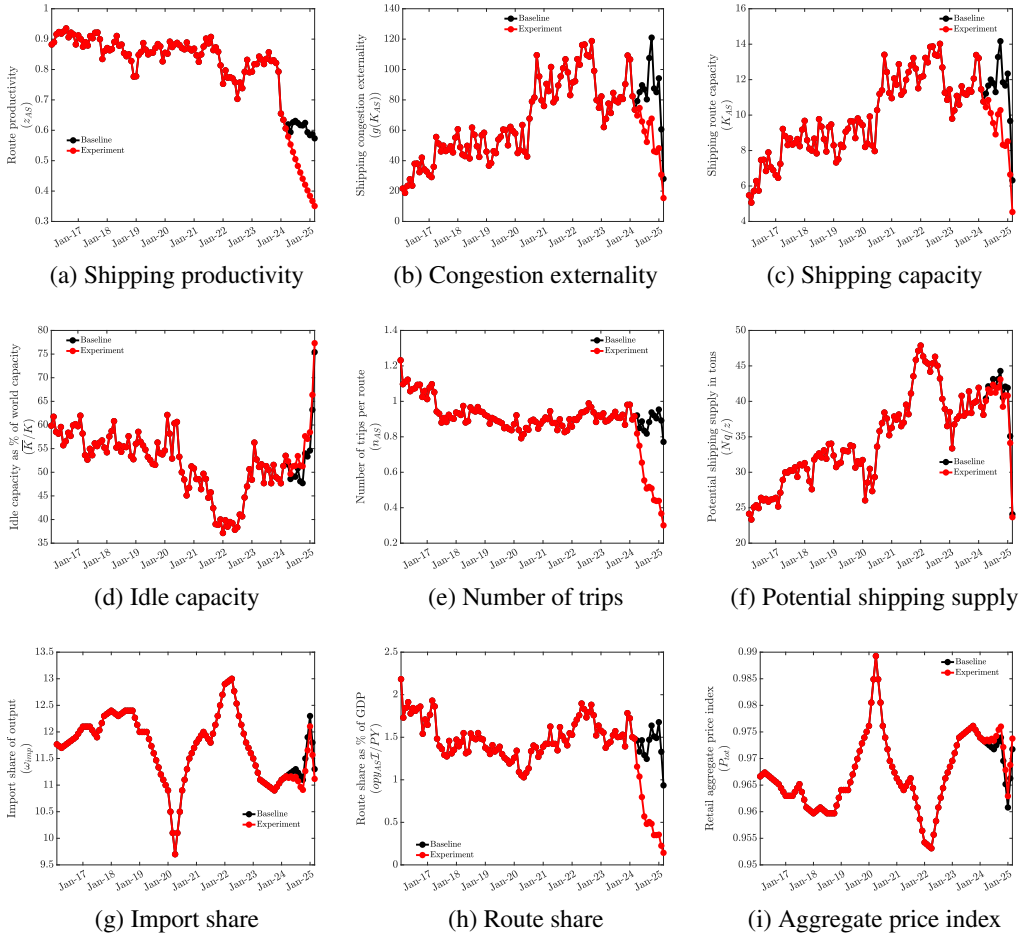
(d) Idle capacity (e) Number of trips (f) Potential shipping supply

(g) Import share (h) Route share (i) Aggregate price index

Note: Panel (a) shows the shipping productivity along the Middle East to the East Coast route. Panel (b) shows the congestion externality along the Middle East to the East Coast route. Panel (c) shows the shipping capacity allocated to the Middle East to the East Coast route. Panel (d) shows the idle capacity as a share of world capacity. Panel (e) shows the number of trips realized along the Middle East to the East Coast route. Panel (f) shows the U.S.-bound potential shipping supply. Panel (g) shows the import share of GDP. Panel (h) shows the Middle East to the East Coast route share of GDP. Panel (i) shows the aggregate price index.

B.2.5. *Impact of Navy's intervention in the Red Sea*

FIGURE B.8.—Evolution of selected aggregates: baseline vs. no Navy support along the Asia to the East Coast route via the Suez Canal, 2017-2025



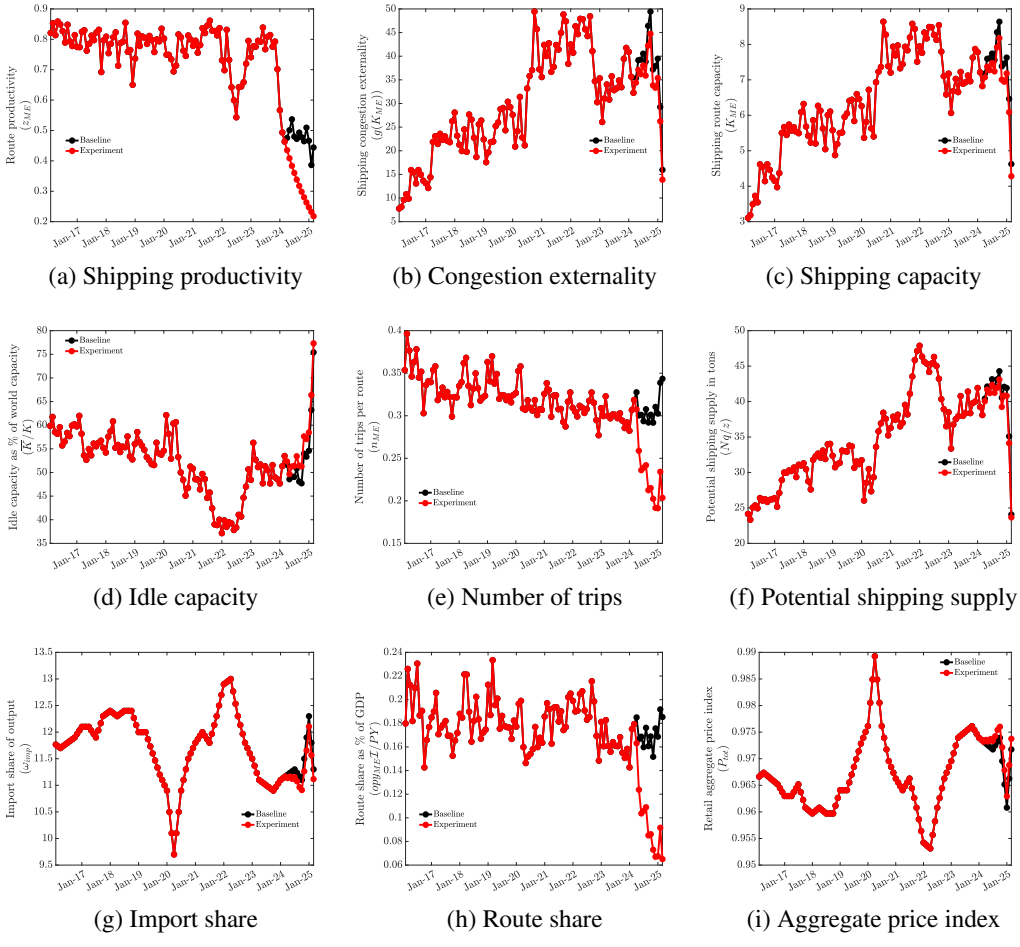
(a) Shipping productivity (b) Congestion externality (c) Shipping capacity

(d) Idle capacity (e) Number of trips (f) Potential shipping supply

(g) Import share (h) Route share (i) Aggregate price index

Note: Panel (a) shows the shipping productivity along the Asia to East Coast via the Suez Canal route. Panel (b) shows the congestion externality along the Asia to East Coast via the Suez Canal route. Panel (c) shows the shipping capacity allocated to the Asia to East Coast via the Suez Canal route. Panel (d) shows the idle capacity as a share of world capacity. Panel (e) shows the number of trips realized along the Asia to East Coast via the Suez Canal route. Panel (f) shows the U.S.-bound potential shipping supply. Panel (g) shows the import share of GDP. Panel (h) shows the Asia to East Coast via the Suez Canal route share of GDP. Panel (i) shows the aggregate price index.

FIGURE B.9.—Evolution of selected aggregates: baseline vs. no Navy support along the Middle East to the East Coast route, 2017-2025



(a) Shipping productivity (b) Congestion externality (c) Shipping capacity

(d) Idle capacity (e) Number of trips (f) Potential shipping supply

(g) Import share (h) Route share (i) Aggregate price index

Note: Panel (a) shows the shipping productivity along the Middle East to the East Coast route. Panel (b) shows the congestion externality along the Middle East to the East Coast route. Panel (c) shows the shipping capacity allocated to the Middle East to the East Coast route. Panel (d) shows the idle capacity as a share of world capacity. Panel (e) shows the number of trips realized along the Middle East to the East Coast route. Panel (f) shows the U.S.-bound potential shipping supply. Panel (g) shows the import share of GDP. Panel (h) shows the Middle East to the East Coast route share of GDP. Panel (i) shows the aggregate price index.

B.2.6. *Impact of tariffs on goods from all regions vs. tariffs on goods from Asia*

TABLE B.3

THE IMPACT OF TARIFFS ON ALL GOODS

		Baseline	Tariffs on Asian goods	Δ%	Tariffs on all goods	Δ%
		(1)	(2)	(3)	(4)	(5)
Shipping market						
Q_r	Effective shipping supply (in DWT), *Total*	18.942	18.059	-4.7	18.552	-2.1
	Asia-EC via Pan.	2.620	2.409	-8.1	2.569	-1.9
	Asia-EC via Suez	1.229	1.119	-9.0	1.206	-1.9
	Asia-West Coast	9.478	8.854	-6.6	9.276	-2.1
	Europe to EC	3.852	3.850	0.0	3.772	-2.1
	Middle East to EC	0.146	0.163	11.1	0.144	-1.7
	South Am. to EC	1.616	1.665	3.0	1.585	-1.9
N	Number of shipping firms	36.000	37.587	4.4	36.698	1.9
$N\overline{\kappa}/K$	Idle capacity share	0.754	0.757	0.3	0.756	0.3
$g(K_r)$	Congestion factor, *Asia-EC via Pan.*	35.109	32.738	-6.8	34.574	-1.5
	Asia-EC via Suez	28.074	26.240	-6.5	27.656	-1.5
	Asia-West Coast	76.507	70.914	-7.3	75.112	-1.8
	Europe to EC	53.651	57.128	6.5	52.758	-1.7
	Middle East to EC	15.958	16.315	2.2	15.704	-1.6
	South Am. to EC	28.179	29.682	5.3	27.739	-1.6
n_r	Number of trips/month, *Asia-EC via Pan.*	0.956	0.866	-9.4	0.931	-2.7
	Asia-EC via Suez	0.771	0.696	-9.7	0.751	-2.6
	Asia-West Coast	1.767	1.609	-8.9	1.715	-2.9
	Europe to EC	1.359	1.372	1.0	1.321	-2.8
	Middle East to EC	0.343	0.358	4.3	0.335	-2.6
	South Am. to EC	0.774	0.789	1.9	0.754	-2.7
p_r	Shipping prices, *Asia-EC via Pan.*	0.004	0.004	-6.8	0.004	-1.5
	Asia-EC via Suez	0.006	0.006	-6.5	0.006	-1.5
	Asia-West Coast	0.004	0.004	-7.3	0.004	-1.8
	Europe to EC	0.006	0.007	6.5	0.006	-1.7
	Middle East to EC	0.010	0.011	2.2	0.010	-1.6
	South Am. to EC	0.005	0.005	5.3	0.005	-1.6
$N\pi_r$	Shipping profits, *Asia-EC via Pan.*	0.002	0.002	-14.3	0.002	-3.4
	Asia-EC via Suez	0.002	0.001	-14.9	0.001	-3.3
	Asia-West Coast	0.008	0.007	-13.4	0.008	-3.9
	Europe to EC	0.005	0.005	6.4	0.005	-3.7
	Middle East to EC	0.000	0.000	13.6	0.000	-3.3
	South Am. to EC	0.002	0.002	8.5	0.001	-3.5
Retail market						
$\mathcal{I}$	Measure of retailers	1.000	1.596	59.6	1.872	87.2
o_r	Specialization, *Asia to EC via Pan.*	0.166	0.166	0.1	0.166	0.2
	Asia to EC via Suez	0.165	0.165	0.4	0.166	0.5
	Asia to West Coast	0.173	0.170	-1.2	0.170	-1.5
	Europe to EC	0.169	0.168	-0.4	0.168	-0.5
	Middle East to EC	0.163	0.164	0.7	0.165	0.9
	South Am. to EC	0.165	0.165	0.4	0.166	0.5
ω_o	Import share of output, *Total*	0.113	0.116	2.7	0.119	4.9
	Asia	0.073	0.073	0.7	0.076	4.8
	Europe	0.029	0.031	5.4	0.030	4.9
	Middle East	0.002	0.002	12.5	0.002	5.3
	South America	0.009	0.010	7.4	0.010	5.1
P^{tot}/p_d	Retail price (rel. to domestic goods), *All goods*	0.972	0.968	-0.3	0.966	-0.6
P^{imp}/p_d	*Imported*	0.017	0.017	-3.0	0.016	-5.2
p_o/p_d	*Asia*	0.005	0.005	-2.3	0.005	-5.2
	Europe	0.007	0.007	-3.8	0.007	-5.2
	Middle East	0.003	0.003	-5.9	0.003	-5.4
	South Am.	0.004	0.004	-4.4	0.004	-5.3
Government						
T/Y	Tax revenues (% of GDP)		0.894		0.862	
Welfare						
	Equivalent variation rel. to domestic goods (% of income)		1.334		1.635	

Note: The experiment is based on the model calibrated to March 2025 data.

B.2.7. *Impact of port fees*

To get an estimate of the port fees, $\mathfrak{f}_o$, we first compute an implied price per ton per voyage. This is achieved by dividing the value of containerized shipping imports from the Census by our measure of effective shipping supply by region. The implied price per ton per trip for ships originating from Asia corresponds to about \$5,000. Hence, a fee of \$50 per ton per voyage would represent 1% of the implied price per ton per voyage. The model counterpart for the price per ton per voyage is $\overline{p}_o$. We thus set $\mathfrak{f}_o = 0.01 \times \overline{p}_o$. We follow the same strategy as above and compute two counterfactual economies, one which the port fees are leveraged only on shipping firms operating the Asian routes and another applied to all routes. Table `tab:exp_PortFees` presents the results and the discussion follows.